

**Alma Mater Studiorum – Università di Bologna**

**DOTTORATO DI RICERCA IN**

**Scienze e Tecnologie Agrarie, Ambientali e Alimentari**

**Ciclo XXVII**

**Settore Concorsuale di afferenza: 07/E1**

**Settore Scientifico disciplinare: AGR/14**

**WATER, SEDIMENT AND SOIL PHYSICOCHEMICAL INTERACTIONS IN  
FRESHWATER, BRACKISH AND SALINE SYSTEMS**

**Presentata da: Ferronato Chiara**

**Coordinatore Dottorato**

**Relatore**

**Ch.mo Prof. Giovanni Dinelli**

**Dott.ssa Livia Vittori Antisari**

**Esame finale anno 2015**



All things are engaged in writing their history. The planet, the pebble, goes attached by its shadow.

The rolling rock leaves its scratches on the mountain; the river, its channel in the soil; the animal, its bones in the stratum; the fern and leaf, their modest epitaph in the coal. The falling drops make its sculpture in the sand or the stone. Not a foot step into the snow or along the ground, but print its character more or less lasting, a map of its march. [...].  
The ground is all memoranda and signatures.

*Ralph Waldo Emerson (1850)*



## Abstract

The present work is the result of a three-years-long research, which explored a wide range of freshwater, brackish, saline subaqueous environments with the aim of understanding the main physicochemical processes involved between water and sediments, and between water and soil.

In a freshwater system (Reno river basin, Northern Italy), the physicochemical characterization of water and sediment of some watercourses led to highlight the issue of the environmental quality of both submerged and dredged sediments. For this reason, the risk assessment of heavy metals was performed by comparing different techniques. Subsequently, some bench-scale experiments were performed to test new eco-friendly techniques for water remediation and for the prevention of sediment contamination. For this purpose, zeolites (e.g. clinoptilolite), clays (e.g. vermiculite) and permeable bio-barriers were used for entrapping heavy metals ions at the water/sediment interface.

In a brackish system (San Vitale park, Northern Italy), the presence of a *soil continuum* from the subaqueous to the hydromorphic environment was investigated in two soil sequences. This research highlighted some common feature among similar soils subjected to different saturation degrees. Moreover, both field and physicochemical indicators were used to define the main variables which describe the transition from the subaqueous to the hydromorphic soil into the *soil continuum*.

In a saline system (Grado lagoon, Northern Italy), the biodiversity of different salt marshes and the effect of the tide oscillation on soil, permitted to investigate the relationship between soil development and landscape features in both subaqueous and hydromorphic environment. It was thus recognized the mutual influence of halophyte species colonization and of the tide oscillation, on soil development.



## Acknowledgments

This research has been supported by the financial contribution of the *Consorzio di Bonifica Renana* (BO) and by the collaboration with the following researchers and professors:

- Dr. Alessandro Buscaroli<sup>1</sup>, Dr. Gloria Falsone<sup>2</sup>, Dr. Denis Zannoni<sup>1</sup> (BiGEA<sup>1</sup> and DipSA<sup>2</sup>-University of Bologna) for their pedologic support and their knowledge of the S. Vitale park.
- Prof Teresa Tavares, Dr. Filomena Costa, Dr. Bruna Silva (IBB-University of Minho), for the study of bioremediation techniques.
- Prof. Maria de Nobili, Dr. Elisa Pellegrini (DISA- University of Udine) for saline systems investigations and botanical expertise of the Grado lagoon.

A particularly thanks goes to my supervisor, Dr. Livia Vittori Antisari, who supported my work at each step, and to Prof. Teresa Tavares, who supported a piece of this research at University of Minho (Portugal).

A special thanks goes to Prof. Gilmo Vianello, who followed all my sampling surveys and solved all my technical problems.

I express my gratitude to all the people who supported me day by day, both professionally and personally, and in particular Dr. Andrea Simoni, Dr. Paola Gioacchin, Dr. Monica Modesto, Dr. Sonia Blasioli, Dr. Enrico Biondi, Dr. Emilio Rosales, Dr. Luigi Sciubba, Dr. Serena Carbone, Dr. Verena Stenico. Last but not least, thanks to Dr. Marco Natale, for his precious moral support.

Thanks to all the people who walked with me during these three years, and to those who followed me from far away: my family, my friends, my comrades and colleagues.





	<i>pp.</i>
Abstract.....	i
Acknowledgments .....	ii
<b>Index.....</b>	<b>iii</b>
1. Introduction and literature review.....	1
1.1. Water, sediment and soil interactions: definitions.....	1
1.1.1. Water.....	1
1.1.2. Sediment.....	2
1.1.3. Soil.....	3
1.2. Water, sediment and soil interactions: weathering processes.....	5
1.2.1. Weathering process .....	5
1.2.2. Time of submergence and reductive processes.....	7
1.3. Water, sediment and soil interactions: ecosystem variability .....	12
1.3.1. Freshwater ecosystems.....	12
1.3.2. Marine and brackish ecosystems.....	13
1.4. Aim of the thesis.....	15
1.5. References.....	16
2. Freshwater systems: The Reno river basin.....	23
2.1. The study area.....	24
2.2. Materials and methods.....	25
2.2.1. Sampling and experimental design.....	25
2.2.2. Water physicochemical analysis.....	26
2.2.3. Sediment physicochemical analysis.....	27
2.2.4. Heavy metals partitioning .....	29
2.2.5. Heavy metals sequential extraction.....	30
2.2.6. Data analysis.....	31
2.3. Results.....	32
2.3.1. Water physicochemical characterization.....	33
2.3.2. Sediment physicochemical characterization.....	35
2.3.3. The risk assessment of heavy metals.....	38
2.4. Discussion.....	42
2.4.1. Water and sediments characterization.....	42
2.4.2. The risk assessment of heavy metals.....	43
2.5. Conclusion.....	44
2.6. References.....	46

3.	The environmental protection: remediation experiments.....	49
3.1.	Clinoptilolite experiments.....	49
3.1.1.	Materials and methods.....	51
3.1.2.	Results.....	52
3.1.3.	Discussion.....	53
3.1.4.	Conclusion.....	54
3.2.	Vermiculite experiments.....	55
3.2.1.	Materials and methods.....	57
3.2.1.1.	Vermiculite, sediment and water characterization.....	57
3.2.1.2.	Biofilm cultivation and preparation.....	58
3.2.1.3.	Data analysis.....	59
3.2.2.	Results.....	59
3.2.3.	Discussion.....	64
3.2.4.	Conclusion.....	65
3.3.	References.....	66
4.	Brackish systems: the S. Vitale park.....	70
4.1.	The study area.....	71
4.2.	Materials and methods.....	71
4.2.1.	Sampling and experimental design.....	71
4.2.2.	Morphological description of soil profiles.....	73
4.1.1.	Physicochemical characterization of soil profiles.....	73
4.1.2.	Data analysis.....	74
4.3.	Results.....	75
4.3.1.	Morphological and physicochemical description of soil continuum.....	75
4.3.2.	Soil classification and discriminant function analysis.....	80
4.4.	Discussion.....	83
4.5.	Conclusion.....	85
4.6.	References.....	86
5.	Saline systems: the Grado lagoon.....	90
5.1.	The study area.....	91
5.2.	Materials and methods.....	92
5.2.1.	Sampling and experimental design.....	92
5.2.2.	Morphological and ecological description of soil profiles.....	93
5.2.3.	Water analysis and physicochemical characterization of soil profiles.....	94
5.2.4.	Data analysis.....	94
5.3.	Results.....	95
5.3.1.	Climatic and ecological characterization.....	95

5.3.2. Morphological and physicochemical characterization of soils.....	96
5.3.3. Soil classification and ecological relationship.....	101
5.4. Discussion.....	105
5.5. Conclusion.....	107
5.6. References.....	109
6. Conclusions.....	113
6.1. Freshwater systems.....	113
6.2. Brackish systems.....	113
6.3. Saline systems.....	114
Appendix 1.....	115
Appendix 2.....	121
Appendix 3.....	122
Appendix 4.....	123
Appendix 5.....	125
Appendix 6.....	127
List of tables.....	129
List of figures.....	131
List of papers.....	133



# CHAPTER 1

## INTRODUCTION

*pp.*

1.	Introduction and literature review.....	1
1.1.	Water, sediment and soil interactions: definitions.....	1
1.1.1.	Water.....	1
1.1.2.	Sediment.....	2
1.1.3.	Soil.....	3
1.2.	Water, sediment and soil interactions: weathering processes.....	5
1.2.1.	Weathering process.....	5
1.2.2.	Time of submergence and reductive processes.....	7
1.3.	Water, sediment and soil interactions: ecosystem variability.....	12
1.3.1.	Freshwater ecosystems.....	12
1.3.2.	Marine and brackish ecosystems.....	13
1.4.	Aim of the thesis.....	15
1.5.	References.....	16



# **1. INTRODUCTION AND LITERATURE REVIEW**

## **1.1. WATER, SEDIMENT AND SOIL INTERACTIONS: DEFINITIONS**

Fresh, brackish and saline water bodies map out our planet by interacting with the ground substrate, and form a variety of freshwater, brackish and saline ecosystems, which span from riverine and estuarine environments, wetlands and lagoons. With the aim of approaching the study of water and sediment/soil interactions, this chapter firstly discusses the definition of water, sediment and soil, and how these concepts have changed over time.

### **1.1.1. Water**

Water is one of the most essential compounds in nature (Vepraskas et al., 2000). Almost 97% of the water resources in our planet is present as salt water in oceans and seas (Bouwer, 1978). Of the remaining 3% of water, 2/3 occurs as snow or ice, and only 1% consists in freshwater. Around 98% of freshwater is present in groundwater aquifers, while less than 2% is found in surface waterbodies such as rivers and lakes (Bouwer, 2000).

Water properties reflect the lithologic, atmospheric and anthropogenic inputs of the territory, and are influenced by the climatic and thermodynamic conditions of the surrounding environment (Pejman et al., 2009; Shrestha and Kazama, 2007).

The chemical quality of surface waters cannot be separated from the study of the water interactions with the surrounding biosphere, geosphere or atmosphere, e.g. water interaction with sediment, soil, suspended solids, rocks, groundwater, rainfall depositions, etc. (Hanrahan et al., 2005). According to these physicochemical interactions, waters can be classified as fresh, brackish or saline.

Fresh waters are usually characterized by the predominance of  $\text{HCO}_3^-$  and  $\text{Ca}^{2+}$ ,  $\text{Mg}^{2+}$  or  $\text{SO}_4^{2-}$  ions, which dissolve from the rock material, and by a low ionic strength. Conversely saline waters are characterized by high ionic strength and by the predominance of  $\text{Na}^+$  and  $\text{Cl}^-$  ions.

The increase of industrialization has deeply influenced the quality of water worldwide, and in many cases the excess of both nutrients and pollutants affect the environmental health (Varol, 2011).

The climate change dynamic enhances the saline intrusion on many coastal areas and this problem is seriously affecting agricultural activities and the environmental sustainability (Hu and Schmidhalter, 2005). Where fresh and saline water meet, the equilibrium of the environment is very fragile and its maintenance is strictly linked to the correct management of the water resources (Buscaroli and Zannoni, 2010).

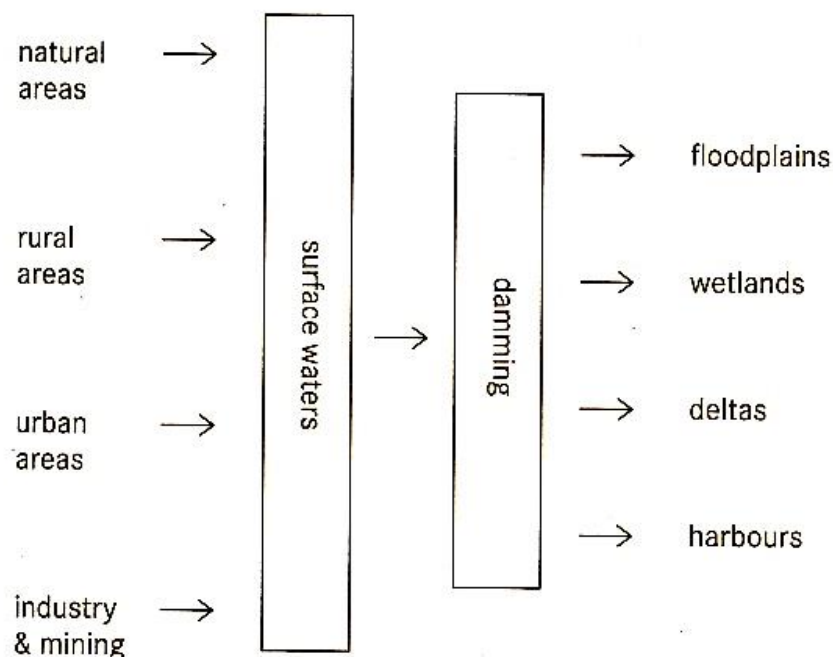
### 1.1.2. Sediment

Krumbein and Sloss (1951) defined sediments as *solid material deposited on the earth's surface from any medium* (air, water, ice, etc.).

This very minimal definition has been enlarged in recent years by some authors, who have defined sediments as *the compartment where substances in the water column tend to accumulate, due to scavenger agents and adsorptive components* (Akcil et al., 2014; Mulligan et al., 2001; Peng et al., 2009). This latter definition, underlines not only the process of erosion, transport and deposition of minerals, organic materials and soil, but also their interaction with the water column through re-suspension and adsorption processes.

A schematic representation of the origin and fate of sediments is shown in Figure 1.1.

**Figure 1.1.** The catchment-coast continuum. Origin, transport and accumulation of sediments and their impact on downstream areas. (European Sediment Research Network, 2004).





The quality and properties of sediments are subjected to several modifications from the upstream areas to the coast (e.g. textural changes, contamination, salinization, organic matter degradation, etc.) due to physical, chemical and biochemical transformations. According to these transformations and to their location, sediments contribute to the formation of a variety of habitats, such as streams and rivers, lakes and reservoirs, floodplain and wetland, estuaries and lagoon, seas and oceans (European Sediment Research Network, 2004). Sediments quality can be also influenced by human activities and discharges. In fact, great attention has been given to the study of sediment contamination and risk assessment (Bat and Raffaelli, 1998; Cowie, 2005; Miniero et al., 2005) because of the toxic effect that polluted sediments can have on the environment and human beings (Crane, 2003; Taylor and Owens, 2009).

Nevertheless, the lack of standardized methodologies and sediment quality standards (SQSs) among countries and jurisdictions, has produced different responses to sediment management (Apitz and Power, 2002; Crane, 2003) and for this reason, many researchers have been focusing on the definitions of adequate and standardized methodologies to define the quality of sediments.

### **1.1.3. Soil**

The first definition of soil was introduced by the Russian school led by Dokuchaiev V. (1846-1903). Soils were conceived as *independent natural bodies with a unique morphology resulting from a unique combination of climate, living matter, earthy parent materials, relief, and age of landforms* (Gedroiz, 1927).

Later, this concept developed considering all biotic and abiotic factors, which interact with the soil components, such as minerals, organic matter, liquid and gasses, *that occur on the land surface, occupy space, and are characterized by one or both of the following: horizons, or layers, that are distinguishable from the initial material as a result of additions, losses, transfers, and transformations of energy and matter, and the ability to support rooted plants in a natural environment* (Soil Survey Staff, 1999).

This definition has been supported by the work of Jenny H. (1899-1992), entitled “Factors of Soil Formation”. In this treatise, he stated the famous state factors equation of soil-forming and development:

$$\text{Soil } (S) = f(C, O, R, P, T) \quad [1]$$

According to this model, soil derives from the interaction of several factors, such as climatic temperature conditions (C), biological activity of soil organisms (O), topographical relief (R), nature of the parent material (P), and time (T).

In the last decades the concept that sediments in shallow water environments undergo soil-forming processes has been investigated by some authors (Balduff, 2007; Bradley and Stolt, 2003; Demas and Rabenhorst, 1999, 2001; Osher and Flannagan, 2007; Payne, 2007).

Their researches demonstrated that subaqueous substrates can be subjected to pedogenetic processes similar to those occurring in subaerial terrestrial soils and the fact that, in some cases, sediments can support rooted plants led soil scientists to verify the possibility to rank these sediment substrates as proper subaqueous soils (Demas et al., 1996).

Recently some American soil scientists (e.g. Demas G., Rabenhorst M.C., Bradley M.P., Stolt M.H., Erich E., Payne M., Balduff D.M.) have therefore proposed a new state factors equation to describe the subaqueous soils-formation and development:

$$\text{Subaqueous Soil } (SAS) = f(C, O, B, F, P, T, W, E) \quad [2]$$

In this model, similarly to terrestrial soils, they recognize the importance of considering climatic temperature conditions (C), biological activity of soil organisms (O), nature of the parent material (P), and time (T). In addition, for subaqueous soil formation, they stress the important role of the bathymetry (B) and of the flow regime (F), the essential role of water characteristics (W) and of catastrophic events (E) (Demas and Rabenhorst, 2001).

The pedological investigation on subaqueous substrates has led to an extension of the definition of soil upper limit in the USDA Sol Taxonomy classification system (Soil Survey Staff, 2010). Since 2010, in fact, the 11<sup>th</sup> approximation of the Soil Taxonomy has included the concept of subaqueous soils (SASs) as *pedons covered by up to 2.5m of water with a positive water potential on the soil surface for at least 21 hours each day* (Soil Survey Staff, 2010).

These soils were thus included in the *Histosol* and *Entisol* orders as belonging to the *Wassist* and *Wassent* sub orders, respectively.

## 1.2. WATER, SEDIMENT AND SOIL INTERACTIONS: WEATHERING PROCESSES

Water is one of the most important soil weathering factor for soil formation and development. The partial or total submergence of sediments or soils induces a number of physical, chemical and biochemical reactions and processes which strictly characterize the subaqueous environments.

### 1.2.1. Weathering processes

Water is a powerful agent of rock and soil physical and chemical weathering. The water flow on a surface primarily results in rocks deterioration, decay, crumbling, decomposition, rotting, disintegration, disaggregation or breakdown (Hall et al., 2012), which can be define as the starting factor of the erosion process of the surface (Moses et al., 2014).

The chemical weathering induced by water can be resumed in three main processes: hydration, hydrolysis and solubility.

During *hydration*, water enters the crystal lattice of a mineral, which does not change its chemical compositions, but results in expansion and mechanical deformation (Schaetzl and Anderson, 2005). Hydration typically affects the weathering of minerals rich in Fe, Mn or S and is strictly linked to oxidation-reduction processes.

*Hydrolysis* occurs when the  $H^+$  proton of water reacts with a silicate mineral inducing a cation exchange mechanism between  $H^+$  and the mineral cation. This reaction generally enhances the solubility of clay minerals and it lowers the pH through acid production. Hydrolysis is typical of silicate weathering, such as the formation of smectite from albite hydrolysis (Schaetzl and Anderson, 2005).

The *solubility* of a mineral depends primarily on the ionic potential of the ions that compose the mineral compound. Ions with low ionic potential are more easily leached and hence more soluble, but all minerals are soluble (Bland and Rolls, 1998). These processes can be accelerated by an increase in temperature and unlike hydration or hydrolysis, it can be reversible: in fact, in supersaturation conditions, dissolved ions may re-

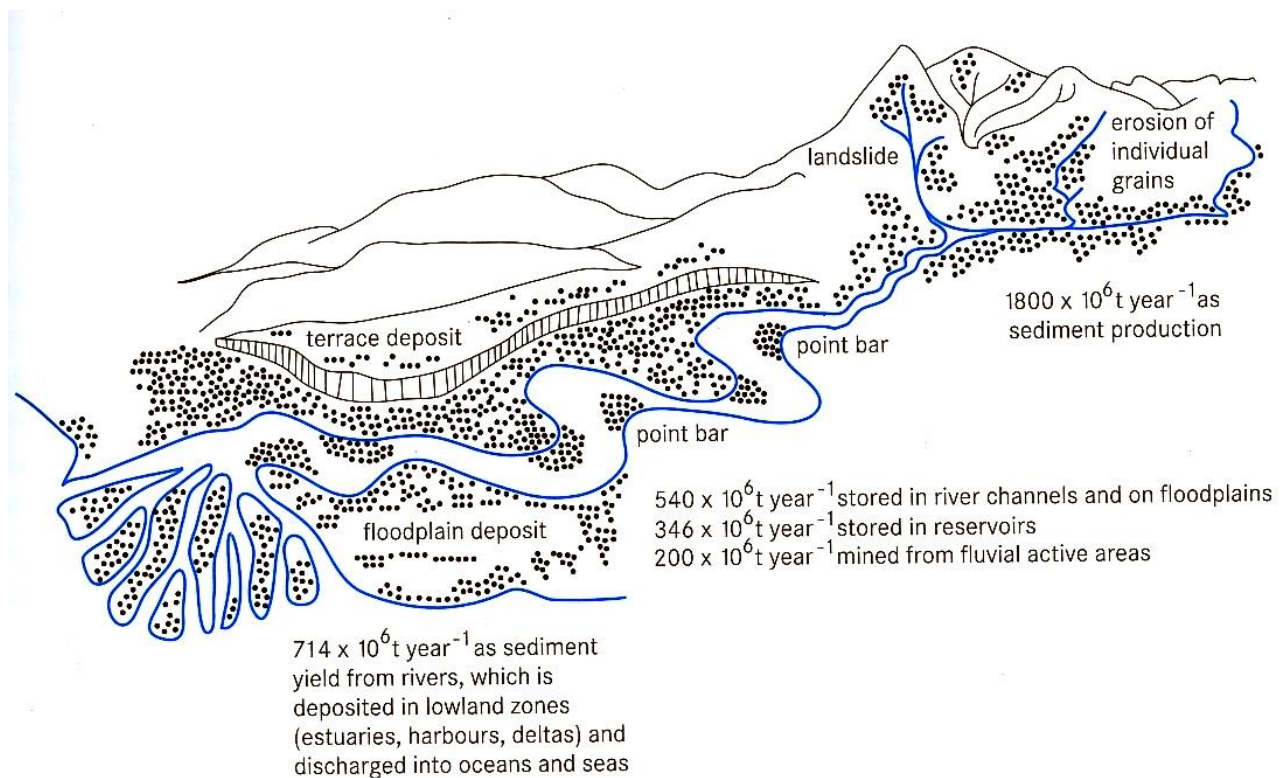
precipitate forming secondarily salts on the top surface. Typical easily soluble minerals found in sediments and soils are halite, potash, gypsum and calcium carbonate.

A great amount of sediments are produced by erosion processes and these materials are subsequently transported and deposited by the water flow. A schematic representation of sediment erosion and transportation budgeting in Europe is offered in Figure 1.2 by Owens and Batalla (2003).

Natural **erosion** is generally the dominant source of sediments but changes in land uses, deforestation, urbanization and agricultural activities have deeply increased the amount of eroded materials, and therefore the accumulation of an excess of sediments in many downstream areas (Kibblewhite et al., 2012).

Sediments are **transported** into rivers, reservoirs and ponds by water hydrodynamics (Wu and Chen, 2012) through time and space, impacting the sustainable use of rivers water (Mukundan et al., 2013; Verstraeten and Poesen, 1999). Coarse material ( $>2\text{mm}$ ) is usually derived from mechanical erosion and does not travel very far from its source, while most fine particles ( $<2\text{mm}$ ) are easily resuspended and transported downstream where floodplains, estuarine and coastal environments are formed.

**Figure 1.2.** Representation of sediment disposal from the river catchment to the estuarine and coastal zones (Owens and Batalla, 2003).



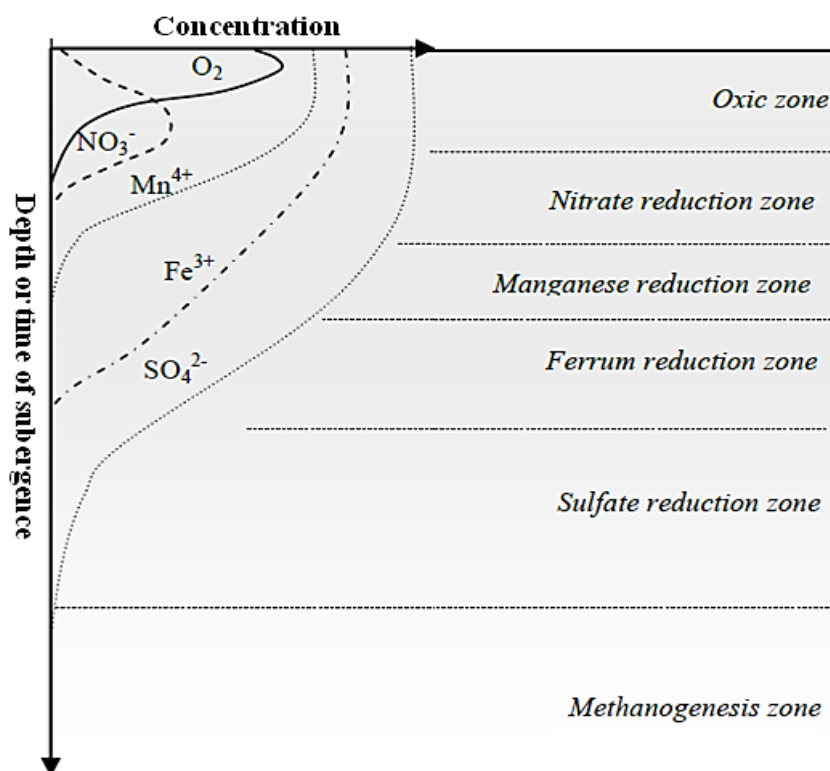
Alluvial deposits may **accumulate** to a large extent in floodplains, estuarine and coastal areas, and they can start a process of layerization and consolidation which may lead to the formation and development of soil. Through infiltration and percolation, water in soil induces mineral dissolution, transports ions colloids and metal organic complexes through the soil profile, and influences the soil redox status (Schaetzl and Anderson, 2005).

Water influences all the soil-forming factors (climate, organisms, relief, parent material, time). Climate influences the amount and timing of water availability in soil. Organisms in soil need water to grow, topography frequently controls water flow, parent materials affect the flow of groundwater and, lastly, time is required for soil development to happen.

### 1.2.2. Time of submergence and reductive processes

The bio-geo-chemical cycle of both nutrients and trace elements at the boundary exchange between water and sediment or soil is strongly regulated by the redox status and by the length of the sediment/soil submergence.

**Figure 1.3.** Schematic presentation of reduction zones in subaqueous sediments/soils (modified from Žilius (2011)).



The diffusion of oxygen through water is approximately 10 000 times slower than the diffusion in air and it is rapidly consumed during aerobic respiration of microorganisms and plants (Reddy and DeLaume, 2008).

Oxygen displacement naturally occurs in poorly drained soils or under saturated conditions, and in many shallow water environments, the thickness of oxic zones may vary from 1 mm to a few centimetres in the upper sediment/soil surface (Žilius, 2011).

Above the oxic zones, reductive conditions may develop in substrates covered with poorly-oxygenated waters, or in deep soil horizons, inducing a number of chemical and biochemical reactions which characterize shallow water environments, as schematically represented in Figure 1.3.

### Oxic Zone

In soil oxic layers,  $O_2$  can be diffused by the atmosphere, the shallow water, or by the plant roots. In this phase, oxygen is the main electron acceptor for biota respiration processes, where microorganisms use  $O_2$  to oxidize organic matter and acquire their energy source.

In hydromorphic conditions, reductive species, such as  $Fe^{2+}$ ,  $Mn^{2+}$  and sulphides, commonly diffuse from the upper anaerobic layer to the aerobic layer and become rapidly oxidized.

**Figure 1.4.** Redoximorphic features on a soil profile (Grado lagoon, Northern Italy).



The alternation of reductive and oxidized forms of Fe and Mn may induce the formation of *redoximorphic features* (Reddy and DeLaume, 2008): these features consist in mottles, nodules, coatings and concentrations along the soil profile, which can be distinguished in the soil matrix for their black, bluish or grey colours

(reductive species) or by reddish colours (oxidized species) as shown in Figure 1.4 (Schaetzl and Anderson, 2005).

Moreover, the sulfidic oxidation in the oxic zone may lead to the acidification of soil, as a consequence of the production of  $\text{H}_2\text{SO}_4$  and gaseous compounds such as,  $\text{SO}_2$ , DMSO (dimethyl sulfoxide) and DMS (dimethyl sulphide) (Bradley and Stolt, 2003; Dent and Pons, 1995).

### **Nitrate reduction zone**

When soil is flooded or waterlogged, the reduction of nitrates ( $\text{NO}_3^-$ ) to  $\text{N}_2$  and  $\text{N}_2\text{O}$  through denitrification processes is the main effect of the microbial respiration. This process primarily occurs below the oxic zone because of the diffusion of nitrates from the top zone (Jensen et al., 1993; Lorenzen et al., 1998; Meyer et al., 2001). Microbial nitrates reduction results in a net mineralization of N compounds, and in a loss of  $\text{N}_2$  evolving to the atmosphere.

Notably the efficiency of the decomposition of organic matter in subaqueous soils is much lower in an anoxic environment than in an oxic one (Reddy and DeLaume, 2008) but, similarly to the terrestrial ecosystem, some authors have investigated the C/N ratio as an indicator of the degradation of organic matter. The lowering of the C/N ratio, in fact, has been found to be related to the microbial transformation of fresh organic matter to other humic substances also in subaqueous sediments of Sinepuxent Bay, Maryland, USA (Demas and Rabenhorst, 1999).

### **Fe and Mn reduction zone**

With the increase in time of submergence and soil depth, other redox couples usually prevail in the system, such as those involved in Fe and Mn redox compounds. Iron is generally abundant in soil and sediments, and is subjected to redox changes depending on the environmental conditions.

Iron and Manganese reduction is one of the most common and well known reactions in soils under water saturated conditions (Munch et al., 1978; Thompson et al., 2006).

In reductive conditions, these elements are usually present in very soluble form, while close to the oxic and aeric zone amorphous and crystalline species prevail (O'Day et al., 2004; Poulton and Canfield, 2005; Vodyanitskii and Shoba, 2014).

The presence of reductive forms of Fe and Mn are generally well distinguished by the Gley colours of the matrix (Munsell colour chart) and characterizes the *gleyfication* process. This process is typically associated with high soluble forms of major elements (Reddy and DeLaume, 2008).

The reduction of  $\text{Fe}^{3+}$  and  $\text{Mn}^{3+}$  forms can be an important path for organic matter degradation (Vandieken et al., 2006; Vodyanitskii and Shoba, 2014) and for the development of *sulfidization processes* (see section below) while the continuous redox changes during dry and wet periods may induce the formation of mottles and depletion, redoximorphic features (see section above) and neoformation of clays (e.g. ferrollysis, Brinkman (1970), Van Ranst et al. (2011)).

### **Sulphate reduction zone**

Reduced sulphur in subaqueous environments is generally bound to organic compounds to form peptides, proteins, and amino acids (Kao et al., 2004; Krairapanond et al., 1992), or it is involved in heavy metals immobilization.

In brackish and salt marsh soils,  $\text{S-SO}_4$  is transported by marine water and in anaerobic conditions it is soon reduced by chemical transformations and microbiological oxidation of the organic matter (Demas and Rabenhorst, 1999).

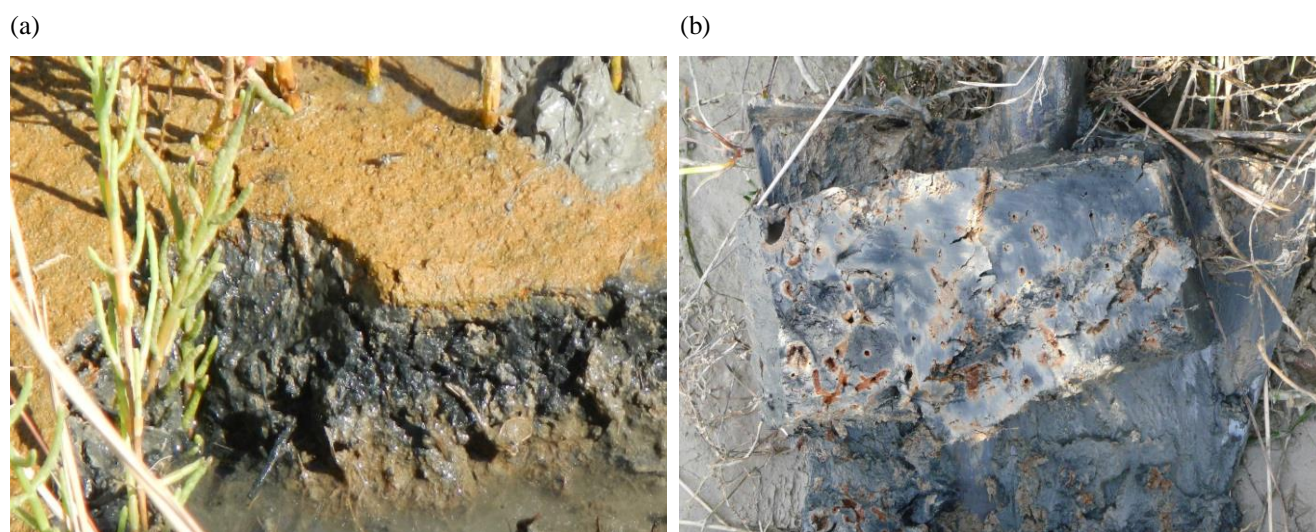
Under strict anoxic conditions, the presence of both reduced S and Fe can lead to the development of *sulfidization* processes, as described by Fanning and Fanning (1989).

The accumulation of reduced S compounds may react with free  $\text{Fe}^{2+}$  forming different sulfidic mineral compounds such as mackinawite ( $\text{FeS}$ ), greigite ( $\text{Fe}_3\text{S}_4$ ), and lastly pyrite ( $\text{FeS}_2$ ), and may lead to the formation of sulfidic horizons (Figure 1.5).

As described above, the oxidation of these compounds is extremely dangerous because of the formation of acid compounds.



**Figure 1.5.** Sulfidic horizon in subaqueous soil (a) and pyrite accumulation associated with Fe oxidation (b).



### **Trace element reduction**

The source of heavy metals can be both geogenic and anthropogenic (Bianchini et al., 2012), and they can be present as free cations in aqueous phase, adsorbed to carbonates, Fe and Mn oxides, sulphides, organic matter or within the crystalline structure of primary minerals (Shannon and White, 1991).

According to their speciation, heavy metals can be more or less toxic to different organisms (Carlson et al., 2004; Farkas et al., 2007): usually their soluble forms are associated with a higher toxicity because of a higher availability (Asa et al., 2013; Stephens et al., 2001b).

The availability of heavy metals is also influenced by the presence of organic matter and clay content, pH and the redox status; moreover, the cycle of sediments or soil wetting and drying can slowly increase the heavy metals mobility over time, and therefore enhance their environmental hazard (Hartley and Dickinson, 2010; Stephens et al., 2001b). Moreover, the mobility of heavy metals in subaqueous and early dredged sediment and soils are strictly linked to the change of the redox status of the environment (Clark et al., 2000; Feng et al., 2005; Gismera et al., 2004; Rao et al., 2008).

### 1.3. WATER, SEDIMENT AND SOIL INTERACTIONS: ECOSYSTEM VARIABILITY

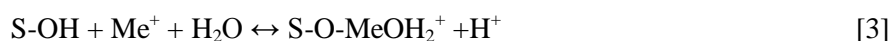
#### 1.3.1. Freshwater ecosystems

Since ancient times, floodplains have attracted humanity because of the high availability of natural resources, fertile soils and relatively flat land for agriculture (European Sediment Research Network, 2004).

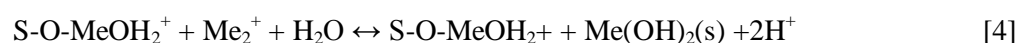
Contaminants and pollutants from different sources (industrial, mining, municipal sewage, agricultural and other activities) nowadays enter watercourses by both natural and anthropic processes (Prica et al., 2010) and sediments often become both a sink and a source of toxic compounds causing environmental problems in most industrialized countries (Choueri et al., 2009; Schwarzenbach et al., 2006).

Heavy metals are considered some of the most harmful inorganic pollutants in sediments and soils (Viganò et al., 2003). Only a small part of free heavy metals ions are dissolved in water while it has been estimated that between 30 to 98% of the total metal load of a river can be transported in a sediment-associated form (Varol and Şen, 2012). In fact, heavy metals can be retained in the solid phase through different sorption mechanisms such as adsorption, precipitation and fixation processes.

**Adsorption** occurs as an electrostatic interaction between the solute and the solid phase, and it largely depends on the pH of the system. Specific adsorption represents an almost irreversible binding of heavy metals to clays, silanol groups, inorganic hydroxyl groups, or organic functional groups (Bradl, 2004; Sahuquillo, 2003). These reactions can be schematically resumed as follows:



**Metal precipitation** occurs as a complexation of metals with oxides, hydroxides, carbonates, sulphides or phosphates present in sediments or soils (Reed and Matsumoto, 1993) and is a reversible reaction. These reactions depend on pH and metal concentrations, resulting in the formation of a new solid phase as explained by the reaction:



**Fixation or absorption** of heavy metals is the mechanism involved in the diffusion of soluble metals into the solid phase. Adsorbed metals, can in fact diffuse into the lattice structure of minerals and be fixed into the pore spaces of the mineral structure (Bradl, 2004).

Notably, the changing of redox status, e.g. sediment oxidation after dredging, seasonal drying of canals bed etc., can deeply affect metals sorption/desorption cycles and precipitation/dissolution processes at the interface between water and sediment (Du Laing et al., 2009; Ho et al., 2012) by enhancing or decreasing their mobility and therefore their environmental hazard (Sahuquillo, 2003).

Early in history, water bodies became pathways for trade, and engineering works have been regularly carried out to improve the flow for navigation, and the safety of territories from flooding. Nowadays, the diffuse problem of sediment contamination and the lack of standardized regulations, cause serious problems to the hydraulic security of a territory (Stephens et al., 2001b) and to the navigability of waterways (Hartley and Dickinson, 2010).

The maintenance of the water level in rivers and reservoirs, and the dredging of the surplus of sediments, are in fact essential to maintain the equilibrium of the territory. On the other hand, the necessity to preserve the environmental health and to reduce the cost of dredging operations, induces scientists and local authorities to study adequate strategies for sediment risk assessment and for preventing sediment contamination.

### **1.3.2. Marine and brackish systems**

The concept that sediments in shallow water environments are capable of supporting rooted plants, and undergo transformation and horizon differentiation, has led soil scientists to consider the hypothesis of a subaqueous pedogenetic process (Demas and Rabenhorst, 1999; Ellis et al., 2002).

Demas and Rabenhorst (1999), in fact, found that, in submerged subaqueous environments, soils may develop similarly to subaerial terrestrial ones. In these contexts, it has been demonstrated that the presence of buried horizons, the accumulation of biogenic  $\text{CaCO}_3$ , the presence of benthic faunal and of organic components, can be considered common **pedogenic additions** (Barko et al., 1991; Demas and Rabenhorst, 1999). Similarly to some subaerial pedons, pedogenetic **losses** of nutrients can be observed through the distribution of organic carbon, which usually decreases with depth along the soil profile. In both systems, in fact, the mineralization

of organic carbon occurs mostly thanks to the microbial metabolism, even if different degradation processes can be recognized (Roden, 2004; Vodyanitskii and Shoba, 2014). The microbial biomass characterization, its enzymatic production and its metabolic path, strongly contribute to **bioturbation processes**, promoting oxygen diffusion or anoxic transformations along the soil profile. Examples of **transfers** include accumulations and depletions of iron and manganese species, diffusion and bioturbation from shellfish and worms (Fanning and Fanning, 1989), which promote soil **horizons differentiation** (Fenchel and Riedl, 1970). In many coastal environments, such as estuaries, coastal wetlands and lagoons, soils may develop under permanently submerged conditions (*subaqueous soils*, Demas and Rabenhorst, 2001). On the other hand, *hydromorphic or hydric soils* develop under partial or provisional water saturation conditions (Federal Register, July 13, 1994; Reddy and DeLaume, 2008) and are characterized by the continuous wetting and drying of soil horizons, and by the alternation of aerobic and anaerobic processes which strongly affect soil pedogenesis (Demas and Rabenhorst, 2001),

The presence of a saline water gradient, the alternation of freshwater and saltwater aquifer and the tide oscillation level, allow the evolution of particular ecosystems where the development of soil and vegetation patterns is strongly linked to the time of submergence, oxygen diffusion mechanisms, and high salinity levels (Ding et al., 2010; Zuo et al., 2012).

The high ecological value of these environments is worldwide recognized, and ranges from regulation of the bio-geo-chemical cycles of nutrients and trace elements, protection of water quality, biodiversity promotion and conservation, fish farming, recreation and many other ecosystem services (Barbier et al., 2011; de Groot et al., 2012).

Despite their values, erosion processes of the coastal area, subsidence and saline intrusion are globally threatening these fragile environments, and changes of both climate conditions and hydrological regimes deeply influence their evolution and health (Halpern et al., 2008; Lotze et al., 2006; Worm et al., 2006).

To study the relationship between subaqueous and hydromorphic soil, or between soils features, vegetation pattern and morphological characters, offers a unique opportunity to increase the knowledge of the ecosystem dynamics, thus to protect these fragile environments and devise strategies for the sustainable management of water and coastal resources (Erich and Drohan, 2012; Surabian, 2007).

## 1.4. THE AIM OF THE THESIS

The physicochemical interaction between water, sediment and soil deeply influence the formation and development of the ecosystem. In this research, different freshwater, brackish and saline subaqueous environments of Northern Italy were investigated to analyze the physicochemical processes which occur at the interface between water and sediments, as well as the effects of soil submergence on soil development.

In the first part of the thesis, a freshwater system (Reno river basin, Northern Italy) was chosen as a study area to explore the physicochemical quality of water and sediments with the aim to:

- highlight how the quality of water affects the sediment contamination;
- assess the risk hazard of heavy metals in both wet and dry sediments by comparing different techniques;
- test new eco-friendly techniques for water remediation and for the protection of sediment contamination.

In the second part of the work, different brackish and saline systems were chosen as study areas to evaluate the effect of water saturation on soil-forming processes and on ecosystem characterization.

In a brackish system (San Vitale park, Northern Italy), some soil sequences were traced from the subaqueous to the hydromorphic environment with the aim to:

- verify the hypothesis of a *soil continuum* from a subaqueous to an hydromorphic environment;
- highlight how the saline water intrusion or surfacing influences the soil development and properties;
- define the common features, the physicochemical variables, and the pedogenetic processes which characterized subaqueous and hydromorphic pedons.

In a saline system (Grado lagoon, Northern Italy), soils from different saltmarshes were collected according to their prevalent vegetation cover with the aim to:

- verify the presence of features, physicochemical variables, and pedogenetic processes which characterized subaqueous and hydromorphic pedons;
- highlight how the tide oscillation influence the soil development and properties;
- define which variables better describe the relationship between soil development, tide oscillation and vegetation cover in lagoon systems.

## 1.5. REFERENCES

- Akcil, A., Erust, C., Ozdemiroglu, S., Fonti, V., Beolchini, F., 2014. A review of approaches and techniques used in aquatic contaminated sediments: metal removal and stabilization by chemical and biotechnological processes. *J. Clean. Prod.* 86, 24–36. doi:10.1016/j.jclepro.2014.08.009
- Apitz, S.E., Power, E.A., 2002. From risk assessment to sediment management an international perspective. *J. Soils Sediments* 2, 61–66. doi:10.1007/BF02987872
- Asa, S.C., Rath, P., Panda, U.C., Parhi, P.K., Bramha, S., 2013. Application of sequential leaching, risk indices and multivariate statistics to evaluate heavy metal contamination of estuarine sediments: Dhamara Estuary, East Coast of India. *Environ. Monit. Assess.* 185, 6719–37. doi:10.1007/s10661-013-3060-3
- Balduff, D.M., 2007. Pedogenesis, inventory, and utilization of subaqueous soils in Chincoteague Bay, Maryland. University of Maryland.
- Barbier, E.B., Hacker, S.D., Kennedy, C., Koch, E.W., Stier, A.C., Silliman, B.R., 2011. The value of estuarine and coastal ecosystem services. *Ecol. Monogr.* 81, 169–193. doi:10.1890/10-1510.1
- Barko, J.W., Gunnison, D., Carpenter, S.R., 1991. Sediment interactions with submersed macrophyte growth and community dynamics. *Aquat. Bot.* 41, 41–65. doi:10.1016/0304-3770(91)90038-7
- Bat, L., Raffaelli, D., 1998. Sediment toxicity testing: a bioassay approach using the amphipod *Corophium volutator* and the polychaete *Arenicola marina*. *J. Exp. Mar. Bio. Ecol.* 226, 217–239. doi:10.1016/S0022-0981(97)00249-9
- Bianchini, G., Natali, C., Giuseppe, D., Beccaluva, L., 2012. Heavy metals in soils and sedimentary deposits of the Padanian Plain (Ferrara, Northern Italy): characterisation and biomonitoring. *J. Soils Sediments* 12, 1145–1153. doi:10.1007/s11368-012-0538-5
- Bland, W., Rolls, D., 1998. *Weathering: An Introduction to the Scientific Principles*. Routledge.
- Bouwer, H., 1978. *Groundwater Hydrology*. McGraw-Hil, New York.
- Bouwer, H., 2000. Integrated water management: emerging issues and challenges. *Agric. Water Manag.* 45, 217–228. doi:10.1016/S0378-3774(00)00092-5
- Bradl, H.B., 2004. Adsorption of heavy metal ions on soils and soils constituents. *J. Colloid Interface Sci.* 277, 1–18. doi:10.1016/j.jcis.2004.04.005
- Bradley, M.P., Stolt, M.H., 2003. Subaqueous Soil-Landscape Relationships in a Rhode Island Estuary. *Soil Sci. Soc. Am. J.* 67, 1487. doi:10.2136/sssaj2003.1487

- Brinkman, R., 1970. Ferrollysis, a soil-forming process in hydromorphic conditions 0000. *Geoderma* 3, 199–206.
- Buscaroli, A., Zannoni, D., 2010. Influence of ground water on soil salinity in the San Vitale Pinewood (Ravenna - Italy). *Agrochimica* 5, 303–320.
- Carlton, C., Dalla Valle, M., Marcomini, a., 2004. Regression models to predict water–soil heavy metals partition coefficients in risk assessment studies. *Environ. Pollut.* 127, 109–115. doi:10.1016/S0269-7491(03)00253-7
- Choueri, R.B., Cesar, A., Abessa, D.M.S., Torres, R.J., Morais, R.D., Riba, I., Pereira, C.D.S., Nascimento, M.R.L., Mozeto, A.A., DelValls, T.A., 2009. Development of site-specific sediment quality guidelines for North and South Atlantic littoral zones: comparison against national and international sediment quality benchmarks. *J. Hazard. Mater.* 170, 320–31. doi:10.1016/j.jhazmat.2009.04.093
- Clark, M.W., Davies-mcconchie, F., Mcconchie, D., Birch, G.F., 2000. Selective chemical extraction and grainsize normalisation for environmental assessment of anoxic sediments: validation of an integrated procedure. *Sci. Total Environ.* 258, 149–170.
- Cowie, G., 2005. The biogeochemistry of Arabian Sea surficial sediments: A review of recent studies. *Prog. Oceanogr.* 65, 260–289. doi:10.1016/j.pocean.2005.03.003
- Crane, M., 2003. Proposed development of Sediment Quality Guidelines under the European Water Framework Directive: a critique. *Toxicol. Lett.* 142, 195–206. doi:10.1016/S0378-4274(03)00069-9
- De Groot, R., Brander, L., van der Ploeg, S., Costanza, R., Bernard, F., Braat, L., Christie, M., Crossman, N., Ghermandi, A., Hein, L., Hussain, S., Kumar, P., McVittie, A., Portela, R., Rodriguez, L.C., ten Brink, P., van Beukering, P., 2012. Global estimates of the value of ecosystems and their services in monetary units. *Ecosyst. Serv.* 1, 50–61. doi:10.1016/j.ecoser.2012.07.005
- Demas, G., Rabenhorst, M.C., 1999. Subaqueous Soils : Pedogenesis in a Submersed Environment. *Soil Sci. Soc. Am. J.* 63, 1250–1257.
- Demas, G.P., Rabenhorst, M.C., 2001. Factors of subaqueous soil formation: a system of quantitative pedology for submersed environments. *Geoderma* 102, 189–204. doi:10.1016/S0016-7061(00)00111-7
- Demas, G.P., Rabenhorst, M.C., Stevenson, J.C., Street, B., Hill, S., 1996. Subaqueous Soils: A Pedological Approach to the Study of Shallow-Water Habitats. *Estuaries* 19, 229. doi:10.2307/1352228
- Dent, D.L., Pons, L.J., 1995. A world perspective on acid sulphate soils. *Geoderma* 67, 263–276. doi:10.1016/0016-7061(95)00013-E
- Ding, W., Zhang, Y., Cai, Z., 2010. Impact of permanent inundation on methane emissions from a *Spartina alterniflora* coastal salt marsh. *Atmos. Environ.* 44, 3894–3900. doi:10.1016/j.atmosenv.2010.07.025

- Du Laing, G., Rinklebe, J., Vandecasteele, B., Meers, E., Tack, F.M.G., 2009. Trace metal behaviour in estuarine and riverine floodplain soils and sediments: a review. *Sci. Total Environ.* 407, 3972–85. doi:10.1016/j.scitotenv.2008.07.025
- Ellis, J., Cummings, V., Hewitt, J., Thrush, S., Norkko, A., 2002. Determining effects of suspended sediment on condition of a suspension feeding bivalve (*Atrina zelandica*): results of a survey, a laboratory experiment and a field transplant experiment. *J. Exp. Mar. Bio. Ecol.* 267, 147–174. doi:10.1016/S0022-0981(01)00355-0
- Erich, E., Drohan, P.J., 2012. Genesis of freshwater subaqueous soils following flooding of a subaerial landscape. *Geoderma* 179–180, 53–62. doi:10.1016/j.geoderma.2012.02.004
- European Sediment Research Network, 2004. Contaminated sediments in European river basins. SedNet.
- Fanning, D.S., Fanning, M.C.B., 1989. Soil: Morphology, genesis, and classification. John Wiley & Sons, New York.
- Farkas, A., Erratico, C., Viganò, L., 2007. Assessment of the environmental significance of heavy metal pollution in surficial sediments of the River Po. *Chemosphere* 68, 761–8. doi:10.1016/j.chemosphere.2006.12.099
- Fenchel, T.M., Riedl, R.J., 1970. The sulfide system: a new biotic community underneath the oxidized layer of marine sand bottoms. *Mar. Biol.* 7, 255–268. doi:10.1007/BF00367496
- Feng, M.-H., Shan, X.-Q., Zhang, S., Wen, B., 2005. A comparison of the rhizosphere-based method with DTPA, EDTA, CaCl<sub>2</sub>, and NaNO<sub>3</sub> extraction methods for prediction of bioavailability of metals in soil to barley. *Environ. Pollut.* 137, 231–40. doi:10.1016/j.envpol.2005.02.003
- Gedroiz, K.K., 1927. Soil-absorbing complex and the absorbed soil cations as a basis of genetic soil classification. *Nossov Agr. Expt. Sta. Paper* 38, 29 pp., Leningrad. Trans. by S.A. Waksman. (Papers on soil reaction, 1912-25.).
- Gismera, M.J., Lacal, J., da Silva, P., García, R., Teresa Sevilla, M., Procopio, J.R., 2004. Study of metal fractionation in river sediments. A comparison between kinetic and sequential extraction procedures. *Environ. Pollut.* 127, 175–182. doi:10.1016/j.envpol.2003.08.004
- Hall, K., Thorn, C., Sumner, P., 2012. On the persistence of “weathering.” *Geomorphology* 149–150, 1–10. doi:10.1016/j.geomorph.2011.12.024
- Halpern, B.S., Walbridge, S., Selkoe, K.A., Kappel, C. V, Micheli, F., D’Agrosa, C., Bruno, J.F., Casey, K.S., Ebert, C., Fox, H.E., Fujita, R., Heinemann, D., Lenihan, H.S., Madin, E.M.P., Perry, M.T., Selig, E.R., Spalding, M., Steneck, R., Watson, R., 2008. A global map of human impact on marine ecosystems. *Science* 319, 948–52. doi:10.1126/science.1149345
- Hanrahan, G., Casey, H., Worsfold, P.J., 2005. Encyclopedia of Analytical Science, Encyclopedia of Analytical Science. Elsevier. doi:10.1016/B0-12-369397-7/00655-5



- Hartley, W., Dickinson, N.M., 2010. Exposure of an anoxic and contaminated canal sediment: mobility of metal(loid)s. *Environ. Pollut.* 158, 649–57. doi:10.1016/j.envpol.2009.10.030
- Ho, H.H., Swennen, R., Cappuyns, V., Vassilieva, E., Van Gerven, T., Tran, T. Van, 2012. Potential release of selected trace elements (As, Cd, Cu, Mn, Pb and Zn) from sediments in Cam River-mouth (Vietnam) under influence of pH and oxidation. *Sci. Total Environ.* 435-436, 487–98. doi:10.1016/j.scitotenv.2012.07.048
- Hu, Y., Schmidhalter, U., 2005. Drought and salinity: A comparison of their effects on mineral nutrition of plants. *J. Plant Nutr. Soil Sci.* 168, 541–549. doi:10.1002/jpln.200420516
- Jensen, K., Revsbech, N.P., Nielsen, L.P., 1993. Microscale distribution of nitrification activity in sediment determined with a shielded microsensor for nitrate. *Appl. Environ. Microbiol.* 59, 3287–96.
- Kao, S.J., Horng, C.-S., Roberts, A.P., Liu, K.-K., 2004. Carbon–sulfur–iron relationships in sedimentary rocks from southwestern Taiwan: influence of geochemical environment on greigite and pyrrhotite formation. *Chem. Geol.* 203, 153–168. doi:10.1016/j.chemgeo.2003.09.007
- Kibblewhite, M.G., Miko, L., Montanarella, L., 2012. Legal frameworks for soil protection: current development and technical information requirements. *Curr. Opin. Environ. Sustain.* 4, 573–577. doi:10.1016/j.cosust.2012.08.001
- Krairapanond, N., DeLaune, R.D., Patrick, W.H., 1992. Distribution of organic and reduced sulfur forms in marsh soils of coastal Louisiana. *Org. Geochem.* 18, 489–500. doi:10.1016/0146-6380(92)90112-B
- Krumbein, W.C., Sloss, L.L., 1951. *Stratigraphy and Sedimentation*, Geological Journal. W. H. Freeman & Co, San Francisco. doi:10.1002/gj.3350010110
- Lorenzen, J., Larsen, L.H., Kjar, T., Revsbech, N.-P., 1998. Biosensor Determination of the Microscale Distribution of Nitrate, Nitrate Assimilation, Nitrification, and Denitrification in a Diatom-Inhabited Freshwater Sediment. *Appl. Environ. Microbiol.* 64, 3264–3269.
- Lotze, H.K., Lenihan, H.S., Bourque, B.J., Bradbury, R.H., Cooke, R.G., Kay, M.C., Kidwell, S.M., Kirby, M.X., Peterson, C.H., Jackson, J.B.C., 2006. Depletion, degradation, and recovery potential of estuaries and coastal seas. *Science* 312, 1806–9. doi:10.1126/science.1128035
- Meyer, R.L., Kjaer, T., Revsbech, N.P., 2001. Use of NO<sub>x</sub>- microsensors to estimate the activity of sediment nitrification and NO<sub>x</sub>- consumption along an estuarine salinity, nitrate, and light gradient. *Aquat. Microb. Ecol.* 26, 181–193.
- Miniero, R., Dellatte, E., Lupi, C., Di, A., Superiore, I., 2005. Problematiche sperimentali inerenti la conduzione di saggi biotossicologici sui sedimenti. *Ann Ist Super Sanità* 41, 381–387.
- Moses, C., Robinson, D., Barlow, J., 2014. Methods for measuring rock surface weathering and erosion: A critical review. *Earth-Science Rev.* 135, 141–161. doi:10.1016/j.earscirev.2014.04.006

- Mukundan, R., Pradhanang, S.M., Schneiderman, E.M., Pierson, D.C., Anandhi, A., Zion, M.S., Matonse, A.H., Lounsbury, D.G., Steenhuis, T.S., 2013. Suspended sediment source areas and future climate impact on soil erosion and sediment yield in a New York City water supply watershed, USA. *Geomorphology* 183, 110–119. doi:10.1016/j.geomorph.2012.06.021
- Mulligan, C.N., Yong, R.N., Gibbs, B.F., 2001. An evaluation of technologies for the heavy metal remediation of dredged sediments. *J. Hazard. Mater.* 85, 145–163. doi:10.1016/S0304-3894(01)00226-6
- Munch, J.C., Hillebrand, T., Ottow, J.C.G., 1978. Transformations in the Fe<sup>o</sup>/Fe<sup>d</sup> ratio of pedogenic iron oxides affected by iron-reducing bacteria. *Can. J. Soil Sci.* 58, 475–486. doi:10.4141/cjss78-054
- O'Day, P.A., Rivera, N., Root, R., Carroll, S.A., 2004. X-ray absorption spectroscopic study of Fe reference compounds for the analysis of natural sediments. *Am. Mineral.* 89, 572–585.
- Osher, L.J., Flannagan, C.T., 2007. Soil/Landscape Relationships in a Mesotidal Maine Estuary. *Soil Sci. Soc. Am. J.* 71, 1323. doi:10.2136/sssaj2006.0224
- Owens, P.N., Batalla, R.J., 2003. A first attempt to approximate Europe ' s sediment budget.
- Payne, M.K., 2007. Landscape-level assessment of subaqueous soils and water quality in shallow embayments in southern New England. University of Rhode Island.
- Pejman, A.H., Bidhendi, G.R.N., Karbassi, A.R., Mehrdadi, N., Bidhendi, M.E., 2009. Evaluation of spatial and seasonal variations in surface water quality using multivariate statistical techniques. *Int. J. Environ. Sci. Technol.* 6, 467–476. doi:10.1007/BF03326086
- Peng, J.-F., Song, Y.-H., Yuan, P., Cui, X.-Y., Qiu, G.-L., 2009. The remediation of heavy metals contaminated sediment. *J. Hazard. Mater.* 161, 633–40. doi:10.1016/j.jhazmat.2008.04.061
- Poulton, S., Canfield, D., 2005. Development of a sequential extraction procedure for iron: implications for iron partitioning in continentally derived particulates. *Chem. Geol.* 214, 209–221. doi:10.1016/j.chemgeo.2004.09.003
- Prica, M., Dalmacija, B., Dalmacija, M., Agbaba, J., Krcmar, D., Trickovic, J., Karlovic, E., 2010. Changes in metal availability during sediment oxidation and the correlation with the immobilization potential. *Ecotoxicol. Environ. Saf.* 73, 1370–7. doi:10.1016/j.ecoenv.2010.06.014
- Rao, C.R., Sahuquillo, A., Lopez Sanchez, J.F., 2008. A review of the different methods applied in environmental geochemistry for single and sequential extraction of trace elements in soils and related materials. *Water Air Soil Pollut.* 189, 291–333.
- Reed, B.E., Matsumoto, M.R., 1993. Modeling CD adsorption in single and binary adsorbent (PAC) systems. *J. Environ. Eng.* 119, 332–348.

- Reddy, R. K., DeLaume, D., 2008. *Biochemistry of wetlands. Science and applications*. Taylor & Francis.
- Roden, E.E., 2004. Analysis of long-term bacterial vs. chemical Fe(III) oxide reduction kinetics. *Geochim. Cosmochim. Acta* 68, 3205–3216. doi:10.1016/j.gca.2004.03.028
- Sahuquillo, A., 2003. Overview of the use of leaching/extraction tests for risk assessment of trace metals in contaminated soils and sediments. *TrAC Trends Anal. Chem.* 22, 152–159. doi:10.1016/S0165-9936(03)00303-0
- Schaetzl, R.J., Anderson, S., 2005. *Soils: Genesis and Geomorphology*. Cambridge University Press.
- Schwarzenbach, R.P., Escher, B.I., Fenner, K., Hofstetter, T.B., Johnson, C.A., von Gunten, U., Wehrli, B., 2006. The challenge of micropollutants in aquatic systems. *Science* (80-. ). 313, 1072–7. doi:10.1126/science.1127291
- Shannon, R.D., White, J.R., 1991. The selectivity of a sequential extraction procedure for the determination of iron oxyhydroxides and iron sulfides in lake sediments. *Biogeochemistry* 14, 193–208. doi:10.1007/BF00000807
- Shrestha, S., Kazama, F., 2007. Assessment of surface water quality using multivariate statistical techniques: A case study of the Fuji river basin, Japan. *Environ. Model. Softw.* 22, 464–475. doi:10.1016/j.envsoft.2006.02.001
- Soil Survey Staff, 1999. *Soil Taxonomy. A basic System of Soil Classification for Making and Interpreting Soil Surveys*, 2nd ed. United States Department of Agriculture.
- Soil Survey Staff, 2010. *Keys to Soil Taxonomy*, 11th ed. United States Department of Agriculture, Natural Resources Conservation Service.
- Stephens, S.R., Alloway, B.J., Parker, a, Carter, J.E., Hodson, M.E., 2001. Changes in the leachability of metals from dredged canal sediments during drying and oxidation. *Environ. Pollut.* 114, 407–13.
- Surabian, D.A., 2007. Moorings: An Interpretation from the Coastal Zone Soil Survey of Little Narragansett Bay , Connecticut and Rhode Island 92, 90–92.
- Taylor, K.G., Owens, P.N., 2009. Sediments in urban river basins: a review of sediment–contaminant dynamics in an environmental system conditioned by human activities. *J. Soils Sediments* 9, 281–303. doi:10.1007/s11368-009-0103-z
- Thompson, A., Chadwick, O. a., Rancourt, D.G., Chorover, J., 2006. Iron-oxide crystallinity increases during soil redox oscillations. *Geochim. Cosmochim. Acta* 70, 1710–1727. doi:10.1016/j.gca.2005.12.005
- Van Ranst, E., Dumon, M., Tolossa, A.R., Cornelis, J.-T., Stoops, G., Vandenberghe, R.E., Deckers, J., 2011. Revisiting ferrollysis processes in the formation of Planosols for rationalizing the soils with stagnic properties in WRB. *Geoderma* 163, 265–274. doi:10.1016/j.geoderma.2011.05.002
- Vandieken, V., Niko Finke, N., Jørgensen, B.B., 2006. Pathways of carbon oxidation in an Arctic fjord sediment (Svalbard) and isolation of psychrophilic and psychrotolerant Fe(III)-reducing bacteria. *Mar. Ecol. Prog. Ser.* 322, 29–41.

- Varol, M., 2011. Assessment of heavy metal contamination in sediments of the Tigris River (Turkey) using pollution indices and multivariate statistical techniques. *J. Hazard. Mater.* 195, 355–64. doi:10.1016/j.jhazmat.2011.08.051
- Varol, M., Şen, B., 2012. Assessment of nutrient and heavy metal contamination in surface water and sediments of the upper Tigris River, Turkey. *Catena* 92, 1–10. doi:10.1016/j.catena.2011.11.011
- Vepraskas, M.J., Craft, C.B., Richardson, J.L., 2000. *Wetland Soils: Genesis, Hydrology, Landscapes, and Classification*.
- Verstraeten, G., Poesen, J., 1999. The nature of small-scale flooding, muddy floods and retention pond sedimentation in central Belgium. *Geomorphology* 29, 275–292. doi:10.1016/S0169-555X(99)00020-3
- Viganò, L., Arillo, A., Buffagni, A., Camusso, M., Ciannarella, R., Crosa, G., Falugi, C., Galassi, S., Guzzella, L., Lopez, A., Mingazzini, M., Pagnotta, R., Patrolecco, L., Tartari, G., Valsecchi, S., 2003. Quality assessment of bed sediments of the Po River (Italy). *Water Res.* 37, 501–18. doi:10.1016/S0043-1354(02)00109-4
- Vodyanitskii, Y.N., Shoba, S.A., 2014. Disputable issues in interpreting the results of chemical extraction of iron compounds from soils. *Eurasian Soil Sci.* 47, 573–580. doi:10.1134/S106422931406009X
- Worm, B., Barbier, E.B., Beaumont, N., Duffy, J.E., Folke, C., Halpern, B.S., Jackson, J.B.C., Lotze, H.K., Micheli, F., Palumbi, S.R., Sala, E., Selkoe, K.A., Stachowicz, J.J., Watson, R., 2006. Impacts of biodiversity loss on ocean ecosystem services. *Science* 314, 787–90. doi:10.1126/science.1132294
- Wu, Y., Chen, J., 2012. Modeling of soil erosion and sediment transport in the East River Basin in southern China. *Sci. Total Environ.* 441, 159–68. doi:10.1016/j.scitotenv.2012.09.057
- Žilius, M., 2011. *Oxygen and nutrient exchange at the sediment-water interface in the eutrophic noreal lagoon (Baltic Sea)*. Klaipeda University.
- Zuo, P., Zhao, S., Liu, C., Wang, C., Liang, Y., 2012. Distribution of *Spartina* spp. along China's coast. *Ecol. Eng.* 40, 160–166. doi:10.1016/j.ecoleng.2011.12.014

# CHAPTER 2

## FRESHWATER SYSTEMS

*pp.*

2.	Freshwater systems: The Reno river basin.....	23
2.1.	The study area.....	24
2.2.	Materials and methods.....	25
2.2.1.	Sampling and experimental design.....	25
2.2.2.	Water physicochemical analysis.....	26
2.2.3.	Sediment physicochemical analysis.....	27
2.2.4.	Heavy metals partitioning.....	29
2.2.5.	Heavy metals sequential extraction.....	30
2.2.6.	Data analysis.....	31
2.3.	Results.....	32
2.3.1.	Water physicochemical characterization.....	33
2.3.2.	Sediment physicochemical characterization.....	35
2.3.3.	The risk assessment of heavy metals.....	38
2.4.	Discussion.....	42
2.4.1.	Water and sediments characterization.....	42
2.4.2.	The risk assessment of heavy metals.....	43
2.5.	Conclusions.....	44
2.6.	References.....	46



## 2. FRESHWATER SYSTEMS: THE RENO RIVER BASIN

Plain areas are impacted by many urban and industrial settlements and superficial waters are often affected by human pressure. With increasing of erosion and runoff processes on superficial waters, natural and anthropic discharges, etc., the quality and safety of the ecosystem can deeply decrease (Varol and Şen, 2012). A high amount of soil loss by land erosion flows into watercourses, increasing dramatically the sediment accumulation in riverbeds, and the hydraulic safety of the territory can be deeply affected. Therefore periodical dredging operations and embankment building are needed to avoid rivers flooding (Stephens et al., 2001a). Sediments can be considered both a sink and a source of nutrients and pollutants (Reddy and DeLaume, 2008) and in view of resource recycling, the application of dredged sediments in the surrounding agricultural land is considered a sustainable practice if sediments are not polluted.

Heavy metals are some of the most harmful substances discharged in river systems and both chemical and physical factors influence their mobility and bioavailability, etc. (Carlon et al., 2004). Therefore the heavy metals risk assessment requires a comprehensive prediction of its potential adverse effects, which involves the study of metal speciation, partitioning, mobility and toxicity.

In this scenario, the objective of this work was (i) to monitor the ecological status of water and sediments in natural and artificial watercourses of the Reno river basin with respect to nutrients and heavy metals, (ii) to assess the heavy metals hazard of sediments by comparing different analytical procedures (e.g. the pseudo-total and available fraction) and different oxidation status (e.g. before and after dredging operations).

The following scientific production resulted from this research:

- Ferronato, C., Modesto, M., Stefanini, I., Vianello, G., Biavati, B., Antisari, L.V., 2013. Chemical and Microbiological Parameters in Fresh Water and Sediments to Evaluate the Pollution Risk in the Reno River Watershed (North Italy). J. Water Resour. Prot. 05, 458–468. doi:10.4236/jwarp.2013.54045
- Ferronato, C., Vittori Antisari, L., Modesto, M., Vianello, G., 2013. Speciation of Heavy metals at water-sediment interface. EQA – Environ. Qual. 10, 51–64. doi:10.6092/issn.2281-4485/3932
- Ferronato, C., Vianello, G., Vittori Antisari, L., 2014. The evolution of the Po Valley and Reno basin (North Italy) through the historical cartography: vicissitude of a land reclamation, in: Regional Symposium on Water, Wastewater and Environment: Traditions and Culture. pp. 741–752. ISBN: 97 8-960-538-921-5
- Ferronato, C., Vianello, G., Vittori Antisari, L., 2015. Heavy metals risk assessment after oxidation of dredged sediments through speciation and availability studies in the Reno river basin, Northern Italy. J. Soil and Sediments. doi: 10.1007/s11368-015-1096-4 - *in press*

## 2.1. STUDY AREA

The Reno river basin is located in the southern part of the Padanian Plain (Northern Italy) and covers an area of 4 930 km<sup>2</sup> between the Apennines and the beginning of the plain. The equilibrium between men and nature in this land has always been linked to the capacity of societies to improve the hydraulic safety and to sanitize the swamps, canalizing the water and managing the excess of transported sediments.

The land colonization of the Po Valley and of the area of the actual Reno river basin, has been characterized by a long term process of drainage operations, which began with the Etruscans and continued with the Romans (Surian and Rinaldi, 2003).

During the Middle Ages the plain was covered with swamps and bogs and all the ancient canalizations have been lost because of the lack of maintenance works; many attempts for water re-canalization were carried out during the following centuries by the Papal State, the Republic of Venice and Napoleon.

Only in the last centuries men have succeeded in building a huge network of artificial canals for water collection and drainage throughout all the plain, and could therefore definitively avoid the continuous flooding of the lands. The final reclamation was carried out thanks to manual excavation works and to the planning of engineering systems (Century XIX-XX) that gave rise to an extensive network of artificial canals. All these works have been fundamental for the management of the swamp and wetlands and their transformation into one of the most productive agricultural land of Italy (Ferronato et al., 2014).

Nevertheless the maintenance of the watercourses through dredging the excess of sediments is still one of the most important activity for the management of the territory equilibrium.

The Reno river basin nowadays is characterized by a network of artificial canals artificially embanked and used as collectors for different purposes, such as for draining water and wastewater from urban and industrial discharges, or for transporting water for irrigation purposes.

In the upper part of the basin watercourses usually have a natural bed and vegetated banks (Vittori Antisari et al., 2010), while in their lower reaches, rivers are characterized by high artificial embankments and cross urban and industrial/craft settlements with spread and point sources of pollution.

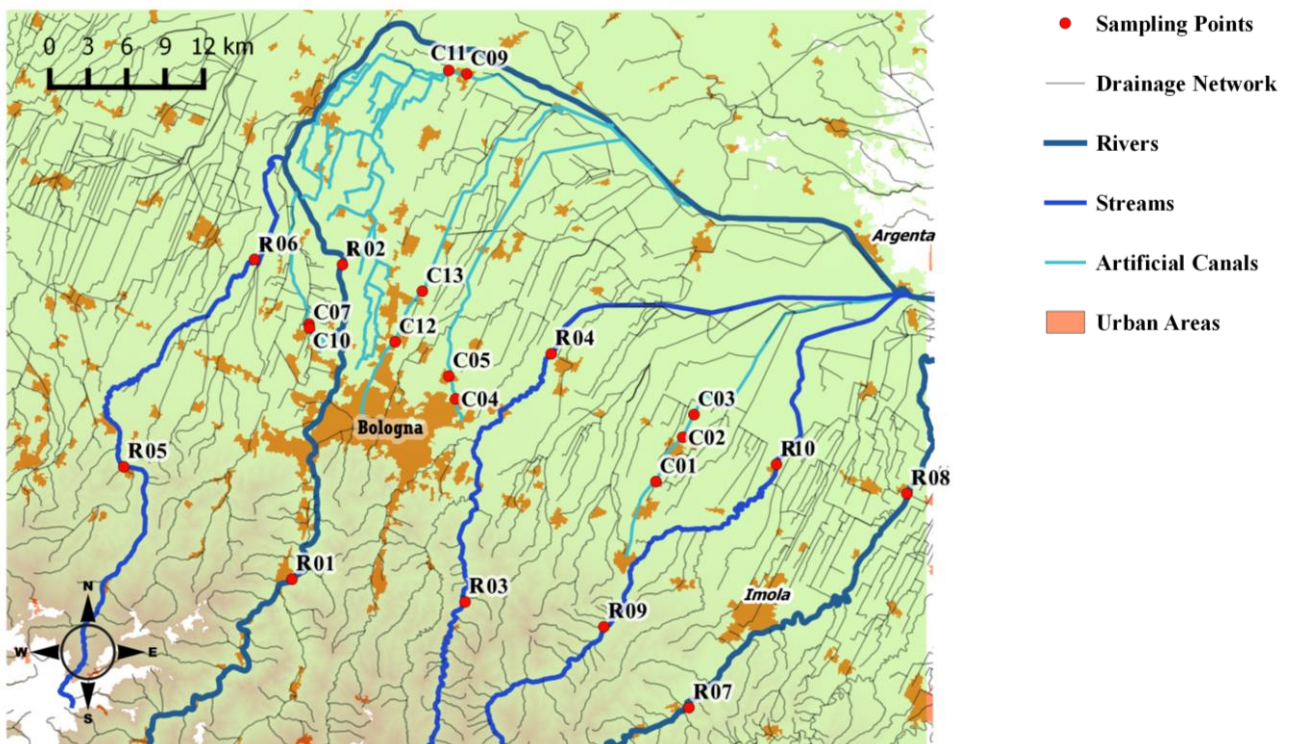


## 2.2. MATERIALS AND METHODS

### 2.2.1. Sampling and experimental design

The Reno River basin and the sampling sites of the studied area are presented in Figure 1.2 while the detailed localization of each site is reported in Appendix 1.

**Figure 2.1.** Reno river basin (Northern Italy) and localization of the monitoring network. Rivers (R) and Canals (C) are shown.



Five natural courses and five artificial canals were chosen in the Reno river basin for a monitoring survey and for assessing their environmental impact. Natural courses included the Reno and Santerno rivers and the Idice, Samoggia and Sillaro streams which cover the area of Bologna district (Figure 2.1). Samples were collected in upstream positions in the Apennine hilly region (R01-05), and downstream from some cities and industrial/craft settlements (R06-10).

Artificial courses included the Dosolo, Navile, Zenetta, Riolo and Medicina canals, which also flow into the Bologna district. Sampling sites were located in the plain area of the district upstream or downstream from

wastewater plants and urban/industrial/craft settlements (C01-05 and C06-13, upstream and downstream, respectively).

The monitoring survey of water and sediments was performed seasonally for 2 years (2012-2013) and the representative samples were collected in the middle section of the watercourse by lowering appropriate instruments connected with a rope down to the course from a bridge.

Water samples were collected with a steam container pre-washed in distilled water. 1 L water was transferred into clean glass bottles, sealed and kept refrigerated at 4° C until analysis. All bottles were pre-cleaned with diluted nitric acid and flushed with milli-Q water to remove trace elements before usage.

Superficial sediment samples (0-10 cm) from both rivers and canals were collected using a Van Veen grab (Idromambiente, Italy) connected to a rope. Three subsamples were collected from each site and subsequently homogenized in order to assure the representativeness of the sample. The collected materials were transferred into appropriate plastic boxes, covered with river/canal water in order to avoid oxidation processes, sealed and kept refrigerated at 4° C until analysis.

All analysis were performed in duplicate or triplicate and reference standard materials were used to verify the accuracy of the measures. The agreement for each datum was always below  $\pm 10\%$ .

### 2.2.2. Water physicochemical analysis

Water samples were processed within 24h from the sampling or appropriately stabilized for the sample conservation (D.M. 23/2000/ITA).

**Electrical conductivity** (*EC*), and **pH** were measured in the field with portable probes (Crison, Spain) and confirmed in laboratory (Compact Titrator, Crison, Spain).

The measurement of the **water alkalinity** was determined through the presence of  $\text{HCO}_3^-$  ions. The concentration of  $\text{HCO}_3^-$  ions was obtained by titrating 40 ml of non-filtrated water sample with 0.02N HCl at the end point of pH 4.4 (D.M. 23/2000/ITA, 2000). The volume of HCl used for titration was then related to the concentration of  $\text{HCO}_3^-$  by the following equation:

$$\text{HCO}_3^- (\text{mg L}^{-1}) = V * N * 1000 * 61 / C \quad [5]$$

where  $V$  was the volume of HCl used for the titration,  $N$  was the normality of the HCl used (0.02N),  $6I$  was the equivalent weight of the acid and  $C$  was the volume of the water sample used.

**Dissolved organic C and N** (DOC and DON respectively) were determined by TOC-L analyser (TOC-UV series, Shimadzu Instruments) on unfiltered samples. The TOC analyser adopts the 680°C combustion catalytic oxidation method, which achieves total combustion of samples by heating them in an oxygen-rich environment. The carbon dioxide generated by oxidation is detected using an infrared gas analyser (NDIR) and it has a range of detection between 0.4  $\mu\text{g L}^{-1}$  and 30,000  $\text{mg L}^{-1}$ . Through the combustion catalytic oxidation method it is possible to efficiently oxidize easily-decomposed compounds, low-molecular-weight organic compounds, but also hard-to-decompose insoluble and macromolecular organic compounds.

The quantification of both **macro and micro elements** was determined by *Inductive Coupled Plasma-Optical Emission Spectroscopy* (ICP-OES, Spectro Arcos, Germany). The methodology used inductively coupled plasma to produce excited atoms and ions from the sample solution, and an optic interface to record the electromagnetic radiation produced by the atoms. 50 ml was filtered on Wathman 42 within 24 h from the sampling and stabilized with 1:100 w:w suprapure  $\text{HNO}_3$  (Carlo Erba). ICP-OES measures were performed in triplicate and the instrument calibration was performed using international standard solution (BCR -610).

The concentrations of Na, Mg and Ca ions ( $\text{meq L}^{-1}$ ) were used to calculate the **Sodium Adsorption Rate**, as reported in the following equation:

$$\text{SAR} = \text{Na}^+ / [\sqrt{(\text{Ca}^{2+} + \text{Mg}^{2+})/2}] \quad [6]$$

### 2.2.3. Sediment analysis physicochemical analysis

Superficial sediments were wet sieved at 2 mm and subsequently split into two subsamples. The first subsample was maintained in wet conditions, covered with fresh water and stored at 4°C for maximum one week. A second subsample was air dried and stored at room temperature for further analysis.

**Soil particle size distribution** was determined by the pipette method after dispersion of the sample with a Na-hexametaphosphate solution (Gee and Bauder, 1986). 10g of dry sediment was used for the analysis and the dispersion time was 2h. The suspension was transferred into a graduated cylinder, brought to volume and

sealed with parafilm. After homogenization, the suspension was left undisturbed to sediment. The measurement of the different textual classes involved particles of  $D < 2\mu\text{m}$  (clay),  $2-50\mu\text{m}$  (silt) and  $50-2000\mu\text{m}$  (sand) and they were carried out according to the calculation of the sedimentation times. 10 ml of suspension was then collected in pre-weight quartz capsules at the appropriate time. The suspension was dried at  $105^\circ\text{C}$  for 24h and the dry weight was then related to the Sand, Silt or Clay percentage.

In accordance with the law of Stokes, the sedimentation times ( $\Gamma$ ) were calculated as a function of the particles diameter ( $D$ ) and density ( $\rho_s$ ), the depth of the liquid ( $s$ ), its density ( $\rho_l$ ) and viscosity ( $\eta$ ,  $10^{-3}$  Pas) and the constant of gravity ( $g$ ). The sedimentation time was then calculated for each fraction as follows:

$$\Gamma = (18s\eta) / D^2 (\rho_s - \rho_l) * g \quad [7]$$

The **pH** was determined in a 1:2.5 ratio w:v with distilled water. 10g of dry samples and 25 ml of distilled water were shaken for 2 h at room temperature and the measurement of pH was performed through a glass electrode (Compact Titrator, Crison, Spain). The suspension was filtered on Wathman 42 and the **electrical conductivity** ( $EC$ ) was subsequently detected on the supernatant with a glass electrode (Orion, Germany).

**Carbonate content** ( $\text{CaCO}_3$ ) was calculated by volumetric method, according to Loeppert and Suarez (1996). The carbonate content is determined by the acid dissolution of the carbonates and the measurement of the production of  $\text{CO}_2$ . 1 g of dry sample and 5ml of HCl 6N were used for the  $\text{CO}_2$  development and A Dietrich calcimeter was used for the volumetric quantification of the carbonates (MiPAF, 2000). The volume of  $\text{CO}_2$  produced by the reaction was related to the carbonate content as follows:

$$\text{CaCO}_2 \text{ (g kg}^{-1}\text{)} = V_0 * 0.0044655 * 1000 / m \quad [8]$$

where  $m$  was the mass of the sample (g),  $V_0$  was the volume of  $\text{CO}_2$  produced and 0.0044655 was the gas volumetric correction factor.

**Total organic carbon (TOC) and total nitrogen (TN)** were detected by *CHN elemental analyser* (EA 1110, Thermo Fisher, USA) by Dumas combustion. The method used the gas chromatography technique to detect the  $\text{CO}_2$  and  $\text{N}_2$  produced from the combustion of the sample at  $1100^\circ\text{C}$ . A further subsample of the dry fraction was finely ground with an agate mill and 5-15 mg of samples were weighed with thin capsules.

Samples were pre-treated firstly with 2M HCl and then with 1M HCl in order to dissolve all carbonates present and subsequently submitted to the analysis.

**Total content of K, P, Fe, Mn, Cd, Cr, Co, Cu, Ni, Pb and Zn** was detected by *Inductive Coupled Plasma – Optical Emission Spectroscopy* (ICP –OES, Spectro Arcos, Germany) as described in section 2.2.2.

Previously, samples were finely grounded and pre-treated with *aqua regia* (AR: suprapure HCl and HNO<sub>3</sub> 3:1 w:w) in a microwave digestion (Milestone 1200, USA). The mineralization cycle was performed for 3 min at 250 Watt, 4 min at 450 Watt and 3 minutes at 700 Watt. Reference materials (BCR-320R and BCR-142) and reagent blanks were used to check the accuracy of data and all analyses were performed in duplicate. Samples were brought to volume (20ml) and filtered with Wathman 42 before ICP-OES analysis.

#### **2.2.4. Heavy metals partitioning**

**The soluble fraction** of metals was determined on both dry and wet samples using MilliQ water according to Jung et al (2005). 10g of sediment were weighed in a polyethylene container with 100 ml of MilliQ water and shaken for 16h in order to reach the equilibrium of the extraction.

The suspension was then centrifuged at 10000 rpm for 15 min and filtrated by Whatman 42. The supernatant was stabilized with HNO<sub>3</sub> suprapure (Carlo Erba) at 1:100 w:w ratio and the content of heavy metals in solution was detected by ICP –OES as described in section 2.2.2 .

A reagent blank solution (MilliQ water) was also analysed for the correction of the measures.

The concentration of soluble metals was calculated through the coefficient of partitioning (log Kd) as follows:

$$\text{LogKd} = \text{Me}_{\text{tot}} / \text{Me}_{\text{sol}} \quad [9]$$

where  $\text{Me}_{\text{tot}}$  was the amount of pseudo-total metal detected in aqua regia (mg kg<sup>-1</sup>) while  $\text{Me}_{\text{sol}}$  was that obtained by water extraction (mg L<sup>-1</sup>) according to Jung et al. (2005).

**The available fraction** of metals for calcareous sediments was extracted with DTPA (diethylenetriamine pentacetic acid, pH 7.3) according to Lindsay and Norvell (1978). DTPA is a chelant agent which is widely used for the extraction of available metals in non-acidic soils (MiPAF, 2000).

10g of sediment (both wet and dry samples) were put in suspension with 20ml of DTPA and shaken for 2h in order to reach the equilibrium of the extraction. The suspension was then centrifuged at 10000 rpm for 15 min, filtrated by Whatman 42 and the supernatant was soon analysed by ICP-OES for heavy metals content as previously described (section 2.2.2).

A reagent blank solution (DTPA solution) was also analysed for the correction of the measures.

The available percentage of metals was subsequently calculated as the ratio between the DTPA metal fraction ( $\text{mg kg}^{-1}$ ) and its pseudo-total fraction ( $\text{mg kg}^{-1}$ ).

### **2.2.5. Heavy metals sequential extraction**

A Five-step sequential extraction was performed according to the procedure developed by Tessier et al (1979) and modified by Hartley and Dickinson (2010) and Ciceri et al. (2008). 1g of freeze-dry sediment was weighed in a nalgene polypropylene centrifuge tube. The procedure steps used were as follows:

1. (*Exchangeable phase*): 10 ml of 1M  $\text{MgCl}_2$  (pH 7) were added to the sediment samples and shaken for 60 min at room temperature. After the equilibration period, samples were centrifuged at 10000 rpm for 20 min and the supernatant was filtered through a cellulose filter (Wathman 42). 10ml of MilliQ water were added for few minutes in order to wash the sample from the residual reagent, centrifuged at 10000 rpm for 10 min and the supernatant discarded.
2. (*pH-dependent phase – Carbonate bond*): 20 ml of 1M  $\text{CH}_3\text{COONa}$  (pH 5) were added to the residue and shaken for 5h at room temperature. The supernatant was separated by centrifugation at 10000 rpm for 20 min, filtrated with Wathman 42. The residue was washed with MilliQ water as described for Step 1.
3. (*Reducible phase - Oxide and Hydroxide bond*): 20 ml of 0.04M  $\text{NH}_2\text{OH}\cdot\text{HCl}$  in 25%  $\text{CH}_3\text{COOH}$  w:v (pH 2) were added to the residue and the samples were shaken for 16h at room temperature as reported in Ciceri et al. (2008). The supernatant was separated by centrifugation and filtration and the residue was washed with MilliQ water as described for Step 1.
4. (*Oxidable phase - Sulphur and Organic bond*): 5ml of 30%  $\text{H}_2\text{O}_2$  + 3ml of 0.02M  $\text{HNO}_3$  were added to the residue and left to equilibrate for 1h at room temperature and 2h in a water bath at 85°C. A further aliquot

of 3ml of 30% H<sub>2</sub>O<sub>2</sub> was added to the mixture and heated for other 2h at 85°C. Samples were then left to cool down at room temperature; then 10ml of 1M CH<sub>3</sub>COONH<sub>4</sub> were added to the mixture and the samples were shaken for 30 min at room temperature. The supernatant was separated by centrifugation and filtration and the residue was washed with MilliQ water as described for Step 1.

5. (*Residual phase*): the residue from Step 4 was died at 60°C overnight and finally digested with aqua regia (6ml HCl + 2ml HNO<sub>3</sub>) using a microwave oven.

All the supernatants were analysed by ICP-OES for Cd, Cr, Cu, Mn, Fe, Ni, Pb, Zn content as previously described (Section 2.2.2). A reagent blank solution for each fraction was also analysed for the correction of the measures. All analyses were performed in triplicate by ICP-OES and each geochemical fraction was presented as percentage value on the total fraction found.

### 2.2.6. Data analysis

The ***geo-accumulation Index (I<sub>geo</sub>)*** was calculated to observe the anthropogenic contribution to the sediment contamination. The *I<sub>geo</sub>* was calculated for some metals as follows:

$$I_{geo} = \log_2 (C_n / 1.5 B_n) \quad [10]$$

where *C<sub>n</sub>* is the metal concentration of sediment determined using acqua regia, *B<sub>n</sub>* is the mean regional reference background values reported by the Emilia Romagna region soil services (determined in the study area only for Cu 57.6 mg kg<sup>-1</sup>, Zn 72.9 mg kg<sup>-1</sup>, Cr 144 mg kg<sup>-1</sup>, Ni 58.5 mg kg<sup>-1</sup>, Pb 48 mg kg<sup>-1</sup> according to Amorosi et al (2005) and 1.5 is the correction factor (Müller, 1969). The *I<sub>geo</sub>* was associated with a qualitative scale of pollution intensity according to Müller et al (1969) where samples were classified as:

- unpolluted (*I<sub>geo</sub>* ≤ 0),
- unpolluted to moderately polluted (0 ≤ *I<sub>geo</sub>* ≤ 1),
- moderately polluted (1 ≤ *I<sub>geo</sub>* ≤ 2),
- moderately to strongly polluted (2 ≤ *I<sub>geo</sub>* ≤ 3),
- strongly polluted (3 ≤ *I<sub>geo</sub>* ≤ 4),
- strongly to extremely polluted (4 ≤ *I<sub>geo</sub>* ≤ 5),
- extremely polluted (≥ 5).

All *statistical analyses* were performed with SPSS software 15.0.1 (IBM, Armonk, New York, USA) or with Statistica10 software (StatSoft, Tulsa, OK, USA).

*Descriptive statistics* involved the calculation of Mean, Minimum (min), Maximum (max) and Standard Deviation (SD) values and were performed to summarize the variability of data. The *analysis of variance* was performed with one-way ANOVA test and Fisher's least significance difference or Pearson correlation were performed as post-hoc tests.

*Hierarchical cluster analysis* was performed using squared euclidean distances and complete linkage method. Cluster analysis primary purpose is to assemble objects based on the characteristics they possess. The dendrogram provides a visual summary of the clustering processes, presenting a picture of the groups and their proximity, with a dramatic reduction in dimensionality of the original data

A *Principal Component Analysis (PCA)* was performed to reduce the number of variables and to detect the structure of the relationships between variables explaining as much as possible their variance using few composite variables (PC, Principal Components). Two Principal Components (PC1 and PC2) were extracted, and the Factor Loadings were used to highlight the most meaningful parameters of the data set, affording data reduction with minimum loss of original information. The statistical significance of each component was checked the analysis of the eigenvalues and of the explained variance for each component. Factor scores were used to display the groups of samples in a scatter plot, according to the two principal components that defined the relationship between variables.

A *Discriminant function analysis (DFA)* was performed with forward stepwise method to identify the continuous variables of the dataset, which could discriminate samples according to their membership to pre-define groups. In contrast to PCA and Cluster analysis, DFA provides a statistical classification of samples, grouping them according to their similar and it is performed with prior knowledge of membership of samples to a particular group. The statistical significance of each discriminant function (Function 1 and Function 2) was checked with Wilk's lambda test and the SCDC was used to rank the importance of each variable. The canonical scores of each sample was used to perform a canonical score plot and display the different groups of samples according to the two dimensions that better separate the groups.



## 2.3. RESULTS

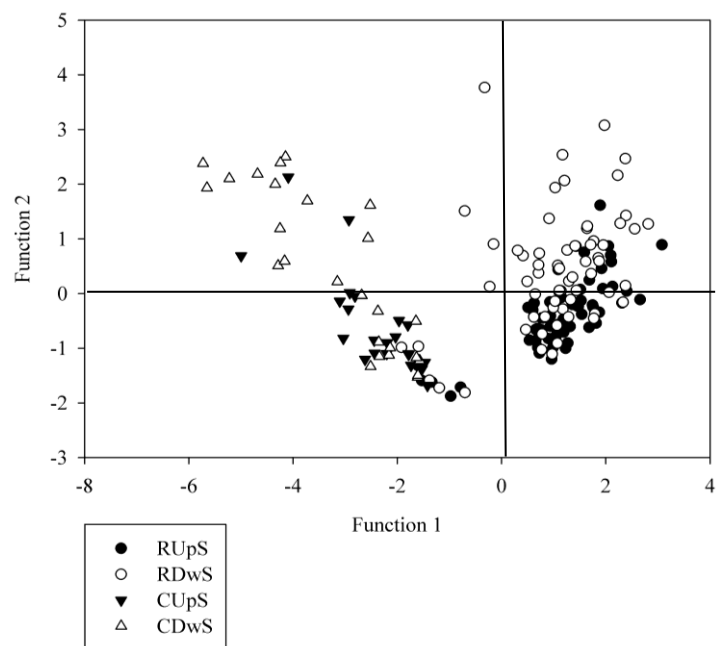
### 2.3.1. Water physicochemical characterization

The variability of all the physicochemical properties of water samples were evaluated through time and space. Since no significant differences were noticed over time within the watercourses, the samples were grouped according to their origin (rivers, R and canals, C) and to their spatial position (upstream, UpS and downstream, DwS). The summary of the main physicochemical properties of waters and the significant difference level between groups are shown in Appendix 2 and it showed that generally canals were significantly richer in nutrient contents than rivers.

With the aim to classify samples according to their origin and position (RUpS, RDwS, CUpS, CDwS). a Discriminant Function Analysis was performed on some chemical variables (e.g. SAR, pH, CE, Alkalinity and nutrients content), and both the summary of the standardized coefficients (SCDC) and the canonical scatter plot is shown in Figure 2.2.

**Figure 2.2:** Standardized coefficients (SCDC) and scatter plot of the Discriminant Function Analysis (DFA) based on the macro physicochemical properties of water samples. Only significant variables included in the model are shown.

	Function 1	Function 2
SAR	-2.16	0.34
PH	0,07	0.07
CE	-0.10	0.00
HCO <sub>3</sub>	-0.26	-0.14
DOM	-0.43	0.31
DON	-0.26	0.53
P	0.78	0.67
Mg	-0.15	-0.07
Na	2.02	-0.21
Eigenval	3.23	0.18
% Var	92.19	5.24



Wilks' Lambda approx: 0.18;  $p < 0.05$

The first two functions could explain 97.4% of the total variance and according to their significance level, SAR, DOM, DON and P had the highest discriminant power. These variables represented the positive SCDC (e.g. P) and the negative SCDC (e.g. SAR, DOM, DON) of Function 1, and they could discriminate the group of rivers waters from that of canals. The latter, in fact, were characterized by higher SAR levels and DOM concentration, while in rivers, a higher P amount could be found. Function 2 could explain only 5% of the total variance and could not be used to discriminate upstream from downstream waters.

Heavy metals were compared with the legislative limits established by Italian law for the reuse of water for agricultural purposes (D.lgs 152/2006) and for the definition of the “good ecological status” defined by the European Framework Directive (Directive 200/60/EC and D.lsg ITA/152/2006).

A summary of the heavy metals concentration in river and canal water during the monitoring survey is shown in Table 2.1.

**Table 2.1:** Summary of heavy metals concentration in river (a) and canal (b) waters according to their upstream (UpS) and downstream (DwS) position. Data are presented as  $\mu\text{g L}^{-1}$ .

<b>(a) Rivers</b>									
	UpS	DwS	UpS	DwS	UpS	DwS	UpS	DwS	ANOVA
	<i>Mean</i>		<i>Min</i>		<i>Max</i>		<i>SD</i>		
<b>Cu*</b>	11.0	49.9	0.6	1.3	134.0	430.0	17.6	83.8	0.0
<b>Zn</b>	9.4	11.0	0.1	3.2	25.5	30.6	6.9	7.9	0.5
<b>Cd</b>	2.2	3.3	0.8	0.7	4.5	13.2	1.5	3.8	0.2
<b>Co</b>	10.4	19.2	1.1	1.1	64.4	64.6	18.6	23.0	0.4
<b>Cr</b>	1.3	1.1	0.0	0.0	3.5	4.6	0.8	0.8	0.4
<b>Ni</b>	26.4	39.2	1.5	1.3	122.0	173.0	35.6	51.8	0.2
<b>Pb</b>	4.8	4.4	0.1	0.8	10.1	10.1	3.8	3.6	0.8

<b>(b) Canals</b>									
	UpS	DwS	UpS	DwS	UpS	DwS	UpS	DwS	ANOVA
	<i>Mean</i>		<i>Min</i>		<i>Max</i>		<i>SD</i>		
<b>Cu</b>	16.7	18.3	0.9	0.9	35.0	52.0	9.2	9.7	0.4
<b>Zn</b>	81.0	44.5	3.5	4.9	429.0	323.0	124.3	50.8	0.1
<b>Cd</b>	1.6	1.5	1.2	1.2	1.9	1.9	0.2	0.2	0.4
<b>Co</b>	14.4	11.3	0.5	1.7	102.0	64.8	24.6	15.7	0.6
<b>Cr</b>	2.5	1.8	1.1	0.9	5.7	2.6	1.3	0.5	0.1
<b>Ni</b>	6.0	7.4	1.7	1.7	29.6	21.9	6.2	5.4	0.3
<b>Pb</b>	9.0	10.4	3.6	3.9	22.5	19.7	4.7	4.4	0.3

\*=  $p < 0.05$

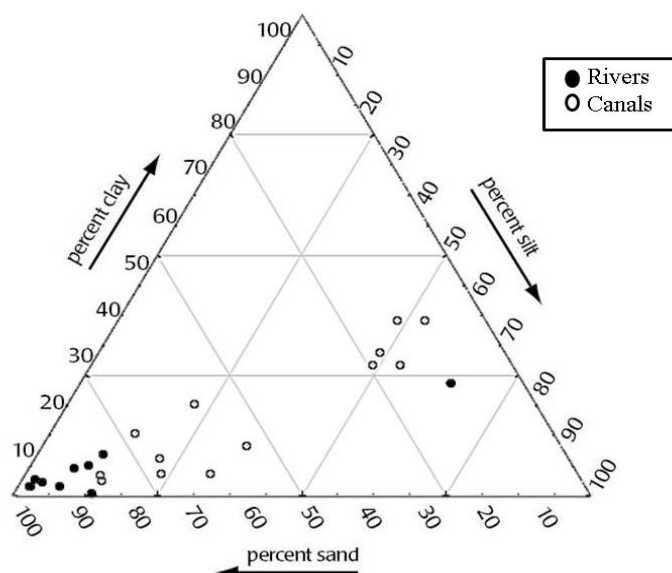
Both river and canal waters respected the limits of water reuse in agriculture while considering the threshold for the definition of the good ecological status (D.lsg.152/2006 ITA: 1, 50, 20 and  $10 \mu\text{g L}^{-1}$  for Cd, Cr, Ni and

Pb respectively), both rivers and canals presented an excess of Cd, Ni and Pb. Canal waters had higher concentrations of heavy metals than rivers ( $p < 0.05$ ) with the exception of Cd and Ni, which were higher in river waters ( $p < 0.05$ ). The increase of contamination from upstream to downstream was more evident in rivers than in canals but only Cu concentration was significantly different ( $p < 0.05$ ). Some extremely high values of Ni (122 and 173  $\mu\text{g L}^{-1}$  up and downstream respectively) and Cu (134 and 430  $\mu\text{g L}^{-1}$  up and downstream respectively) were noted in some hotspots in river waters as shown by the max values reported in the table. In canals, hotspots were recorded for Zn (429 and 323  $\mu\text{g L}^{-1}$  up and downstream respectively) and Co (102 and 64  $\mu\text{g L}^{-1}$  up and downstream respectively) but generally no significant differences were recorded among the samples.

### 2.3.2. Sediment physicochemical characterization

Sediment distribution according to their textural composition is presented in Figure 2.3.

**Figure 2.3:** Texture triangle of river and canal sediments.



The texture triangle showed that all river samples had a sandy or loamy-sand texture with the exception of one sample (F09, Sillaro Upstream), which had a silt-loam texture. Notably, canal texture mostly varied from loamy sand, sandy loam and sandy clay loam texture. while a small group of canal samples had a silty clay loam texture (P9 and P11, Riolo canal, P2 and P3, Medicina canal and P13, Navile canal).

The summary of the chemical properties of sediments from natural rivers (R) and artificial canals (C) in both upstream (UpS) and downstream (DwS) sites is shown in Appendix 3.

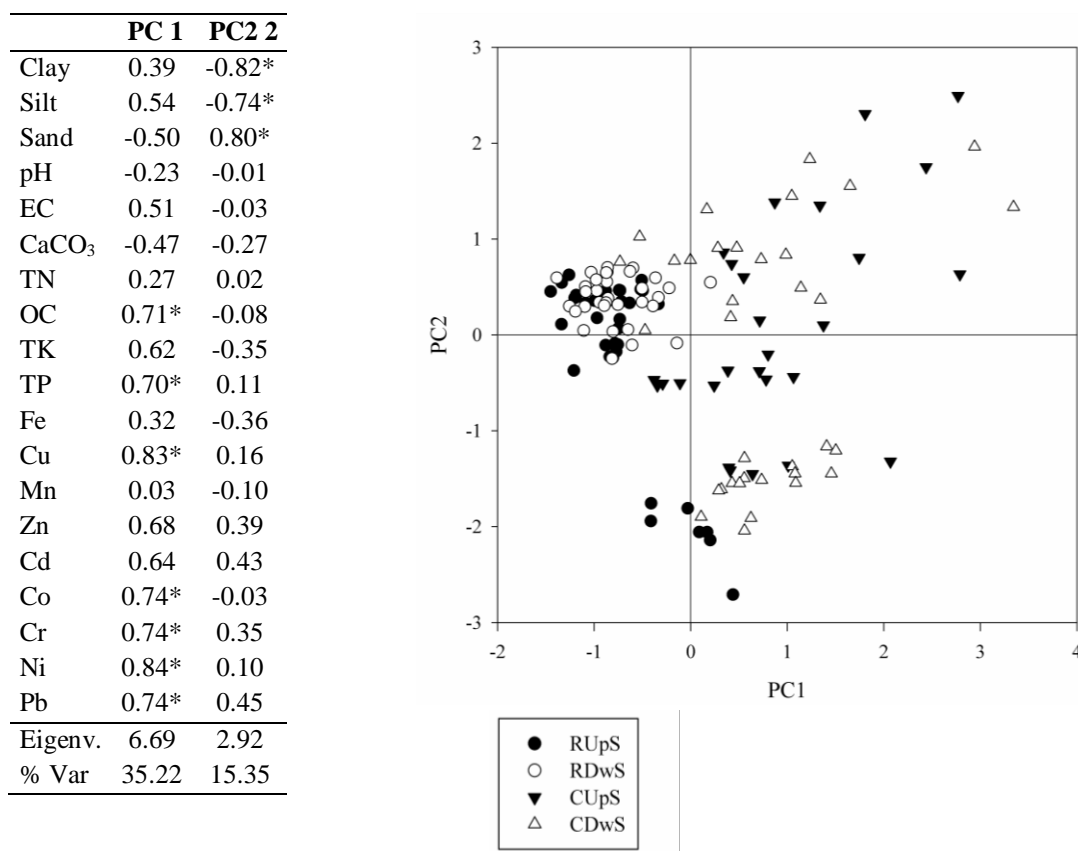
Artificial canal sediments were enriched by organic matter and nutrients content (e.g. TOC, TN and TP), while their pH values and total  $\text{CaCO}_3$  content were lower than those of rivers.

Heavy metals concentration increased from upstream to downstream and from rivers to canals as follows:  $\text{RUpS} < \text{RDwS} < \text{CUpS} < \text{CDwS}$ . Some hotspots were detected in river sediments of both UpS and DwS stations for Zn (189.1-192.2  $\text{mg kg}^{-1}$  UpS and DwS respectively), Cr (222.4-239.8  $\text{mg kg}^{-1}$  UpS and DwS respectively), Co (33.7-32.0  $\text{mg kg}^{-1}$  UpS and DwS respectively), Pb (171.8  $\text{mg kg}^{-1}$  in DwS); these values slightly exceed the Italian legislative thresholds of 150, 120, 20 and 100  $\text{mg kg}^{-1}$ , for Zn, Cr, Co and Pb, respectively. The artificial canal sediments showed mean values significantly higher than the thresholds for Cu (161.9-234  $\text{mg kg}^{-1}$  UpS and DwS respectively), Zn (595.9-862  $\text{mg kg}^{-1}$  UpS and DwS respectively), Cr (149.4-174.8  $\text{mg kg}^{-1}$  UpS and DwS respectively) and hotspots were found for all metals in both DwS and UpS sites, with the exception of Cd.

A Principal Component Analysis was applied to the physicochemical parameters in order to detect the structure of the relationships between variables explaining as much as possible their variance among the samples and to highlight the most meaningful variables which describe and characterize samples (Figure 2.4). The two components extracted could explain only 50% of the variance, however some interesting considerations could be carried out. PC1 represents the chemical composition of sediments, while PC2 represent the textural parameters. The factor scores displayed the samples association and could separate rivers from canals according to the PC1, but no separation was appreciated between Up and Downstream sampling points. As shown in the scatter plot, the PC1 could highlight that river sediments had very similar physicochemical characteristics and no dispersion, while canals presented higher variability and generally a higher content of both nutrients (e.g. OC and P) associated to some heavy metals (Cu, Co, Cr, Ni, Pb), as suggested by the factors loading.

Moreover, according to PC2, a small group of both river and canal sediments were separated due to their high content of silt and clay materials. This group consisted of specific sampling points (R09, C05 and C07) which displayed some differences in terms of texture and geochemical composition.

**Figure 2.4.** Factor loadings of Principal Component Analysis (PCA) and score plot obtained from the analysis.



\*= Factor loading >0.70

### 2.3.3. The risk assessment of heavy metals

Based on the physicochemical characterization of sediments during the monitoring survey (Appendix 3), the geo-accumulation index (*I<sub>geo</sub>*), was calculated to evaluate the anthropogenic enrichment of heavy metals on the superficial layers of sediments as shown in Table 2.2. The river stations were mainly unpolluted (*I<sub>geo</sub>*<0) for all the metals considered in both UpS and DwS but an increase of Zn pollution level was observed in the DwS stations after the urban settlements (unpolluted to moderately polluted).

The highest heavy metal pollution level in canal sediments ranged from moderate to strong/extreme (*I<sub>geo</sub>*>5) with Cu and Zn, while an unpolluted to moderate pollution level was observed for all the other metals. No marked difference was observed in UpS and DwS stations of the canal network.

**Table 2.2.** Geoaccumulation Index and qualitative classification in river and canal sediments, in upstream and downstream stations (Muller, 1969).

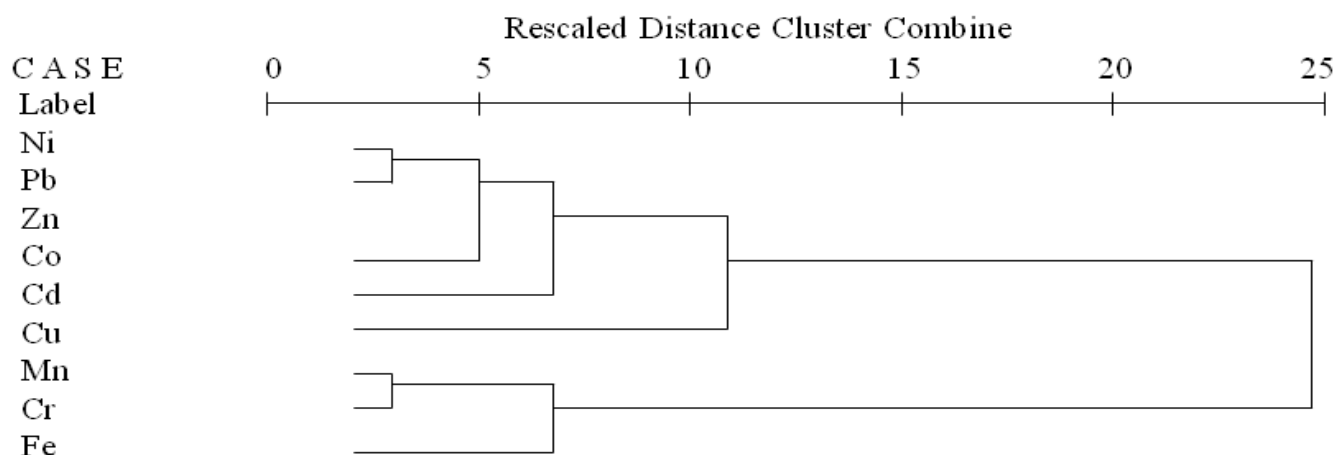
		Rivers		Canals		Rivers		Canals	
		UpS	DwS	UpS	DwS	UpS	DwS	UpS	DwS
Cu	mean			0.64	1.05				
	min			$\leq 0$	$\leq 0$				
	max	$\leq 0$	$\leq 0$	2.64	2.53	unpolluted	Unpolluted	moderate to strongly polluted	moderate to strongly polluted
	SD			0.91	0.80				
Zn	mean	$\leq 0$	$\leq 0$	2.06	1.98				
	min	$\leq 0$	$\leq 0$	$\leq 0$	0.26	unpolluted to moderately polluted	unpolluted to moderately polluted	moderate to extreme polluted	moderate to extreme polluted
	max	0.79	0.82	5.49	5.11				
	SD	0.67	0.73	1.64	1.25				
Cr	mean			0.44	0.51				
	min			$\leq 0$	$\leq 0$				
	max	$\leq 0$	$\leq 0$	0.88	0.81	unpolluted	unpolluted	unpolluted to moderately polluted	unpolluted to moderately polluted
	SD			0.68	0.69				
Ni	mean	$\leq 0$	$\leq 0$	0.02	$\leq 0$				
	min	$\leq 0$	$\leq 0$	$\leq 0$	$\leq 0$	unpolluted to moderately polluted	unpolluted to moderately polluted	unpolluted to moderately polluted	unpolluted to moderately polluted
	max	0.22	0.26	1.00	1.43				
	SD	0.61	0.63	0.58	0.67				
Pb	mean			0.01	0.09				
	min			$\leq 0$	$\leq 0$				
	max	$\leq 0$	$\leq 0$	2.35	1.53	unpolluted	unpolluted	unpolluted to moderately polluted	unpolluted to moderately polluted
	SD			1.18	0.76				

Heavy metals were extracted with different reagents with the aim to investigate their mobility, availability and affinity with the mineralogical phase of sediments before and after drying.

The coefficient  $\log K_d$  was used to describe the heavy metals partitioning through the water/sediment interface during the oxidation process of sediments after dredging. The lower the  $\log K_d$ , the higher was the solubility of the metal (Jung et al., 2005), and it ranged between 0 and 4.5 according to the kind of metal and its dry or wet condition. Generally the  $\log K_d$  was lower in canal than in river sediments and in dry conditions than in wet one. Nevertheless only Cu and Cd were significantly more soluble in dry conditions than in wet and no significant differences were found between UpS and DwS sites.

Cluster analysis was therefore performed to highlight similar behaviours of all heavy metals and two groups were identified, as shown in Figure. 2.5: the first was composed of Cd, Co, Cu, Zn, Ni and Pb and it was characterized by a  $\log K_d < 2.8$ , while the second group was formed by Fe, Mn and Cr. The latter always showed a  $\log K_d > 2.8$  in both wet and dry conditions.

**Figure 2.5.** Dendrogram obtained by cluster analysis of log (Kd) values.



The percentage of available fraction was performed by DTPA-extraction, which simulates the effect of metals solubility in the rhizosphere environment. The summary of sediments availability in wet and dry samples is shown in Table 2.3.

**Table 2.3.** Availability percentage of metals, determined by DTPA extraction of rivers and canals sediments in wet and dry samples. Data presented as percentage values of DTPA extract on the total fraction.

		Rivers					Canals				
		Wet		Dry		<i>p</i>	Wet		Dry		<i>p</i>
		Mean	SD	Mean	SD		Mean	SD	Mean	SD	
Cd	Up	nd	nd	nd	nd		36.84	32.5	14.51	6.5	
	Down	nd	nd	nd	nd		27.54	20.7	17.59	6.6	
Co	Up	1.35	0.6	0.52	0.4	*	2.47	1.3	1.41	1.7	
	Down	1.56	0.8	0.39	0.3		3.86	2.5	2.22	1.8	
Cr	Up	0.20	0.0	nd	nd		0.18	0.1	nd	nd	
	Down	0.23	0.1	nd	nd		0.14	0.0	nd	nd	
Cu	Up	5.27	7.1	9.26	6.2		4.37	4.0	16.68	5.2	**
	Down	6.96	9.7	15.98	17.3		3.07	3.7	14.89	7.6	
Fe	Up	0.08	0.1	0.07	0.0		0.39	0.2	0.23	0.2	*
	Down	0.40	0.5	0.12	0.1		0.74	0.4	0.34	0.2	
Mn	Up	0.70	0.6	0.54	0.4		5.06	4.4	2.12	2.7	*
	Down	1.37	1.5	0.58	0.3		3.26	3.1	1.94	1.5	
Ni	Up	1.07	1.1	0.92	0.7		2.12	1.0	2.41	1.7	
	Down	1.39	0.9	0.99	0.9		3.51	1.7	3.68	1.8	
Pb	Up	5.64	3.6	5.58	3.1		12.56	8.7	14.74	13.8	
	Down	9.75	5.3	10.09	5.9		8.17	5.9	13.01	5.6	
Zn	Up	1.60	0.8	2.69	1.8		11.09	11.2	32.15	28.0	*
	Down	2.61	2.0	4.15	2.9		11.09	9.3	46.71	40.2	

\* =  $p < 0.05$ ; \*\* =  $p < 0.001$

Generally, the mean values of most metals available fraction in wet sediments were slightly higher than those determined in dry ones.

On the contrary, high percentages of available Cu and Zn ( $p < 0.05$ ) were detected in dry sediments of artificial canals. In the latter, dry sediments released +14% of Cu and +28% of Zn while river sediments showed no significant differences between extraction conditions.

Notably, canal dry sediments released larger amounts of Pb than wet ones but the statistical difference was negligible ( $p > 0.05$ ).

The sequential extraction of heavy metals in dry sediment samples allowed to distinguish the affinity of each metal for the different mineralogical phases (exchangeable, carbonates, Fe/Mn oxides, organic/sulphides, residual) of both UpS and DwS sites in river and canal sediments. The histograms of the sequential extraction are shown in Figure 2.6.

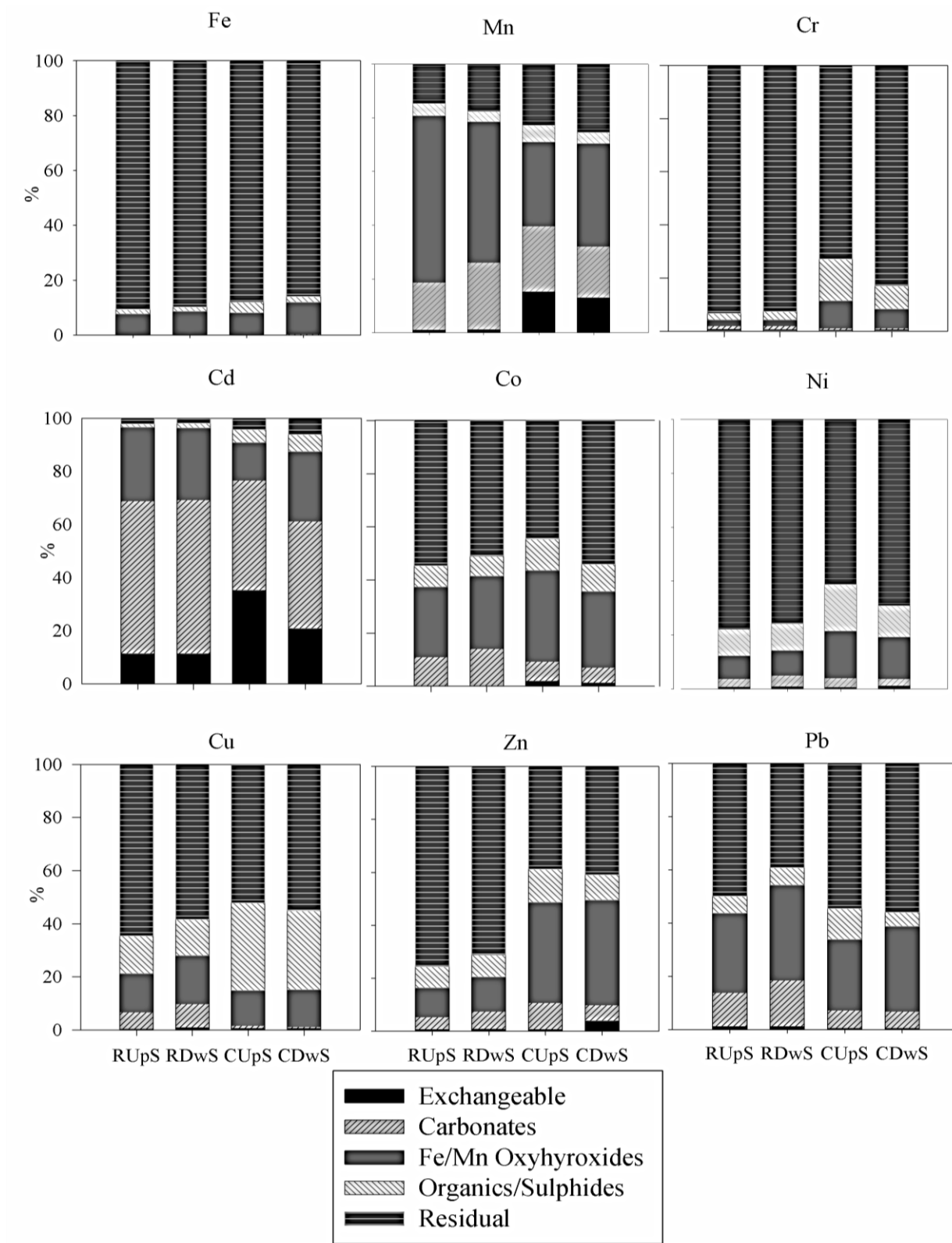
Generally, in river sediments, metals were mainly associated with the residual fraction. Iron was mainly detected in the residual phase of both rivers and canals, while Mn was mostly related to the exchangeable and carbonate-bound phase in canals and to Fe/Mn oxides in rivers.

High residual fraction characterized the Cr distribution in river sediments (92-93%), while a rise in oxide/hydroxide (15.8-8.7%) and sulphur/organic fractions (10.2-6.2%) was observed in canal sediments. Similarly, all the other studied metals showed a higher affinity for the labile and/or organic phases in canals than in rivers. This was true for Ni and Cu, which were mainly linked to the residual phase in rivers, and to the organic/sulphides phase in canals (9.8-17.1% for Ni and 33.1-29.8% for Cu in UpS-DwS respectively), and for Zn, which was mainly residual in rivers and highly affine with the oxide/hydroxide fraction in canals (37.8-39.4%).

On the contrary, Co and Pb bound on carbonates were higher in rivers than in canals. The distribution of Cd highlighted that a high amount of this metal was concentrated in the most labile phases, which includes the exchangeable phase (11% in rivers and 20-35% in canals), and the carbonate-bound phase (58% in rivers and 41-40% in canals).



**Figure 2.6.** Histograms of metals distribution between Exchangeable, Carbonate, Oxide/ Hydroxide bonds, Sulphur/ Organic bonds and Residual phase according to a five-step sequential extraction. Data are presented as % values.



## **2.4. DISCUSSION**

### **2.4.1. Water and sediments characterization**

Both river and canal water systems presented neutral-alkaline pH and a carbonate origin. The different chemical composition of water in rivers and canals was highlighted by the DFA, and it was shown that canal waters have higher nutrient content than that in rivers, due to the increase of run-off from the agricultural lands, discharges from the urban areas and other anthropogenic sources (Vittori Antisari et al., 2010). Considering the heavy metals load, from a legislative point of view, the waters of the Reno river basin are in agreement with the parameters for water reuse in agriculture while in sediments the pseudo total heavy metals often exceed the legislative threshold for the land disposal of dredged materials (D. lgs 152/2006). Their concentration and distribution, in fact, suggest a different pollution hazard in fluvial and canal ecosystems, characterized by some site-dependent hotspots in rivers and a heavy, widespread pollution in canals.

Sediments are deeply affected by a strong exchange dynamic with the water column (Du Laing et al., 2009). Texture, carbonates and organic C content are an important sink of nutrients, but they also represent some important controlling factors for heavy metals adsorption in sediments (Rubio et al., 1999). Fine-grained sediments, in fact, have a high surface area and ionic attraction capacity which increases the retention of both organic matter and heavy metals from the water column (Horowitz and Elrick, 1987; McCave, 1984).

The PCA analysis could explain only 50% of the total variance and this can be due to the moderate homogeneity of the samples population, as expected from sediments of the same origin. However, by analysing the distribution of the factor scores, river sediments formed a homogeneous group associated with sandy texture, which reduces the possibility of metals and nutrients to be adsorbed from the water column onto the sediments structure, while canal sediments displayed a high variability in terms of both textural parameters and nutrients (e.g. OC and P), which were associated with an accumulation of total Cu, Co, Cr, Ni and Pb.

The nutrients content in both systems represents an important resource for soil fertility that could be useful during land disposal, but the high concentration of heavy metals in the canals sediments prevents their reuse on agricultural soil and justifies their management as waste materials.

## 2.4.2. The risk assessment of heavy metals

The geoaccumulation index (*I<sub>geo</sub>*) and the Muller qualitative scale of pollution (Farkas et al., 2007; Müller, 1969) highlighted that the fluvial system is generally *unpolluted* whereas some hazardous points are observed in the artificial canal network: here *moderate to extreme* pollution levels are present (e.g from Cu and Zn).

The analysis of total metals concentration is an essential and rapid way to assess sediment quality from a legislative point of view, but gives no information about metals fractionation and mobility which are fundamental in such environments where redox conditions periodically change in dry seasons, or after dredging operations (Maes et al., 2003).

The analysis of metals log *K<sub>d</sub>* through cluster analysis highlighted a group of metals with high affinity with sediments (log *K<sub>d</sub>* ≥ 2.8, e.g. Fe, Mn, Cr), and another one with low affinity (log *K<sub>d</sub>* ≤ 2.8, e.g. Cu, Pb, Co, Ni, Zn, Cd) (Jung et al., 2005).

In the first group, it is interesting to note that the total Cr has a high affinity with sediments. According to this analysis, Cr is quickly immobilized in low soluble compounds and its environmental risk can be considered low. This result is also confirmed by the Cr low DTPA-extractable percentage and by its sequential extraction. In particular, the high Cr residual fraction of river sediments sequential extraction highlights the geogenic origin of Cr as reported in other studies on the Po Valley sediments and soils (Bianchini et al., 2012; Di Giuseppe et al., 2014).

The second cluster, Cu, Pb, Co, Ni, Zn, Cd was characterized by greater solubility and weak adsorption onto the sediment surface, suggesting their anthropogenic origin. These results are in agreement with both DTPA-extraction and fractionating studies.

The sequential extraction, for example, underlines that Cd is mainly retained by weak electrostatic interaction (e.g. exchangeable phase) or to a loosely bound phase (e.g. carbonate phase), and this result is also confirmed by the Cd low log *K<sub>d</sub>* mean value and its high DTPA-extractable percentage. These findings demonstrate that the pseudo-total concentration of Cd found in sediments is not sufficient to predict its environmental hazard, since Cd solubility and therefore its environmental hazard is high.

The enhancement of metals hazard was also detected for Cu, Ni, Pb and Zn according to the change from wet to dry status of sediments. In fact, both water and DTPA extractions showed that the mobility and therefore

the risk hazard of these metals is higher when sediments are dried after dredging than when they are submerged.

As confirmed by some authors (Borne et al., 2014; Maes et al., 2003), the dredging of submerged sediments leads to a rapid oxidation of organic matter and of the reductive sulfidic compounds, resulting in the increase of metals availability (Prica et al., 2010; Stephens et al., 2001a).

Sequential extraction highlights the strong affinity of Cu with organic matter which usually retains this and other metals (e.g. Ni, Zn) through chelation processes (Durand et al., 2004). As soon as sediments are dried, the oxidation of organic matter becomes faster and its structure less complex (Reddy and DeLaume, 2008), giving rise to the release of metals (Kashem and Singh, 2001; Stietiya and Wang, 2006). Therefore Cu environmental risk can seriously increase after sediment dredging .

In this study, the high affinity of Zn with carbonates and hydroxides in canal sediments (Dudka and Chlopecka, 1990; Stietiya and Wang, 2006) suggests that the mobility of this element is mainly controlled by pH-dependent mechanisms, rather than organic matter interaction.

In submerged environments exposed to the air, oxidation of sulfidic materials leads to a slight acidification of the system (Kazi et al., 2005), thus dissolving carbonates. When these processes occur, metal bound to carbonates and hydroxides can be easily released and intensify their environmental hazard.

## **2.5. CONCLUSION**

The monitoring of water and sediments in a natural system is fundamental to evaluate the quality of the ecosystem. This work has demonstrated that the analysis of sediments can give much more useful informations about the quality and the management of these natural resources than the analysis of waters. In fact, due to the carbonate origin of waters of the Reno river basin, and to their high pH values, most of the pollutants tend to precipitate or to be adsorbed into sediments.

The pseudo total concentration of metals in sediments of the Reno basin network shows that an important source of nutrients can be found in both river and canal beds. Conversely, an environmental hazard is observed in canal sediments, even if a different degree of pollution can be highlighted using different calculations (e.g. legislative limits or *Igeo*).

The investigations on metal availability suggests that the total metal fraction does not always represent the real environmental risk for these pollutants, as in the case of the high Cr amount, which is strongly linked to the sediment structure, or in the case of the low amount of Cd, which is actually present in soluble form. Moreover the availability of some metals (e.g. Cu, Pb and Zn) strongly changes when sediments oxidation occurs. In such a changing environment, it is more and more important to understand and predict the fate of metals as a function of redox processes and the use of partial and sequential dissolution techniques, in both wet and dry conditions, is strongly suggested for assessing the environmental hazard of dredged sediments. From an operative point of view the necessity to find eco-friendly techniques for sediment protection is highly recommended.

## 2.6. REFERENCES

- Amorosi, A., M. C. Centineo, M. L. Colalongo, and F. Fiorini. 2005. Millennial-scale depositional cycles from the Holocene of the Po Plain, Italy. *Marine Geology* 222-223:7–18.
- Bianchini, G., C. Natali, D. Giuseppe, and L. Beccaluva. 2012. Heavy metals in soils and sedimentary deposits of the Padanian Plain (Ferrara, Northern Italy): characterisation and biomonitoring. *Journal of Soils and Sediments* 12:1145–1153.
- Borne, K. E., E. a Fassman-Beck, and C. C. Tanner. 2014. Floating Treatment Wetland influences on the fate of metals in road runoff retention ponds. *Water research* 48:430–42.
- Carlón, C., M. Dalla Valle, and a. Marcomini. 2004. Regression models to predict water–soil heavy metals partition coefficients in risk assessment studies. *Environmental Pollution* 127:109–115.
- Ciceri, E., B. Giussani, A. Pozzi, C. Dossi, and S. Recchia. 2008. Problems in the application of the three-step BCR sequential extraction to low amounts of sediments: an alternative validated route. *Talanta* 76:621–6.
- D.M. 23/2000/ITA. 2000. Metodi ufficiali di analisi delle acque per uso agricolo e zootecnico. *Gazzetta Ufficiale* n 87, 13 aprile 2000. Franco Angeli.
- Dudka, S., and A. Chlopecka. 1990. Effect of solid-phase speciation on metal mobility and phytoavailability in sludge-amended soil. *Water, Air, and Soil Pollution* 51:153–160.
- Durand, C., V. Ruban, and A. Amblès. 2004. Mobility of trace metals in retention pond sediments. *Environmental technology* 25:881–8.
- Farkas, A., C. Erratico, and L. Viganò. 2007. Assessment of the environmental significance of heavy metal pollution in surficial sediments of the River Po. *Chemosphere* 68:761–8.
- Ferronato, C., G. Vianello, and L. Vittori Antisari. 2014. The evolution of the Po Valley and Reno basin (North Italy) through the historical cartography: vicissitude of a land reclamation. Pages 741–752 *Regional Symposium on Water, Wastewater and Environment: Traditions and Culture*.
- Gee, G. W., and J. W. Bauder. 1986. Methods of Soil Analysis: Part 1—Physical and Mineralogical Methods. Pages 383–411 *Methods of Soil Analysis: Part 1—Physical and Mineralogical Methods*. Soil Science Society of America, American Society of Agronomy.
- Di Giuseppe, D., L. Vittori Antisari, C. Ferronato, and G. Bianchini. 2014. New insights on mobility and bioavailability of heavy metals in soils of the Padanian alluvial plain (Ferrara Province, northern Italy). *Chemie der Erde - Geochemistry*.

- Hartley, W., and N. M. Dickinson. 2010. Exposure of an anoxic and contaminated canal sediment: mobility of metal(loid)s. *Environmental pollution (Barking, Essex : 1987)* 158:649–57.
- Horowitz, A. J., and K. A. Elrick. 1987. The relation of stream sediment surface area, grain size and composition to trace element chemistry. *Applied Geochemistry* 2:437–451.
- Jung, H.-B., S.-T. Yun, B. Mayer, S.-O. Kim, S.-S. Park, and P.-K. Lee. 2005. Transport and sediment–water partitioning of trace metals in acid mine drainage: an example from the abandoned Kwangyang Au–Ag mine area, South Korea. *Environmental Geology* 48:437–449.
- Kashem, M. A., and B. R. Singh. 2001. Metal availability in contaminated soils: I. Effects of flooding and organic matter on changes in Eh, pH and solubility of Cd, Ni and Zn. *Nutrient Cycling in Agroecosystems* 61:247–255.
- Kazi, T. G., M. K. Jamali, G. H. Kazi, M. B. Arain, H. I. Afridi, and A. Siddiqui. 2005. Evaluating the mobility of toxic metals in untreated industrial wastewater sludge using a BCR sequential extraction procedure and a leaching test. *Analytical and bioanalytical chemistry* 383:297–304.
- Du Laing, G., J. Rinklebe, B. Vandecasteele, E. Meers, and F. M. G. Tack. 2009. Trace metal behaviour in estuarine and riverine floodplain soils and sediments: a review. *The Science of the total environment* 407:3972–85.
- Lindsay, W. L., and W. A. Norvell. 1978. a DTPA soil test for zinc, iron, manganese and copper. *Soil Sci Soc Am* 42:421–428.
- Loeppert, R.H., Suarez, D.L., 1996. Carbonate and gypsum. In: Sparks, D.L. (Ed.), 532 *Method of Soil Analysis. Part 3, Chemical Methods*. SSSA and ASA, Madison, pp. 437–533 474. (n.d.). . USDA-ARS/UNL Faculty.
- Maes, a, M. Vanthuyne, P. Cauwenberg, and B. Engels. 2003. Metal partitioning in a sulfidic canal sediment: metal solubility as a function of pH combined with EDTA extraction in anoxic conditions. *The Science of the total environment* 312:181–93.
- McCave, I. N. 1984. Size spectra and aggregation of suspended particles in the deep ocean. *Deep Sea Research Part A. Oceanographic Research Papers* 31:329–352.
- MiPAF. 2000. *Analisi chimica del suolo*. Franco Angeli, Milano.
- Müller, G. 1969. Index of geoaccumulation in sediments of the Rhine River. *Geological Journal* 2:109–118.
- Prica, M., B. Dalmacija, M. Dalmacija, J. Agbaba, D. Krcmar, J. Trickovic, and E. Karlovic. 2010. Changes in metal availability during sediment oxidation and the correlation with the immobilization potential. *Ecotoxicology and environmental safety* 73:1370–7.
- Reddy, R. K., and D. DeLaume. 2008. *Biochemistry of wetlands. Science and applications*. Taylor & Francis.

- Rubio, R., G. Rauret, A. Sahuquillo, J. F. Lo, R. P. Thomas, C. M. Davidson, and A. M. Ure. 1999. Use of a certified reference material for extractable trace metals to assess sources of uncertainty in the BCR three-stage sequential extraction procedure 382.
- Stephens, S. R., B. J. Alloway, J. E. Carter, and a Parker. 2001. Towards the characterisation of heavy metals in dredged canal sediments and an appreciation of “availability”: two examples from the UK. *Environmental pollution* (Barking, Essex : 1987) 113:395–401.
- Stietiya, M. H., and J. J. Wang. 2006. Effect of organic matter oxidation on the fractionation of copper, zinc, lead, and arsenic in sewage sludge and amended soils. *Journal of environmental quality* 40:1162–71.
- Surian, N., and M. Rinaldi. 2003. Morphological response to river engineering and management in alluvial channels in Italy. *Geomorphology* 50:307–326.
- Varol, M., and B. Şen. 2012. Assessment of nutrient and heavy metal contamination in surface water and sediments of the upper Tigris River, Turkey. *Catena* 92:1–10.
- Vittori Antisari, L., C. Trivisano, C. Gessa, M. Gherardi, A. Simoni, G. Vianello, and N. Zamboni. 2010. Quality of Municipal Wastewater Compared to Surface Waters of the River and Artificial Canal Network in Different Areas of the Eastern Po Valley (Italy). *Water Quality, Exposure and Health* 2:1–13.



# CHAPTER 3

## THE ENVIRONMENTAL PROTECTION

*pp.*

3.	The environmental protection: remediation experiments.....	49
3.1.	Clinoptilolite experiments.....	49
3.1.1.	Materials and methods.....	51
3.1.2.	Results.....	52
3.1.3.	Discussion.....	53
3.1.4.	Conclusion.....	54
3.2.	Vermiculite experiments .....	55
3.2.1.	Materials and methods.....	57
3.2.1.1.	Vermiculite, sediment and water characterization.....	57
3.2.1.2.	Biofilm cultivation and preparation.....	58
3.2.1.3.	Data analysis.....	59
3.2.2.	Results.....	59
3.2.3.	Discussion.....	64
3.2.4.	Conclusion.....	65
3.3.	References.....	66



### 3. THE ENVIRONMENTAL PROTECTION: REMEDIATION EXPERIMENTS

In the last decades a number of studies have focused on different strategies for water remediation using eco-friendly materials but to our knowledge few works focused on the possibility to extend these low-cost techniques to the prevention of sediment contamination (Rakowska et al., 2012).

Among different techniques for heavy metals remediation in canal systems, the concept of metal entrapment at the interface between water and sediment through low-cost and eco-friendly materials appears to be an interesting strategy for environmental preservation (Wang and Chen, 2009). In this study, different experiments were performed with the aim to investigate eco-friendly solutions for water remediation and for the protection from sediment contamination.

A part of the research was carried out thanks to the collaboration of CEB-IBB (University of Minho, PT) and produced these scientific publications:

- Ferronato, C., Vianello, G., Vittori Antisari, L., 2015. Adsorption of pathogens microorganisms,  $\text{NH}_4^+$  and heavy metals of wastewater through a clinoptilolite using bed laminar flow. Clay minerals. Clay Minerals, *in press*.
- Ferronato, C., Silva, B., Costa, F., Tavares, T., 2015 Vermiculite bio-barriers for Cu and Zn remediation: an eco-friendly approach for freshwater and sediments protection. Int. J. of Environ. Sci. and Tech. *submitted*.

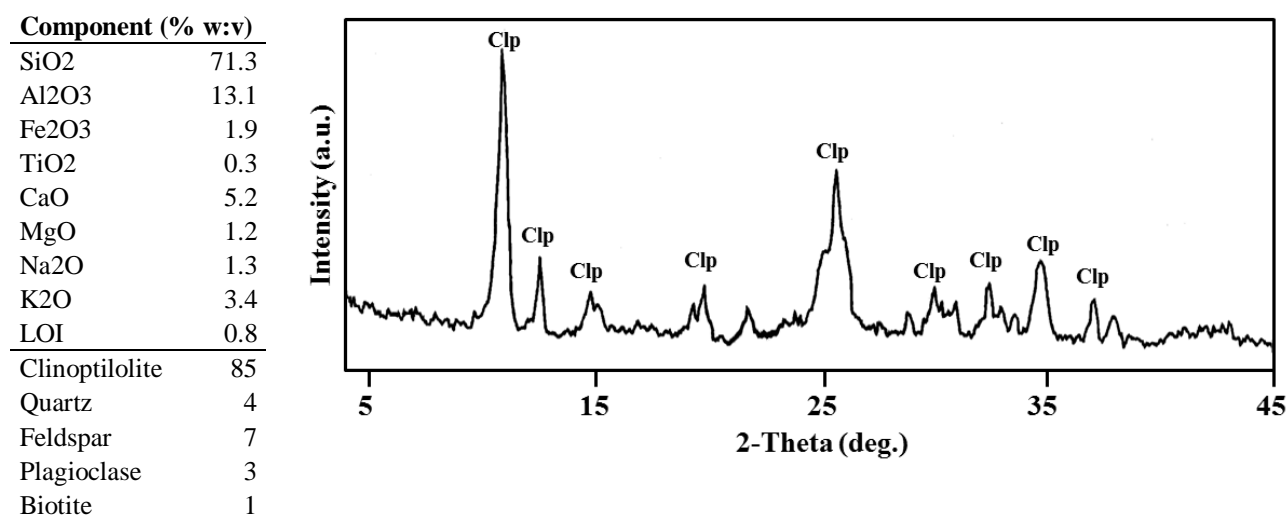
#### 3.1. CLINOPTILOLITE EXPERIMENTS

Among many zeolite types, clinoptilolite is a natural mineral formed by the alteration of glass-rich volcanic rocks with fresh water in lakes or seawater systems, comprising a microporous arrangement of silica and alumina tetrahedral, forming tabular monoclinic tectosilicate crystals.

This material has a high attractive selectivity for certain heavy metals, such as Pb, Cu, Zn, Cd and it can be used as an ion exchanger for the removal of ammonium (Englert and Rubio, 2005; Erdem et al., 2004; Shaheen et al., 2012). Moreover, clinoptilolite can be suitable for entrapping microorganisms in its microporous structure (Chen et al. 2009) due to Van der Waals interactions, hydrogen bonding or ion bridging (Chen et al., 2009; Park et al., 2002; Stotzky, 1985).

Clinoptilolite was used to improve the remediation of the outflow water of an old wastewater treatment plant, which discharges its water in an artificial irrigation canal of the Po Plain in the Bologna District (Northern Italy). The zeolite used in this study was marketed by ECOLIN srl. Its chemical and mineralogical composition is shown in Figure 3.1.

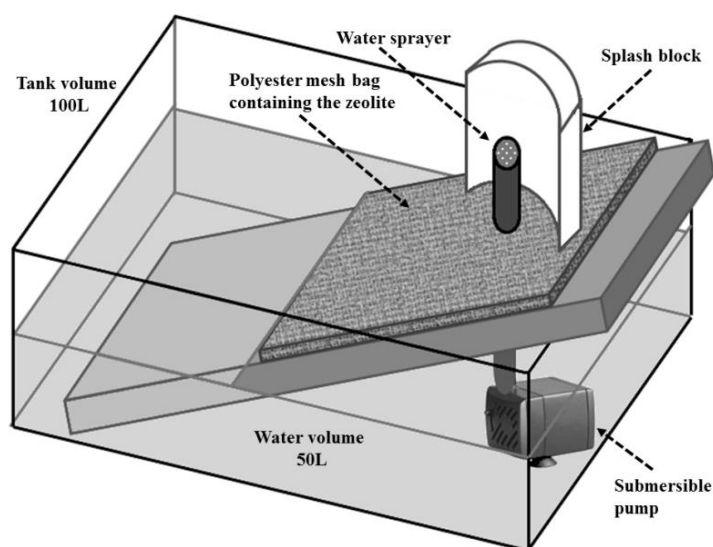
**Figure 3.1.** Chemical and mineralogical composition of Ecolin clinoptilolite sample obtained by X-ray diffraction pattern.



**Experiment 1** studied the efficiency of the zeolites to reduce  $\text{NH}_4^+$  content and pathogenic microorganisms (e.g. faecal coliforms and *Escherichia coli*). Different amounts of zeolite (20, 40, 50, 100 g) were put in contact with 500 ml of wastewater in a glass mesocosm for 24 h without shaking (static system). The concentration of faecal coliforms and *Escherichia coli* colony forming unit (CFU 100ml<sup>-1</sup>) and the amount of  $\text{NH}_4^+$  (mg L<sup>-1</sup>) in the effluent were measured before and after the experiment.

**Experiment 2** investigated the efficiency of clinoptilolite to remediate wastewater from some major elements (Ca, Mg, K, P, Na) and heavy metals (As, Cu, Ni, Zn) using a continuous flow system as shown in Figure 3.2. The experiment was performed in an open system by fluxing 50 L of wastewater with a flow rate of 4 L/min in a clinoptilolite laminar inclined bed of clinoptilolite (35\*35\*1 cm). Water was sampled for heavy metals analysis before and after 2 and 12h of water flow.

**Figure 3.2.** Laminar flux system for water remediation in a clinoptilolite bed.



### 3.1.1. Materials and methods

Water analysis of *Electrical Conductivity (EC)*, *pH*, and *heavy metals* were performed as described in previous section 2.2.2. *Redox potential* was measured with a portable probe (Hach Lange, USA) while  $NH_4^+$  was detected calorimetrically using an Hach-Lange kit (DR3900 spectrometer),

*Faecal coliform and Escherichia coli* quantification water samples were first diluted (until 1:10,000) in Phosphate Buffered Saline (Oxoid) and filtered through nitrocellulose membranes ( $\phi$  0.45 $\mu$ m, Sartorius). Filters were placed on solid selective media for the detection and enumeration of faecal indicators. Chromcult Coliformen Agar (Merck) was used for *Escherichia coli* and faecal coliform detection after incubation in aerobic conditions at 44°C for 24h. *E. coli* typically appears as blue/purple colonies whereas coliforms appear as red/pink colonies.

*Clinoptilolite uptake* ( $Q$ , mg g<sup>-1</sup>) and *removal percentage* ( $D$ , %) of both macro and trace elements were calculated as follows:

$$Q = (C_f - C_i) * V/m \quad [11]$$

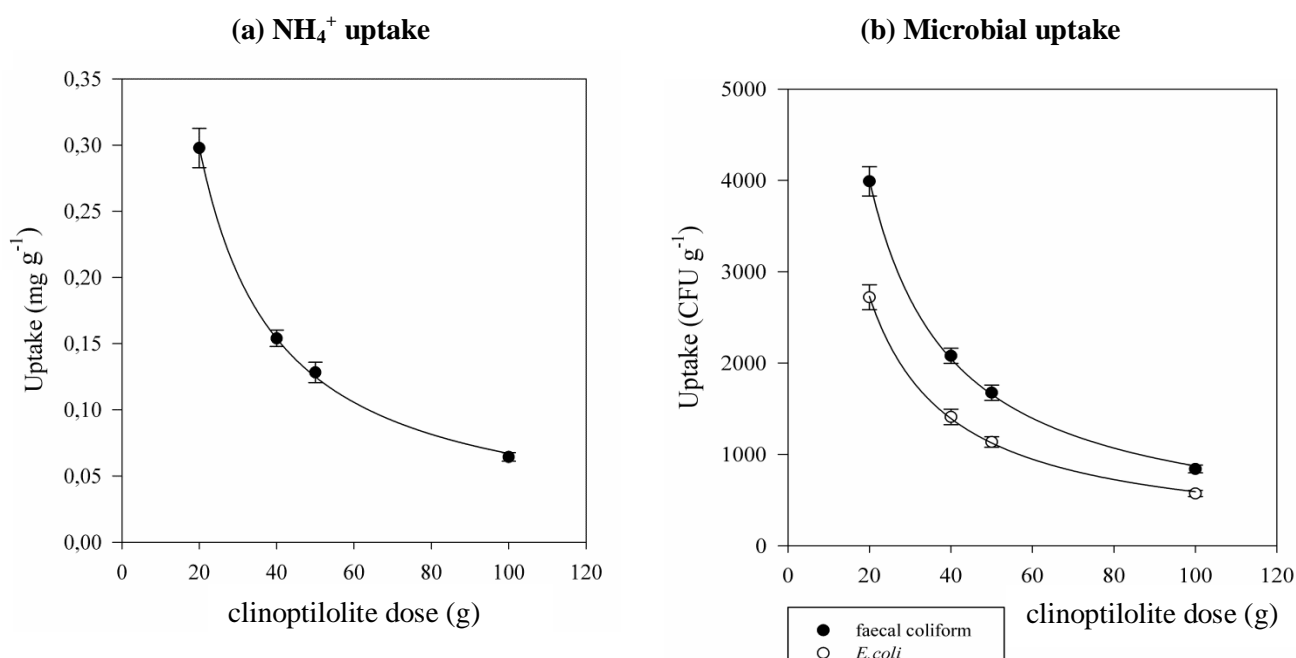
$$D = 100 * (C_f - C_i)/C_i \quad [12]$$

where  $C_f$  and  $C_i$  (mg L<sup>-1</sup>) are the final and the initial concentration of metal in solution respectively,  $V$  is the working volume (L) and  $m$  (g) is the mass of vermiculite used.

### 3.1.2. Results

In *Experiment 1*, pH and electrical conductivity (EC), dissolved oxygen (OD) and redox potential (Eh) showed no significant change during time: pH ranged between 7.4 and 7.9, while EC ranged from 773 to 767  $\mu\text{S cm}^{-1}$ . Dissolved Oxygen (DO) slightly varied from 6.4 to 7.3  $\text{mg dm}_3^{-1}$  while Eh went from 126 to 164 mV. The initial content of total coliform and *E. coli* was 177 33 and 12 333 CFU  $100\text{cm}_3^{-1}$  respectively, while  $\text{NH}_4^+$  concentration was 13.9  $\text{mg dm}_3^{-1}$ . The uptake trend of both  $\text{NH}_4^+$  and pathogens is shown in Figure 3.3.

**Figure 3.3.** Uptake of ammonium (3.2.a) and microbial faecal indicators (3.2.b) at different sorbent: adsorbate ratio.



Generally, both pathogens and  $\text{NH}_4^+$  removal increased with the increase of adsorbent:adsorbate ratio. The almost complete removal was observed for  $\text{NH}_4^+$ , total coliform and *E. coli* with sorbent: adsorbate ratio 1:5 (92.7, 94.8, 95.2%, respectively). By increasing the clinoptilolite dose, ammonium uptake decreased from 0.3 to 0.06  $\text{mg g}^{-1}$  (Figure 3.3.a) because of the high availability of clinoptilolite binding sites for  $\text{NH}_4^+$  ions.

The uptake of faecal coliforms and *E. coli* was similar and it increased likewise with the lowering of the adsorbent dose (Figure 3.3.b). The removal percentage of pathogen colonies with the lowest dose of clinoptilolite were 89.9 and 90.4% for faecal coliform and *E. coli*, respectively, with an active uptake of 3 989 and 2 732 cfu  $\text{g}^{-1}$ .

Table 3.1 shows the results obtained from *Experiment 2*, and it shows that after 2 h no active uptake of elements on clinoptilolite surfaces occurred, while after 12 h all major elements, heavy metals and metalloids were strongly removed from aqueous solution. The initial concentration of nutrients and heavy metals in the wastewater was 75, 22, 22, 193 mg dm<sup>-1</sup> for Ca, K, Mg and Na, respectively and 14.93, 19, 4.86 and 31 µg dm<sup>-1</sup> for As, Cu, Ni and Zn, respectively.

**Table 3.1.** Removal percentage and uptake of macro elements and heavy metals in the effluent after 2 and 12h of laminar flux on a clinoptilolite bed.

		Water flow (mg L <sup>-1</sup> )		Removal (%)		Uptake (µg g <sup>-1</sup> )	
		2h	12h	2h	12h	2h	12h
Ca	mg L <sup>-1</sup>	85.7	10.1	-14.0	86.6	-350.0	2170.0
K		29.7	2.5	-29.7	89.0	-226.7	679.7
Mg		19.1	2.4	14.0	89.4	103.3	661.3
Na		182.4	19.9	5.5	89.7	356.7	5773.3
As	µg L <sup>-1</sup>	14	0	5.1	97.7	25.3	486.0
Cu		22	4	0.0	78.0	0.0	497.0
Ni		4.44	0.22	8.6	95.5	14.0	154.7
Zn		32.7	2.5	0.0	92.0	0.0	970.3

The removal percentage of all elements analysed ranged from 78 to 92% and from a legislative point of view, the treated wastewater reached the “good a positive ecological status” required by the European Directive (EC 2000/60) and could be recycled in surface water (D.lsg 152/2006). The uptake values showed that the selectivity among nutrients was Na<sup>+</sup>>Ca<sup>2+</sup>> K>Mg<sup>2+</sup>>P while that of metalloids and metals was As>Zn>Ni>Cu.

### 3.1.3. Discussion

The reduction of both NH<sub>4</sub><sup>+</sup> and pathogen concentration in *Experiment 1* allowed for the sanitization of wastewater for recycling purposes in surface waters. Clinoptilolite shows a high adsorption rate of NH<sub>4</sub><sup>+</sup> as confirmed by many authors (Burgess et al., 2004; Guo et al., 2008; Karadag et al., 2006).

Several factors influence the relationship between the sorbent and the adsorbate, such as pH, temperature, initial concentration and structure of zeolites (Guo et al., 2008) and both adsorption isotherms and kinetics are largely available in literature (Farkas et al., 2005; Jorgensen and Weatherley, 2003; Weatherley and Miladinovic, 2004). In our system, the pH slightly increases with the increase of the sorbent dose, and at this condition the NH<sub>4</sub><sup>+</sup> should slightly decrease in favour of NH<sub>3</sub> formation. However, Guo et al (2008) confirmed

that  $\text{NH}_4^+$  adsorption at pH from 7 to 9 does not produce significant differences. Moreover, the high reduction of microbial contamination of wastewater confirms the capacity of microorganisms to be attracted by weak electrostatic or binding forces on the inter/intra layer sheets of zeolites and clays, forming a compact biofilm on their surface (Lameiras et al., 2008; Stotzky, 1985).

Also in **Experiment 2**, the high reduction of heavy metals in the water was achieved after flowing the wastewater in a clinoptilolite laminar bed for 12 h while the negative removal percentage obtained after 2h flow for K and Ca may be linked to the partial dissolution of the clinoptilolite  $\text{K}_2\text{O}$  and  $\text{CaO}$ , which could interfere with the water composition and sampling. As expected, the negative charge of the clinoptilolite structure is counterbalanced by monovalent and divalent cations (e.g.  $\text{Na}^+$ ,  $\text{K}^+$ ,  $\text{Ca}^{2+}$  and  $\text{Mg}^{2+}$ ), even under basic conditions (Doula et al., 2002). The relatively low pollutant concentration in the effluent favours an almost complete adsorption of all heavy metals considered (As, Cu, Ni, Zn) on the adsorbent sites. At neutral pH, some metals (e.g. Cu and Zn) tend to precipitate as oxide or hydroxides and their soluble species can be easily adsorbed at the sorbent surface of natural zeolites and clays (Abollino et al., 2006; Berber-Mendoza et al., 2006; Malandrino et al., 2006; Nyembe et al., 2010). In our study, since the pH was constant at 7.4, the different efficiency in heavy metals adsorption can be due to the different affinity of the metal with the silicate structure and to competition for the binding sites of the clinoptilolite structure (Srivastava et al., 2009). It is well known that clinoptilolite absorbed anionic forms like phosphorus and arsenic, which are present in the water as phosphates and arsenates. Their removal can be linked to the formation of salts binding or to the direct participation of these compounds in the adsorption process at the edges of the mineral (specific adsorption mechanism).

### 3.1.4. Conclusion

The study of the laminar flux prototype for wastewater remediation showed that this system can performs water remediation rapidly and efficiently. Few studies were found about the interaction of different pollutants so it was concluded that the interaction and the competition of metals and organics in zeolite/wastewater need to be better understood. Nevertheless, further application of this model on a larger scale is needed in order to test clinoptilolite performances on high volumes of wastewater.



### 3.2. VERMICULITE EXPERIMENTS

Natural clays (e.g. vermiculite) have often been studied for water remediation of heavy metals (Malamis and Katsou, 2013; Quintelas et al., 2011). The tetra and octahedral structure of phyllosilicates, in fact, favors a high surface area and high availability of negative charges. Vermiculite, among smectites, can capture heavy metals by cation exchange mechanisms between metal ions and the negative permanent charge at the planar sites (outer-sphere complexes), or by the formation of SiO-/AlO- metal bound at the clay particle edge (inner-sphere complexes) (Malandrino et al., 2006).

In recent years, many efforts have been made to increase the performance of clay adsorption, and a vast array of biological materials has been explored for heavy metals removal (Costa et al., 2012; Lameiras et al., 2008; Bruna Silva et al., 2012; Wang and Chen, 2009). Many authors reported that microorganisms, organized in biofilm on different adsorbent supports, can promote active and passive mechanisms for metal uptake and stabilization (Cobas et al., 2013; Ferreira et al., 2013; Pazos et al., 2010) such as native biosorption, enzymatic transformations, metal precipitation, synthesis of extracellular substances (Kazy et al., 2002; Valls and de Lorenzo, 2002).

Vermiculite was used to model Vermiculite Permeable Barriers (VPB) for fast removal of Cu and Zn from water. To improve the efficacy of VPB, Permeable Bio-barriers (VPB-Bio) were constructed by promoting the formation of *Pseudomonas putida* biofilm on vermiculite.

The water remediation efficacy of VPB and VPB-Bio and their efficiency in protecting sediment from metal contamination were evaluated in different experimental assays.

**Experiment 1** evaluated Cu or Zn uptake by simple vermiculite barriers (VPB) in order to clarify some fundamental parameters in remediation studies (e.g. equilibrium, adsorption kinetics, uptake and removal percentage). 150 ml of aqueous solution of Cu or Zn 100 mg L<sup>-1</sup>, were added to different vermiculite amounts from 0.5 to 2 g and stirred at 140 rpm for 24 h.

Solution samples were periodically collected and analyzed for their Cu and Zn concentrations by ICP-OES (Perkin Elmer, USA).

In **Experiment 2**, Cu and Zn uptake from the solution was performed by both VPB and VPB.Bio to evaluate the contribution of *Pseudomonas putida* biofilm in water remediation. For this reason, in VPB.Bio, biofilm adhesion had been previously promoted and observed as described further in section 3.2.1. VPB and VPB.Bio system were prepared in batch, and 100 mg L<sup>-1</sup> of Cu and Zn were added in a separate assay. Each experiment was performed in three different growth medium in order to evaluate the microbial efficiency at different nutrition stress conditions. Samples were stirred at 140 rpm at 26°C for 96 h in order to reach the equilibrium condition of the system, while the metals concentration in the supernatant was periodically monitored by ICP-OES (Perkin Elmer, USA) as described in section 3.2.1.

**Experiment 3** was performed in order to test the efficiency of vermiculite permeable barriers (VPB) and bio-barriers (VPB-Bio) to prevent Cu and Zn contamination of sediments, and it was carried out in some continuous assays at lab-scale using plexiglas columns (height: 33 cm, internal Ø 3.5 cm). Distinct columns were provided for Cu and Zn contamination as shown in Figure 3.4.

**Figure 3.4.** Plexiglas column and open-system set-up (*Experiment 3*).



For each metal treatment, two columns (VPB and VPB-Bio) were filled with 96cm<sup>3</sup> of VPB and pre-treated VPB-Bio respectively and 192cm<sup>3</sup> of fresh sediment from Dosolo canal (Bologna, IT); a third column with sediment alone was provided as control (Ct). Distinct water solutions containing 10 mg L<sup>-1</sup> of Cu or Zn were fluxed upwards though the system using a peristaltic pump (flow rate 0.5 L h<sup>-1</sup>) for 24 h and the metals concentration in the outflow was periodically monitored by ICP-OES. At the end of the experiment, sediment and vermiculites were characterized as described in section 3.2.1.1.

### 3.2.1. Materials and methods

#### 3.2.1.1. Vermiculite, sediment and water characterization

Vermiculite clay (Sigma-Aldrich; specific surface area  $39 \text{ m}^2 \text{ g}^{-1}$ ; mean particle  $\phi$  0.5mm; porosity 10%) was selected as adsorbent material for batch and open system assays due to its low cost and eco-friendly characteristics.

Sediment for open system assay was collected in the Dosolo canal, one of the monitored artificial canals located in the urban area of Bologna, Italy.

Water solution for both batch and open system assay was contaminated with nitrate salts of Cu and Zn ( $\text{CuSO}_4 \cdot 5\text{H}_2\text{O}$  and  $\text{ZnSO}_4 \cdot 7\text{H}_2\text{O}$ , Pancreac).

All tests were performed considering the metals separately, in order to avoid metal competition which could affect the interpretation of the data (Fonseca et al., 2012) and within 24 h in order to simulate the short contact time between the adsorbent and the adsorbate in a natural system (e.g. riverine system). All analyses were performed in duplicate.

The *elemental composition of vermiculite* and sediment samples was determined by *Inductive Coupled Plasma Optical Emission Spectroscopy* (ICP –OES, Spectro, Arcos, Germany) after acid digestion of samples with aqua regia as described in section 2.2.3.

The *Cu and Zn concentration in water* was performed by ICP-OES (Perkin Elmer, USA). Samples were periodically collected, centrifuged at 120.000 rpm for 15 min and stabilized with  $\text{HNO}_3$  suprapure 1:100 w:w before analysis. Certified reference materials (Optima Multi-Element Standard, PerkinElmer Pure) were used to verify the analytical accuracy and the agreement was typically  $<\pm 5\%$ .

The *characterization of the functional groups* of vermiculite was performed by Fourier-Transform Infrared Spectroscopy (FT-IR, BOMEM MB 104) on pressed KBr pellets. The pellet was obtained by grounding 1mg of each sample and 100 mg of KBr in an agate mortar.

Background correction for atmospheric air was used and spectra were obtained in the range  $500\text{--}4000 \text{ cm}^{-1}$  with a minimum of 30 scans and a resolution of  $4 \text{ cm}^{-1}$ .

### 3.2.1.2. Biofilm cultivation and preparation

*Pseudomonas putida* strain was obtained from the Spanish Type Culture Collection of the University of Valencia. *Pseudomonas putida* strain was cultivated for 24 h at 26°C in Luria Bertani broth (LB: 10 g L<sup>-1</sup> tryptone; 5 g L<sup>-1</sup> yeast extract; 5 g L<sup>-1</sup> NaCl).

The growth curve of the microorganism was determined by measuring the Optical Density (OD) of the suspension at 620 nm (T60-UV Visible Spectrophotometer, PG Instruments) for 24 h.

The OD measurement was related to the mass of the microbial cells (g) through a calibration curve. For this reason *Pseudomonas putida* was grown until its exponential phase and the OD of both the original suspension and its scalar dilutions (up to 1:50), were measured. At the same time, 10 ml of each sample was filtered on pre-weight nitrocellulose filters ( $\phi = 45\mu\text{m}$ ) and oven dried at 105°C.

The dry mass of the filtered culture was then related to its OD through linear regression. The regression equation ( $y=0,9091x+0,0029$ ) was consequently applied to correlate the OD measurement (x) to the mass of the culture (y).

**Vermiculite bio-barriers (VPB.Bio)** were constructed by promoting the formation of biofilm on 1g of vermiculite in batch assays. Three different nutrient conditions were tested for biofilm promotion: Luria Bertani broth (LB), 1:10 w:w diluted Luria Bertani broth (Dil.LB) and distilled water (W).

*Pseudomonas putida* was cultivated in LB medium in order to obtain a pure culture with a final concentration of 3g L<sup>-1</sup>. 500ml of the bacterial suspension was centrifuged in sterilized polypropylene centrifuge tubes at 7000 rpm for 15 min and subsequently re-suspended in 30ml of the three different medium (LB, DLB, W).

Erlenmeyer flasks containing 1g of sterilized vermiculite was added to the concentrated microbial suspension and the system was left to equilibrate for 48 h with moderate agitation speed in order to promote microbial adhesion on vermiculite particles (Ollos et al., 2003).

The best medium solution was selected for further experiments in open system assays.

Vermiculite permeable bio-barriers (VPB-Bio) for open system experiments were designed following the method described above, using 12g of vermiculite and re-suspending the concentrated culture in DLB medium for 48h.

A *Scanning Electron Microscope* (SEM – Leica Cambridge S360) was used for observing the biofilm evolution throughout the metal treatment.

VPB and VPB-Bio sub-samples were dehydrated through a graded ethanol series (10%, 25%, 50%, 80%, 100%) and gold covered for SEM analysis (Chen et al., 2009).

### 3.2.1.3. Data analysis

Vermiculite *uptake* ( $Q$ , mg kg<sup>-1</sup>) and *removal percentage* ( $D$ , %) of Cu and Zn were calculated as reported in section 3.1.1.

Pseudo-first order and pseudo-second order *kinetics models* were applied according to Rosales et al (2012) to compare the kinetics of metal sorption at different conditions, with the following equations:

$$\text{Pseudo first order (Lagergren, 1907): } dq/dt = k_1 \times (q_e - q_t) \quad [13]$$

$$\text{Pseudo second order (Ho and McKay, 1999): } dq/dt = k_2 \times (q_e - q_t)^2 \quad [14]$$

where  $q_t$  is the mass of metal adsorbed at time  $t$  (mg g<sup>-1</sup>);  $q_e$  is the mass of metal adsorbed at equilibrium (mg g<sup>-1</sup>);  $k_1$  (L/min) and  $k_2$  (g<sub>verm</sub>/(mg<sub>metal</sub>·t)) are the pseudo first and pseudo second order constants respectively. Both equations were derived in linear form and according to Azizian (2004), and  $q_e$  and  $k_2$  were related to the slope and to the intercept respectively of the resulting graphs.

A *mass balance approach* was used to evaluate the metal partitioning in each component of the column set-up. Total Cu and Zn amount released in water was calculated as the residual part of the total metal flowed into the system.

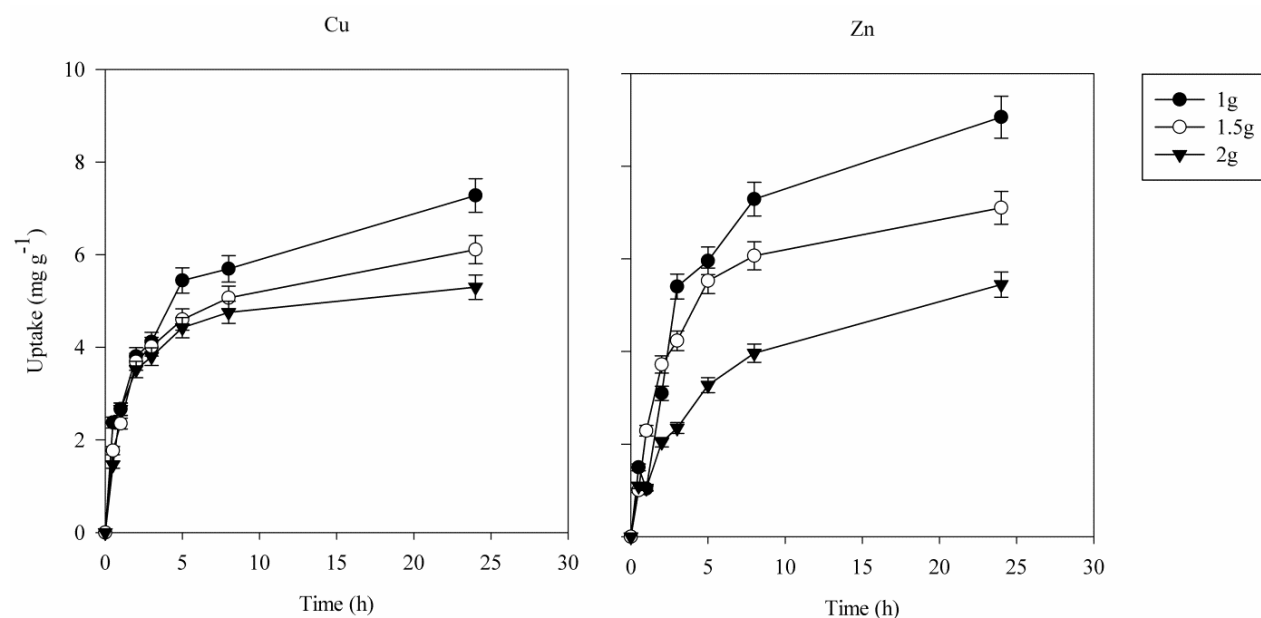
### 3.2.2. Results

**Experiment 1** aimed to evaluate the uptake of both Cu and Zn metals by different amounts of vermiculite and the results are shown in Figure 3.5.

Both metals uptake increased with decreasing the adsorbent dose; for each assay the uptake increases rapidly during the first 8h and it started to reach the equilibrium after 24h.

The maximum Cu and Zn uptake after 24h was 7.28 and 9.06 mg g<sup>-1</sup> respectively, and the best performance in terms of the highest metals uptake was obtained by the lowest vermiculite dose.

**Figure 3.5.** Cu and Zn removal percentage (D) and uptake (Q) from different amounts of vermiculite



**Experiment 2** evaluated the biofilm contribution to metals removal from solution. The lowest dose of vermiculite was chosen to test Cu and Zn removal (D, %) and uptake (Q, %) by VPB and VPB.Bio, and each experiment was replicated by suspending Cu and Zn on three different medium (LB, Dil.LB and W).

The results of the different assays showed that the removal efficiency increased as follows: W>Dil.LB>LB (data not shown).

In each assay, after 24 h of contact the uptake equilibrium was reached and the presence of *Pseudomonas putida* increased VBP performance by enhancing the remediation efficiency of vermiculite.

The contribution of *Pseudomonas putida* biomass on water remediation was appreciable only in the presence of nutrient starvation conditions (W medium): in this case, the metal uptake increased by about 3mg g<sup>-1</sup> as

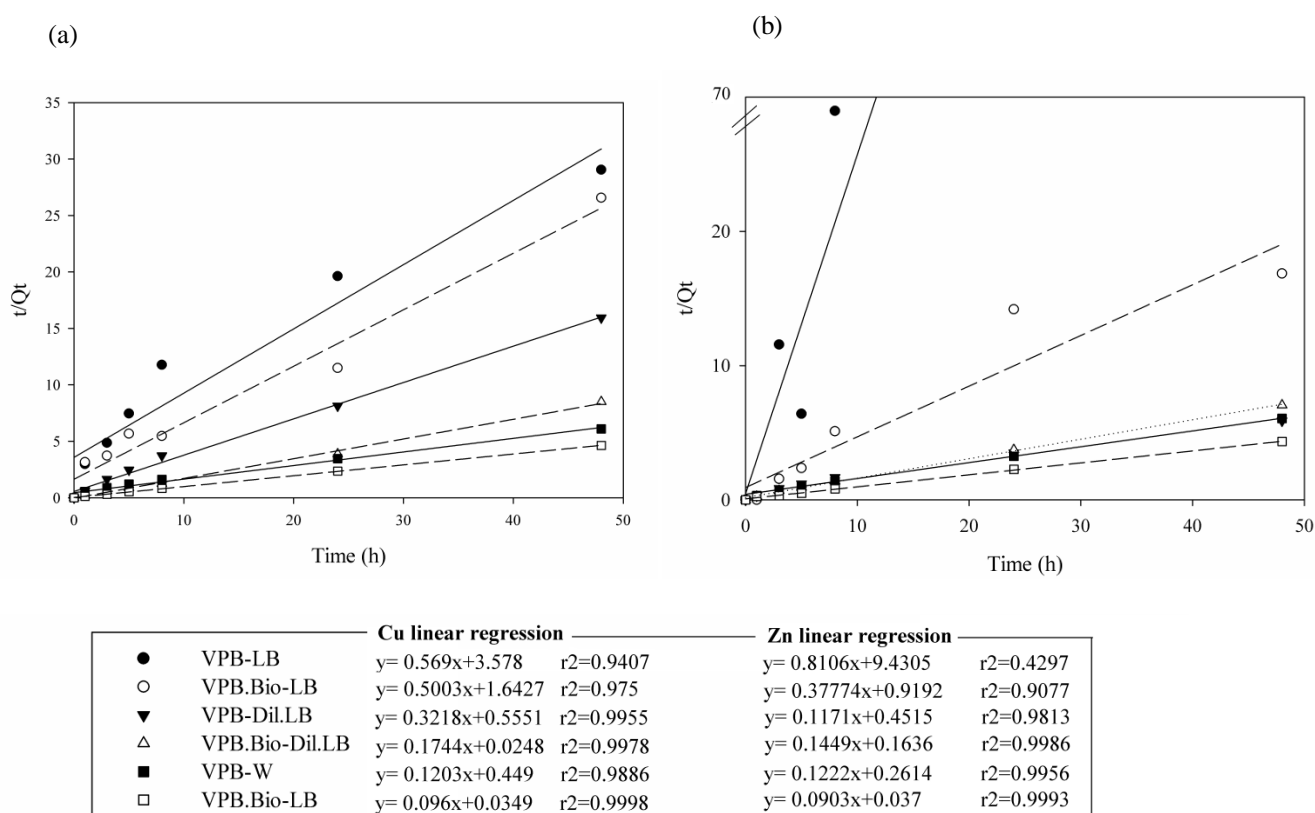
compared to the control (VPB). In absolute terms 84% of Cu (+34.4%) and 74.6% of Zn (+27%) were removed from solution thanks to the contribution of *Pseudomonas putida*.

The application of the kinetics adsorption models revealed that the *pseudo-first order model* did not fit the experimental data and presented low  $R^2$  values (data not shown) while the *pseudo-second order model* could better describe the adsorption kinetic of the system (Figure 3.6).

According to Azizian (2004), the sorption process generally obeys the pseudo-first order kinetic at high solute concentration, while it obeys the pseudo second-order model at lower initial concentration solution. Moreover, by deriving the pseudo-second order equation, the lower the slope of the curve is, the faster the kinetic is (Azizian, 2004).

In both Cu and Zn adsorption kinetics, VBP.Bio systems showed lower  $k_2$  than VPB for each experimental condition and the lowest  $k_2$  was obtained in the assays performed in water.

**Figure3.6.** Adsorption kinetic of Cu (a) and Zn (b), on vermiculite permeable barrier (VPB) and bio-barrier (VPB.Bio). Standard Deviation was always  $< \pm 5\%$ .



**Experiment 3** tested the suitability of VPB and VPB-Bio in an open system for water remediation and verify their efficiency to prevent sediment contamination. VPB-Bio was constructed on DLB as described in section 3.1.2 and the structure of the biofilm was observed through SEM before and after the assay.

As shown in Figure 3.7 the SEM images displayed a well compact biofilm on the vermiculite VPB-Bio surface (Figure 3.7) before starting the column experiment, while after the water flow the shape and the density of the *Pseudomonas putida* biofilm was strongly reduced (data not shown).

**Figure.3.7.** SEM image of the biofilm grown in Dil.LB medium and supported on vermiculite.

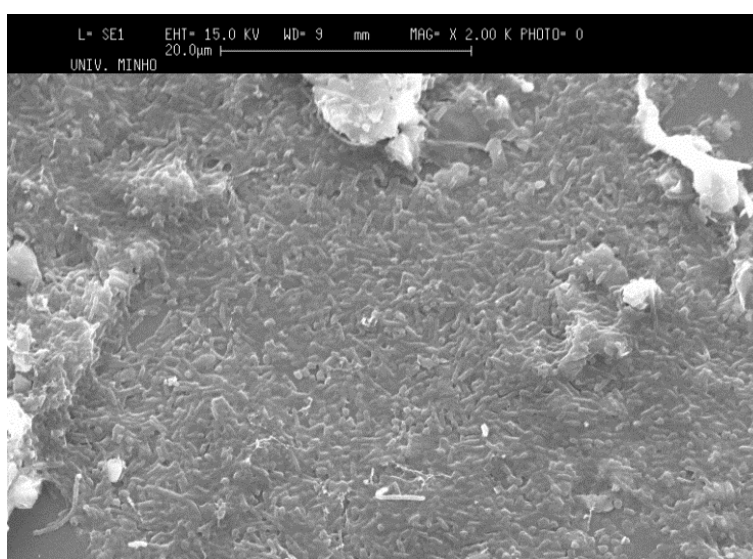


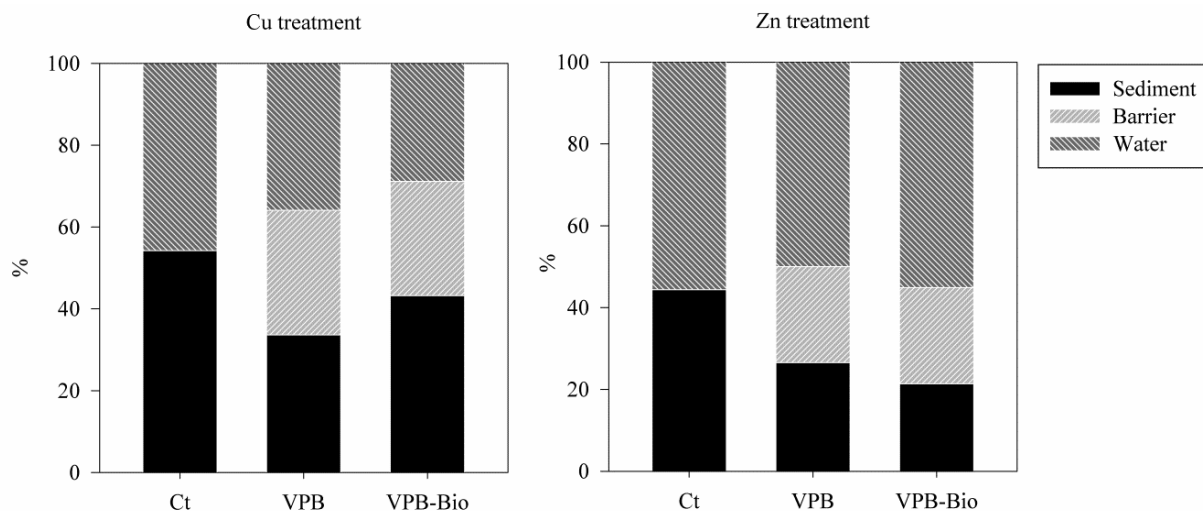
Figure 3.8 displays the percentage of metal distributed in water, VPB or VPB-Bio and sediment for each column. After 24 h treatment, Cu concentration in sediments varied as follows: Ct>VPB-Bio>VPB.

In Ct column, 45% of Cu was released in the water outflow, while in VPB and VPB-Bio columns the metal released was 35 and 28% respectively. These results confirm that the use of a permeable barrier at the interface between water and sediment can reduce the Cu concentration up to 20% in sediments and up to 10% in water outflow.

After Zn treatment the metal concentration in sediment was: Ct>VPB>VPB-Bio, while in water no significant difference between the systems was noticed. The application of the permeable barrier could reduce metal contamination by 18% in sediments. The use of VPB-Bio successfully contributed to sediment mitigation up to 23%.

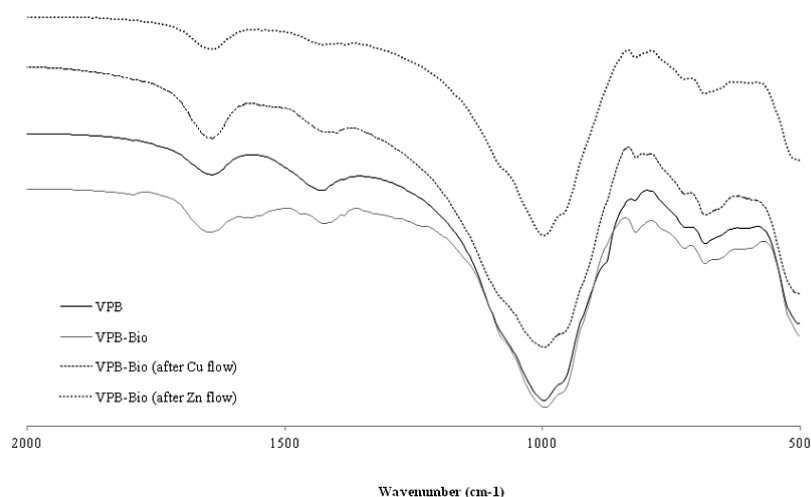


**Figure 3.8.** Mass balance of Cu and Zn throughout sediment, barrier and water the open system assay. VPB is vermiculite barrier while VPB-Bio is vermiculite bio-barrier system. Standard Deviation was always  $< \pm 5\%$ .



The FTIR spectra of VPB-Bio before and after metal treatment are presented in Figure 3.9 and it shows the alteration that surface chemical groups suffered before and after the metals flow. The presence of the bacterial biomass could be faintly detected by a weak band at  $1550\text{ cm}^{-1}$  which corresponds to the vibration of the amide II, N–H or C–N from proteins, where vermiculite does not adsorb (Rong et al, 2010). No characteristic bands of organic matter were found on VPB-Bio samples, probably due to the low amount of biomass. Moreover, SEM images showed that the biofilm size was strongly reduced after the metal treatment (data not shown) and this hypothesis was confirmed from metals quantification through ICP analysis of vermiculite, where no significant differences between the VPB and VPB-Bio were detected (Figure 3.8).

**Figure 3.9.** FT-IR spectra of characteristic functional groups of pure vermiculite (VPB) and vermiculite loaded with biomass (VPB-Bio) before and after metals treatment.



### 3.2.3. Discussion

It is well known that the dynamic of metal cations adsorption on clays is fast, due to the significant cation exchange capacity of these minerals and to their high specific surface area associated with the small particle size (Abollino et al., 2006).

In *Experiment 1*, the different Cu and Zn uptake on vermiculite after 24 h suggests that these metals have different affinity with the vermiculite surface. In fact, the Zn ion has higher electrostatic attraction than Cu and can be easily adsorbed into surface sites. On the contrary, Cu ion has tetragonal distortion and its adsorption into the intra-lamellar sites is more difficult (Abollino et al., 2006; Vieira dos Santos and Masini, 2007). The lowest vermiculite amount tested in this study, showed the best performance in terms of uptake capacity and velocity of adsorption, confirming that this material is very suitable for metal remediation in freshwater open systems.

*Experiment 2* in batch assay tested the possibility to increase metal adsorption of clay from water solution by exploiting *Pseudomonas putida*'s ability to entrap Cu and Zn ions. In this experiment, the efficiency of the surface attached growth of microbial biofilm predominates in low-nutrient mediums, probably due to the higher capacity of microorganisms to produce self-defence mechanisms for their survival (Soini et al., 2002). These mechanisms (e.g. EPS extracellular substances) are important for both biofilm protection and heavy metals binding (Fang et al., 2011; Gadd, 2009; González et al., 2010; Quintelas et al., 2011; Pal and Paul, 2008; Sutherland, 2001) and further studies should investigate how to enhance their production. In this assay, in fact, the presence of the biofilm acts as a kind of catalyst in the adsorption process (B. Silva et al., 2012).

The low kinetics of LB and Dil.LB assay can be due to the presence of  $\text{Na}^+$  and phosphate groups in LB medium, which may interfered with vermiculite negative charges, causing a reduction in the distances between layers of vermiculite (Müller and Défago, 2006) and therefore a reduction of metals entrapment.

In *Experiment 3* (open system), the presence of a permeable barrier at the interface between water and sediment could reduce the Cu adsorption up to 20% in sediments and up to 10% in water outflow. The application of VPB can also reduce Zn contamination by 18% in sediments and the use of VPB-Bio successfully contributed to sediment mitigation up to 23%.

In both cases the immobilization of the biofilm was not strong enough to prevent microbial migration through the column. Some authors indicate that time, nutrient availability and hydraulic stress can deeply affect the attachment and detachment of biofilm from a surface (Percival et al., 1999; Ollos et al., 2003). In this study, the low flow rate and the low contact time may have affected both the thickness and resistance of the biofilm on VPB-Bio, resulting in partial detachment of the microbial biomass during flow (Soini et al., 2002). Therefore metals retained by the biomass might migrate through the column and be subjected to a number of chemical and biochemical transformations which typically occur in soil and sediment (Fonseca et al., 2009; Kashem and Singh, 2001; Stietiya and Wang, 2006).

### **3.2.4. Conclusion**

Vermiculite is an interesting, eco-friendly material, for water remediation and sediment protection. *Pseudomonas putida* supported on vermiculite contributes to metal adsorption, as demonstrated in adsorption studies at batch-scale, and confirm the possibility to increase vermiculite efficiency by exploiting microbial biofilm potentialities.

The application of VPBs successfully has proved their ability to protect both water and sediment from metal contamination but some limitations have been observed in the barriers retention of the microbial biofilm over time. Studying bio-recovery of metals from a complex system such as water and sediments will required more experimentation on biofilm immobilization by modelling different flow rates and contact times, and by monitoring the biofilm diffusion through the water and sediment layers.

### 3.3. REFERENCES

- Abollino, O., A. Giacomino, M. Malandrino, and E. Mentasti. 2006. The Efficiency of Vermiculite as Natural Sorbent for Heavy Metals. Application to a Contaminated Soil. *Water, Air, and Soil Pollution* 181:149–160.
- Azizian, S. 2004. Kinetic models of sorption: a theoretical analysis. *Journal of colloid and interface science* 276:47–52.
- Berber-Mendoza, M. S., R. Leyva-Ramos, P. Alonso-Davila, L. Fuentes-Rubio, and R. M. Guerrero-Coronado. 2006. Comparison of isotherms for the ion exchange of Pb(II) from aqueous solution onto homoionic clinoptilolite. *Journal of colloid and interface science* 301:40–5.
- Burgess, R. M., M. M. Perron, M. G. Cantwell, K. T. Ho, J. R. Serbst, and M. C. Pelletier. 2004. Use of zeolite for removing ammonia and ammonia-caused toxicity in marine toxicity identification evaluations. *Archives of environmental contamination and toxicology* 47:440–7.
- Chen, X., S. Hu, C. Shen, C. Dou, J. Shi, and Y. Chen. 2009. Interaction of *Pseudomonas putida* CZ1 with clays and ability of the composite to immobilize copper and zinc from solution. *Bioresource technology* 100:330–7.
- Cobas, M., L. Ferreira, T. Tavares, M. A. Sanromán, and M. Pazos. 2013. Development of permeable reactive biobarrier for the removal of PAHs by *Trichoderma longibrachiatum*. *Chemosphere* 91:711–6.
- Costa, F., C. Quintelas, and T. Tavares. 2012. Kinetics of biodegradation of diethylketone by *Arthrobacter viscosus*. *Biodegradation* 23:81–92.
- Doula, M., a Ioannou, and a Dimirkou. 2002. Copper adsorption and Si, Al, Ca, Mg, and Na release from clinoptilolite. *Journal of colloid and interface science* 245:237–50.
- Englert, A. H., and J. Rubio. 2005. Characterization and environmental application of a Chilean natural zeolite. *International Journal of Mineral Processing* 75:21–29.
- Erdem, E., N. Karapinar, and R. Donat. 2004. The removal of heavy metal cations by natural zeolites. *Journal of colloid and interface science* 280:309–14.
- Fang, L., X. Wei, P. Cai, Q. Huang, H. Chen, W. Liang, and X. Rong. 2011. Role of extracellular polymeric substances in Cu(II) adsorption on *Bacillus subtilis* and *Pseudomonas putida*. *Bioresource technology* 102:1137–41.
- Farkas, A., M. Rozić, and Z. Barbarić-Mikočević. 2005. Ammonium exchange in leakage waters of waste dumps using natural zeolite from the Krapina region, Croatia. *Journal of hazardous materials* 117:25–33.
- Ferreira, L., M. Cobas, T. Tavares, M. a Sanromán, and M. Pazos. 2013. Assessment of *Arthrobacter viscosus* as reactive medium for forming permeable reactive biobarrier applied to PAHs remediation. *Environmental science and pollution research international* 20:7348–54.

- Fonseca, B., H. Maio, C. Quintelas, A. Teixeira, and T. Tavares. 2009. Retention of Cr(VI) and Pb(II) on a loamy sand soil. *Chemical Engineering Journal* 152:212–219.
- Fonseca, B., M. Pazos, T. Tavares, and M. a Sanromán. 2012. Removal of hexavalent chromium of contaminated soil by coupling electrokinetic remediation and permeable reactive biobarriers. *Environmental science and pollution research international* 19:1800–8.
- Gadd, G. M. 2009. Biosorption: critical review of scientific rationale, environmental importance and significance for pollution treatment. *Journal of Chemical Technology & Biotechnology* 84:13–28.
- González, a G., L. S. Shirokova, O. S. Pokrovsky, E. E. Emnova, R. E. Martínez, J. M. Santana-Casiano, M. González-Dávila, and G. S. Pokrovski. 2010. Adsorption of copper on *Pseudomonas aureofaciens*: protective role of surface exopolysaccharides. *Journal of colloid and interface science* 350:305–14.
- Guo, X., L. L. Zeng, X. Li, and H.-S. Park. 2008. Ammonium and potassium removal for anaerobically digested wastewater using natural clinoptilolite followed by membrane pretreatment. *Journal of hazardous materials* 151:125–33.
- Ho, Y. ., and G. McKay. 1999. Pseudo-second order model for sorption processes. *Process Biochemistry* 34:451–465.
- Jorgensen, T. C., and L. R. Weatherley. 2003. Ammonia removal from wastewater by ion exchange in the presence of organic contaminants. *Water research* 37:1723–8.
- Karadag, D., Y. Koc, M. Turan, and B. Armagan. 2006. Removal of ammonium ion from aqueous solution using natural Turkish clinoptilolite. *Journal of hazardous materials* 136:604–9.
- Kashem, M. A., and B. R. Singh. 2001. Metal availability in contaminated soils: I. Effects of flooding and organic matter on changes in Eh, pH and solubility of Cd, Ni and Zn. *Nutrient Cycling in Agroecosystems* 61:247–255.
- Kazy, S. K., P. Sar, S. P. Singh, A. K. Sen, and S. F. D. Souza. 2002. Extracellular polysaccharides of a copper-sensitive and a copper-resistant *Pseudomonas aeruginosa* strain : synthesis , chemical nature and copper binding. *World Journal of Microbiology and Biotechnology* 18:583–588.
- Lagergren, S. 1907. Zur Theorie der sogenannten Adsorption gelöster Stoffe. *Zeitschrift für Chemie und Industrie der Kolloide* 2:15–15.
- Lameiras, S., C. Quintelas, and T. Tavares. 2008. Biosorption of Cr (VI) using a bacterial biofilm supported on granular activated carbon and on zeolite. *Bioresource technology* 99:801–6.
- Malamis, S., and E. Katsou. 2013. A review on zinc and nickel adsorption on natural and modified zeolite, bentonite and vermiculite: examination of process parameters, kinetics and isotherms. *Journal of hazardous materials* 252-253:428–61.
- Malandrino, M., O. Abollino, A. Giacomino, M. Aceto, and E. Mentasti. 2006. Adsorption of heavy metals on vermiculite: influence of pH and organic ligands. *Journal of colloid and interface science* 299:537–46.

- Müller, B., and G. Défago. 2006. Interaction between the bacterium *Pseudomonas fluorescens* and vermiculite: Effects on chemical, mineralogical, and mechanical properties of vermiculite. *Journal of Geophysical Research* 111:G02017.
- Nyembe, D. W., B. B. Mamba, and A. F. Mulaba Bafubiandi. 2010. Adsorption mechanisms of  $\text{Co}^{2+}$  and  $\text{Cu}^{2+}$  from aqueous solutions using natural clinoptilolite: equilibrium and kinetic studies. *Journal of Applied Sciences* 10:599–610.
- Ollos, P. J., P. M. Huck, and R. . Slawson. 2003. Factors affecting biofilm accumulation in model distribution systems. *Journal of American Water Works Association* 95:87–97.
- Pal, A., and A. K. Paul. 2008. Microbial extracellular polymeric substances: central elements in heavy metal bioremediation. *Indian journal of microbiology* 48:49–64.
- Park, S. J., H. Sool, and T. Il Yoon. 2002. The evaluation of enhanced nitrification by immobilized biofilm on a clinoptilolite carrier. *Bioresource technology* 82:183–189.
- Pazos, M., M. Branco, I. C. Neves, M. a. Sanromán, and T. Tavares. 2010. Removal of Cr(VI) from Aqueous Solutions by a Bacterial Biofilm Supported on Zeolite: Optimisation of the Operational Conditions and Scale-Up of the Bioreactor. *Chemical Engineering & Technology* 33:2008–2014.
- Percival, S. L., J. S. Knapp, D. S. Wales, and R. G. J. Edyvean. 1999. The effect of turbulent flow and surface roughness on biofilm formation in drinking water. *Journal of Industrial Microbiology and Biotechnology* 22:152–159.
- Quintelas, C., V. B. da Silva, B. Silva, H. Figueiredo, and T. Tavares. 2011. Optimization of production of extracellular polymeric substances by *Arthrobacter viscosus* and their interaction with a 13X zeolite for the biosorption of Cr(VI). *Environmental technology* 32:1541–9.
- Rakowska, M. I., D. Kupryianchyk, J. Harmsen, T. Grotenhuis, and A. A. Koelmans. 2012. In situ remediation of contaminated sediments using carbonaceous materials. *Environmental toxicology and chemistry / SETAC* 31:693–704.
- Rosales, E., M. Pazos, M. a. Sanromán, and T. Tavares. 2012. Application of zeolite-*Arthrobacter viscosus* system for the removal of heavy metal and dye: Chromium and Azure B. *Desalination* 284:150–156.
- Shaheen, S. M., A. S. Derbalah, and F. S. Moghanm. 2012. Removal of Heavy Metals from Aqueous Solution by Zeolite in Competitive Sorption System. *International Journal of Environmental Science and Development* 3:362–367.
- Silva, B., H. Figueiredo, C. Quintelas, I. C. Neves, and T. Tavares. 2012a. Improved biosorption for Cr(VI) reduction and removal by *Arthrobacter viscosus* using zeolite. *International Biodeterioration & Biodegradation* 74:116–123.
- Silva, B., H. Figueiredo, O. S. G. P. Soares, M. F. R. Pereira, J. L. Figueiredo, A. E. Lewandowska, M. A. Bañares, I. C. Neves, and T. Tavares. 2012b. Evaluation of ion exchange-modified Y and ZSM5 zeolites in Cr(VI) biosorption and catalytic oxidation of ethyl acetate. *Applied Catalysis B: Environmental* 117-118:406–413.

- Soini, S. ., K. . Koskinen, M. . Vilenius, and J. . Puhakka. 2002. Effects of fluid-flow velocity and water quality on planktonic and sessile microbial growth in water hydraulic system. *Water Research* 36:3812–3820.
- Srivastava, V. C., I. D. Mall, and I. M. Mishra. 2009. Competitive adsorption of cadmium(II) and nickel(II) metal ions from aqueous solution onto rice husk ash. *Chemical Engineering and Processing: Process Intensification* 48:370–379.
- Stietiya, M. H., and J. J. Wang. 2006. Effect of organic matter oxidation on the fractionation of copper, zinc, lead, and arsenic in sewage sludge and amended soils. *Journal of environmental quality* 40:1162–71.
- Stotzky, G. 1985. Mechanisms of adhesion to clays, with reference to soil systems. Pages 195–253 *in* D. C. Savage and M. Fletcher, editors. *Bacterial adhesion*. Springer US, Boston, MA.
- Sutherland, I. 2001. Biofilm exopolysaccharides: a strong and sticky framework. *Microbiology (Reading, England)* 147:3–9.
- Valls, M., and V. de Lorenzo. 2002. Exploiting the genetic and biochemical capacities of bacteria for the remediation of heavy metal pollution. *FEMS microbiology reviews* 26:327–38.
- Vieira dos Santos, A. C., and J. C. Masini. 2007. Evaluating the removal of Cd(II), Pb(II) and Cu(II) from a wastewater sample of a coating industry by adsorption onto vermiculite. *Applied Clay Science* 37:167–174.
- Wang, J., and C. Chen. 2009. Biosorbents for heavy metals removal and their future. *Biotechnology advances* 27:195–226.
- Weatherley, L. R., and N. D. Miladinovic. 2004. Comparison of the ion exchange uptake of ammonium ion onto New Zealand clinoptilolite and mordenite. *Water research* 38:4305–12.





# CHAPTER 4

## BRACKISH SYSTEMS

*pp.*

4.	Brackish systems: the S. Vitale park.....	70
4.1.	The study area.....	71
4.2.	Materials and methods.....	71
4.2.1.	Sampling and experimental design.....	71
4.2.2.	Morphological description of soil profiles.....	73
4.1.1.	Physicochemical characterization of soil profiles .....	73
4.1.2.	Data analysis.....	74
4.3.	Results.....	75
4.3.1.	Morphological and physicochemical description of soil continuum.....	75
4.3.2.	Soil classification and discriminant function analysis.....	80
4.4.	Discussion .....	83
4.5.	Conclusion.....	85
4.6.	References.....	86



#### 4. BRACKISH SYSTEMS: THE S. VITALE PARK

Soils in estuary and wetland systems are characterized by different degrees of hydromorphism and permanent water saturation conditions due to the dynamism of both surface and ground-water. In these environments, hydromorphic soils can be occasionally flooded or they can be affected by a shallow water table, enhancing the alternation of anaerobic and aerobic conditions along the soil profile (Vepraskas et al., 2000). On the other hand, subaqueous soils (SASs) can develop in permanent saturation conditions, where a water column of up to 2.5 m is present.

The introduction of SASs into USDA soil classification opens a new frontier in soil science because it offers the possibility to investigate the pedological and physicochemical processes occurring in transitional and subaqueous systems (Ferreira et al., 2007). From the point of view of soil forming processes, the soils sequence characterized by partial or permanent water saturation, can be considered a “*soil continuum*” and the key role of the water table level on soil development can be investigated.

The San Vitale park has been chosen to investigate soil development along a soil sequence from a submerged wetlands environment to a hydromorphic interdune one, aiming to: (i) characterize distinct pedons with different hydromorphic degrees from the wetland to the interdune morphological system and (ii) identify which variables, among the soil chemical properties, can better describe the common features and differences in the soil sequence which defines the “*soil continuum*”.

This work have been carried out with the collaboration of colleagues from BIGEA (University of Bologna) and the following scientific production resulted from this research:

- Ferronato, C., Falsone, G., Natale, M., Zannoni, D., Buscaroli, A., Vianello, G., Vittori Antisari, L. Chemical and pedological features of subaqueous and hydromorphic soils sequence in an intradune-wetland system (San Vitale park, Northern Italy). *Geoderma- submitted*.

## **4.1. THE STUDY AREA**

San Vitale park is a protected area of 1 222 ha which stands in the southern part of the Po Estuary Regional Park (Northern Italy). The area emerged between X and XVI centuries from alluvial deposits of an ancient branch of the Po river and of some of the Apennine's watercourses, and it acquired its present appearance before the last intervention of canalization during the XX century (Ferronato et al., 2014). The long sedimentation process allowed for the evolution of a dune/infra-dune coastal system and of an alluvial wetland called "*Pialassa*", which originally created by a sea loch inclusion during the XVIII century (Buscaroli et al., 2011; Veggiani, 1974).

San Vitale park is characterized by a sub continental temperate climate with about 600 mm of annual rainfall during all the year, and an annual mean temperature of about 13°C (Pinna, 1978). Rainfalls, temperature oscillations, and evapotranspiration phenomena deeply affect the groundwater depth and the magnitude of saline intrusion in the deep aquifer (Amorosi et al., 2005; Castiglioni et al., 1999). Moreover, the over-exploitation of freshwater aquifer for agricultural purposes has caused a rise of the fresh vs salt water interface and consequently the increase of saline intrusion problems and the intensification of subsidence (Buscaroli and Zannoni, 2010).

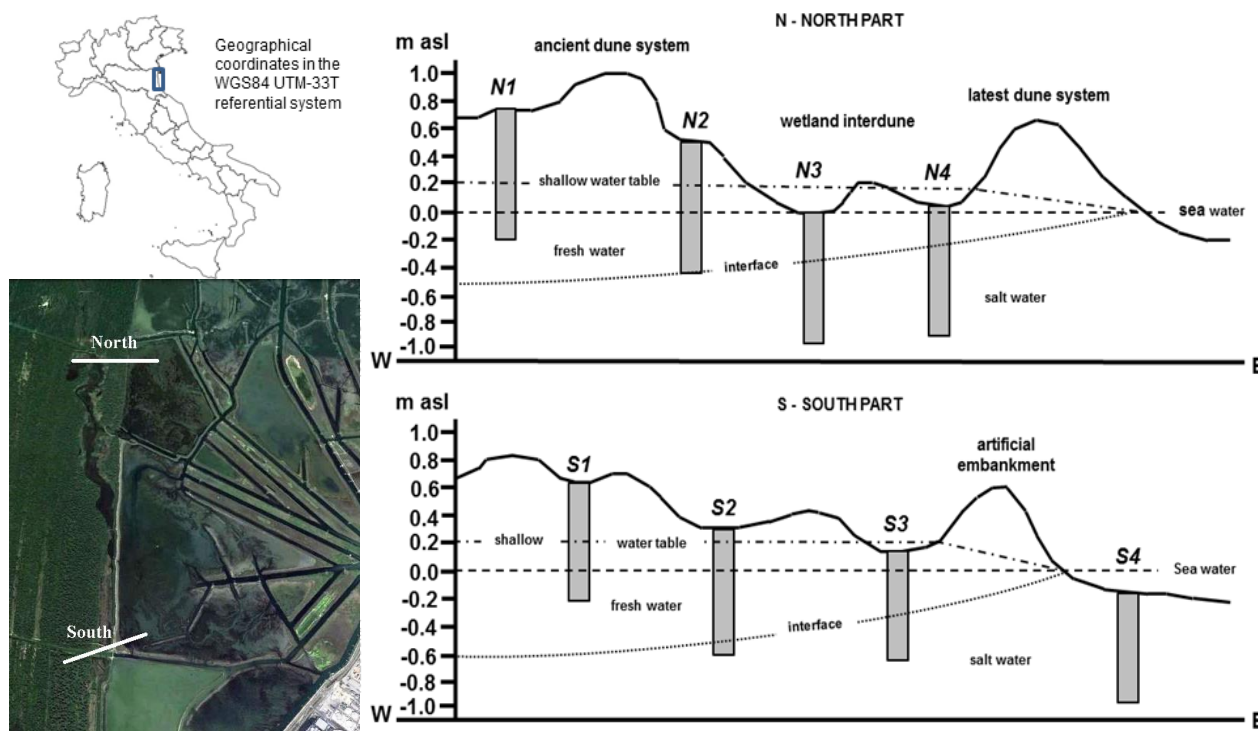
The northern part of the study area is influenced by the Lamone river, while the southern part is crossed by the Cerba canal, which serves as collector of agricultural and landfill discharges of the surrounding area. Due to the intensity of subsidence problems, which increase from north to south, the southern part results morphologically lower than the northern one (Gambolati, 1998; Teatini et al., 2005; Zannoni, 2008).

## **4.2. MATERIALS AND METHODS**

### **4.2.1. Sampling and experimental design**

The soil survey has been carried out in both the northern and southern parts of the park, according to their morphological position (Figure 4.1). Soil samples were collected in both interdunal and wetland areas in order to catch a different hydromorphic degree and the localization of each soil profile and localization is shown in Appendix 4.

**Figure 4.1.** Localization of the study area, and morphological distribution of soil profiles.



Hydromorphic soil profiles in the interdunal sites were excavated and each genetic horizon was described in field according to Schoeneberger et al. (2012).

Subaqueous soil profiles were collected at a depth of 1.5 m using a vibracore sampler, type Becker (Eijkelkamp, NL), equipped with a polyethylene tube with a diameter of 6 cm.

The depth of the water column upon the soil surface was recorded before column extraction. Sample cores were immediately sealed with a tight stopper to avoid oxygen infiltration and stored at 4°C until laboratory analysis.

In both studied sites, the highest and the western-most soil profiles (N1 and S1, about 0.7-0.8 m a.s.l.) have been excavated in ancient interdunal areas, mainly covered by hygrophilous species (e.g. *Fraxinus oxycarpa*, *Populus alba*, *Ulmus minor*) and mesophilous species (e.g. *Quercus robur*, and *Quercus pubescens*).

In the middle position, soil profiles (N2 and S2, about 0.5-0.4 m asl) have been excavated on a recent interdunal area which are seasonally affected by flooding phenomena and which is mainly covered by Gramineae family and *Juncus* spp.

In a lower and more eastern position, subaqueous soils (N3, N4 and S3, around 0 m a.s.l.) were collected in the wetland area characterized by the presence of brackish waterholes and colonized by *Juncus* spp. and halophyte species such as *Arthrocnemum fruticosum*.

In the lowest and most easterly position of the wetland (*Pialassa*), near to the Adriatic sea, a further subaqueous soil profile has been collected (S4, about -0.2 m a.s.l.).

#### **4.2.2. Morphological description of soil profiles**

Each genetic horizon of hydromorphic soil profiles was described in field according to Schoeneberger et al. (2012). The morphological features recorded, included horizon depth, boundary, Munsell color (wet), consistence of the matrix, presence of coats/films and redoximorphic features, roots and biological concentration. Samples were then sealed in polyethylene bags and stored at 4°C until analysis.

Soil columns were extracted in laboratory on a suitable support and each genetic horizon was described for its depth, boundary, Munsell colour, coats/films and redoximorphic features, organic fragments, fluidity class (McVey et al., 2012).

The presence of monosulphides was observed through the colour response of the matrix after adding some drops of 3% H<sub>2</sub>O<sub>2</sub> (McVey et al, 2012) and by recording the odour description of each soil horizon (Fanning and Fanning, 1989; Fanning et al., 2002).

#### **4.2.3. Physicochemical characterization of soil profiles**

All analytical methods for soil physicochemical characterization were accurately described in section 2.2.3.

Briefly, electrical conductivity (EC; conductimeter Orion) and pH (pHmeter, Crison) measures of all samples were performed on 1:2.5 (w:v) soil:distilled water suspension.

Soil particle size distribution was determined by pipette method (Gee and Bauder, 1986) and total carbonates (CaCO<sub>3</sub>) were quantified by volumetric method, according to Loeppert and Suarez (1996).

Total organic carbon (OC) and total nitrogen (TN) were measured by Dumas combustion with a EA 1110 Thermo Fisher CHN elemental analyser after dissolution of carbonates with 2M HCl.

The pseudo-total concentration of macronutrients (P, K, S, Na, Ca, Mg, Fe and Mn) was detected by Inductive Coupled Plasma – Optic Emission Spectroscopy (ICP-OES, Ametek, Germany) after treating samples with aqua regia in microwave oven (Milestone, 1200).

Cation exchange capacity (CEC) was determined after exchange with ammonium acetate (pH 7) according to Summer and Miller (1996) and Vittori Antisari et al. (2015).

All soils samples were air-dried and sieved at 2 mm before analysis (Balduff, 2007). A wet subsample of subaqueous soils had been previously collected and soon incubated aerobically for 8 week in 1:1 w:v soil:distilled water. The pH was recorded periodically during this time, in order to detect the lowering of pH due to acid sulphate weathering oxidation in soil horizon which contain reduced sulphides (Bradley and Stolt, 2003; Soil Survey Staff, 2010).

#### **4.2.4. Data analysis**

All analysis were performed with Statistica 10 software (StatSoft, Tulsa, OK, USA).

*Minimum (Min), Maximum (Max), and quartiles distribution* of some variables were calculated to design some boxplot graphs in order to highlight the variability of the physicochemical properties within and between the soil profiles.

*Matrix correlations* (MX) were performed to highlight the single correlation between variables and significance level ( $p < 0.05$ ) was checked with Fisher approach.

*Discriminant function analysis* (DFA) was performed with stepwise forward method to identify which continuous variables related to the chemical properties (e.g., pH, EC,  $\text{CaCO}_3$ , OC, TN, P, K, S, Na, Ca, Mg, Fe and Mn) could discriminate the distinct pedons according to their great group classification (Soil Survey Staff, 2014). The statistical significance of each discriminant function was checked with Wilk's lambda test and the SCDC was used to rank the importance of each variable as described in section 2.2.6.

## 4.3. RESULTS

### 4.3.1. Morphological and physicochemical description of soil continuum

The summary of the morphological features of each soil profile is presented in Table 4.1 while their chemical properties are shown in Tables 4.2 and 4.3, respectively.

Both hydromorphic and subaqueous soil profiles showed a O/A/AC/C horizon sequence.

The thickness of organic horizons (O) ranged from 5 to 14 cm in the northern part and from 3 to 6 cm in the southern one. Similarly, the organo-mineral A/AC horizons were thicker in the northern sites than in southern ones. Notably, the wetland pedon in the *Pialassa* (S4) showed some intercalations of buried organic matter-rich horizons down to the soil profile.

However, mineral horizons with the presence of organic fragments characterized by different decomposition degree were found in wetland soils (N3-4 and S3-4) at different depths. In these horizons the pH decreased at least of 2.01 point and sulfidic materials were found (Table 4.2).

**Table 4.1.** Morphological features of the hydromorphic (a) and subaqueous soils (b). Codes according to Shoenenberg et al (2012) and McVey et al. (2012) respectively.

(a)	Depth (cm)	Master Horizon	Boundary (D/T)	Matrix Color (WET)	Mottles/RMFs (K/Q/S)	Field texture class	Structure	Organic frags/Roots (Q/S)
N1	5 - 0	Oi	CW	nd		nd	nd	nd
	0 - 5	A1	CW	2,5Y 3/1		S	gr fl	2/f
	5 - 20	A2	AS	2,5Y 3/2		S	sg	1/f-1/m
	20-80	Cg1	CW	2,5Y 5/1	F2M/m/3	S	sg	1/m
	80-100+	Cg2	U	Gley 1 5/1	F2M/c/3	S	sg	
N2	3 - 0	Oi	AW	nd		nd	nd	nd
	0 - 5	A1	CS	2,5Y 2,5/1		S	gr fl	2/f
	5 - 10	A2	CW	2,5Y 3/1		S	gr fl	1/f-1/m
	10 - 35	ACg	AW	2,5Y 3/1	OSF/m/2	S	sg	1/m
	35 - 45	Cg1	CW	Gley 1 5/1	F2M/c/3/1	S	sg	1/f
	45-100	Cg2	U	Gley 1 6/1	F2M/c/3/1	S	sg	
S1	3-0	Oi	AW	nd		nd	nd	
	1 - 0,5	Oe	AW	nd		nd	nd	
	0,5 - 0	Oa	AW	nd		nd	nd	
	0 - 3/8	A	CS	2,5Y 2,5/1		LS	gr fl	
	3/8- 25	ACg	AS	2,5Y 4/2	OSF/c/5/4	LS	gr fl	
	25 - 50	Cg1	CS	2,5Y 5/2	OSF/c/5/4	S	sg	
	50 - 80	Cg2	GS	2,5Y 5/1		S	sg	
	80-100	Cg3	U	Gley 1 6/1		S	sg	
S2	3 - 1	Oi	AW	nd		nd	nd	nd
	1 - 0	Oe	AW	nd		nd	nd	nd
	0 - 2/5	A	AW	2,5Y 2,5/1		LS	gr fl	3/f-3/vf
	2/5- 10	Ag	CS	2,5Y 4/1		SL	sg	2/vf
	10 - 30	Cg1	CS	2,5Y 4/3		LS	sg	1/vf
	30 - 80	Cg2	CS	2,5Y 5/2	OSF/c/5/4	LS	sg	1/vf
	80-100	Cg3	U	Gley 1 6/1	OSF/c/2	S	sg	



(b)	Depth (cm)	Master Horizon	Matrix Munsell Color (WET)	Coarse Frags (%)	Organic frags/Roots(%)	Mottles/RMFs (K/Q/S)	Field texture class	Odor (K/I) HCl	
N3	0-14	Oeg	Gley2 2.5/10B	2	30	FED/m/1	SL	S/MD	S/SL
	14-20	Ase1	Gley1 4/10Y		20	OSF/ m/1	SL	S/MD	S/SL
	20-40	Ase2	Gley1 4/10Y		15	OSF/m/1	LS	S/MD	S/SL
	40-45	Cg1	Gley 1 3/10Y		5	F2M/m/1	S	N	N
	45-100	Cg2	Gley 1 3/10Y	5	5	F2M/m/1	S	N	N
N4	0-8	Oig	Gley2 2.5/5B	15	50			N	S/ST
	8-18	Ase	Gley 2 2.5/10B	10	40		S	N	S/ST
	18-35	Ag	Gley 2 2.5/5Pb	5	20	OSF/f/1	S	N	S/MD
	35-49	Cg1	Gley 2 2.5/10B	5	5	OSF/f/2	S	N	S/MD
	49-80	Cg2	Gley 2 2.5/10B	5	5	OSF/f/1	S	N	S/MD
S3	4-0	Oi	Gley 1 2.5/10Y	nd	25	OAF/c/1	LS	N	S/SL
	0-6	O/Ag	Gley1 3/10Y	3	15	F2M/c/1	LS	N	S/SL
	6-13	A	Gley1 4/10Y	15	15		LS	N	N
	13-20	ACse1	Gley1 2.5/N	0		F2M/c/1	SL	N	S/ST
	20-36	ACse2	Gley1 4/10Y	0	5	F2M/f/2	LS	N	S/SL
S4	36-60	Cg1	5 Y4/1	0		F2M/f/2	S	N	N
	60-83	Cg2	6 Y4/1	0	10	FED/c/4	S	N	S/SL
	0-6	Ag1	Gley1 2.5/N	60			LS	S/MD	S/S
	6-13	Ag2	Gley1 3/N	1			L	S/MD	S/S
	13-20	Ag3	Gley1 3/N	2			SL	S/MD	S/S
S4	20-35	O/Cg	Gley1 3/N		20	OAF/f/2	SCL	S/MD	S/MD
	35-50	Cse1	Gley1 4/N		20	OAF/f/2	CL	S/ST	S/MD
	50-57	Cse2	Gley1 2.5/N		20	OSF/f/2	CL	S/ST	S/S
	57-64	Cse3	Gley1 5/10GY		10	F2M/f/2	CL	S/ST	S/MD
	64-70	Cse4	Gley1 2.5/N	2	1		LS	S/MD	S/ST
S4	70-80	Cg	Gley1 3/10Y	2			LS	S/MD	S/MD
	80-90	O/Cg1	Gley1 5-4/10Y	1			S	S/MD	S/MD
	90-98	O/Cg2	Gley1 5-4/10Y		60	OSF/m/3	S	S/MD	S/MD

**Horizon master:** g=gleying. **Horizon boundary:** (D)Distinctness: A=abrupt, C=clear, G=gradual, D=diffuse - (T) **Topography:** S=smooth, W=wavy, I=irregular, U=unknown. ; **Structure:** (T) Type: GR = granular, ABK= angular blocky, SBK = subangular blocky, PL = platy, SG = single grain / (G) **Grade:** 0 = structureless, 1 = weak, 2 = moderate - (S) **Size:** vf = very fine, f = fine, m = medium; **Field texture class:** S=sand, SL=Sandy Loam, L=Loam, LS=Loamy Sand, SCL= Silty Clay Loam; **Mottles/redoximorphic features (RMFs):** (K) **Kind:** FED=iron depletions, FEF=ferriargillans, F2M=reduced iron FeS, OAF=organoargillans, OSF=organic stains; (Q) **Quantity:** f=few, c=common, m=many; (S) **size:** 1=fine, 2=medium, 3=coarse, 4=very coarse, 5=extremely coarse - **Roots:** (Q) **Quantity:** 1=few, 2=common, 3=many / (S) **Size:** vf=very fine, f=fine, m=medium, co=coarse. **Peroxide color change:** Y=yes; N=no. **Odor:** (K) Kind: N = none, S = sulphurous - (I) Intensity: SL = slight, MD = moderate, ST = strong.

In all pedons, a sandy or sandy-loam texture was noticed, with exception of the *Pialassa* S4 pedon in which some clay and silty-clay-loam deposits were detected (Table 4.1). Moreover, the soil matrix of subaqueous soils was characterized by gley Munsell color, while in hydromorphic soil profiles only deep C horizons showed gley colour (Table 4.1).

**Table 4.2.** Chemical properties of hydromorphic soil profiles sampled in the interdunal area.

Pedon	Horizon	Depth cm	pH		EC mS cm <sup>-1</sup>	ESP %	CEC cmol kg <sup>-1</sup>	OC	TN	Na	P	S g kg <sup>-1</sup>	Ca g kg <sup>-1</sup>	Mg	Al	Fe	Mn	OC/S
			In.	Fin.														
N1	A1	0-5	nd	7,05	1,95	3.1	18.7	71.2	5.5	0.2	0.5	2.1	3.7	2.9	8.7	10.2	0.3	34.4
	A2	5-20	nd	7,58	0,71	1.9	19.7	36.6	2.4	0.1	0.5	1.0	3.4	3.4	12.7	13.2	0.3	37.7
	Cg1	20-50	nd	8,33	0,17	0.3	32.4	1.3	0.7	0.1	0.5	0.1	17.6	3.8	9.6	12.2	0.4	12.3
	Cg2	80-100+	nd	8,22	0,15	0.2	18.9	1.8	0.1	0.1	0.5	0.1	17.5	3.8	9.5	12.6	0.4	15.4
N2	A1	0-5	nd	7,28	5,47	32.3	38.2	76.7	5.7	1.2	0.5	1.6	3.8	3.0	7.7	10.5	0.2	49.0
	A2	5-10	nd	6,76	5,18	23.8	28.2	51.7	3.7	1.4	0.5	1.5	2.9	3.2	9.5	11.1	0.2	35.2
	ACg	10-24	nd	6,96	5,14	47.1	26.5	28.9	2.3	0.9	0.5	0.9	4.0	3.2	10.6	11.7	0.2	33.0
	Cg1	35-45	nd	7,95	2,29	4.9	46.4	4.0	0.3	0.5	0.5	0.4	19.5	3.9	11.9	14.2	0.4	11.3
	Cg2	80-100+	nd	8,20	2,64	21.1	44.9	1.9	0.2	0.6	0.4	0.5	19.4	3.9	9.2	11.8	0.4	4.2
S1	A	0-5	nd	7,4	4,25	41.3	60.5	118.1	7.6	1.3	0.5	2.2	8.7	3.6	10.1	11.4	0.4	54.4
	ACg	5-13	nd	8,1	4,02	23.2	68.5	25.9	2.2	0.9	0.4	0.6	11.4	3.8	10.7	12.8	0.3	38.5
	Cg1	13-50	nd	8,6	1,46	14.2	33.6	4.3	0.7	0.4	0.4	0.1	23.5	4.0	11.5	13.6	0.7	20.6
	Cg2	50-80	nd	8,5	1,24	12.0	51.3	6.3	0.2	0.3	0.4	0.1	23.0	3.9	9.8	12.8	0.5	7.0
	Cg3	80-100+	nd	8,5	1,05	6.4	59.4	2.1	0.2	0.3	0.4	0.1	22.7	4.1	11.8	14.4	0.5	8.0
S2	A	0-5	nd	8,10	3,01	16.8	78.6	49.3	4.1	0.7	0.5	0.9	3.7	3.3	12.0	12.2	0.3	52.6
	Ag	5-10	nd	8,52	3,00	16.3	80.2	21.4	2.1	0.7	0.4	0.6	5.8	3.6	15.4	14.3	0.3	43.3
	Cg1	10-30	nd	8,65	2,28	11.7	77.7	3.9	0.5	0.5	0.4	0.2	19.7	3.7	10.8	13.3	0.4	43.4
	Cg2	30-80	nd	8,48	3,57	0.4	44.9	2.1	0.3	0.8	0.4	0.3	25.3	3.7	9.9	12.1	0.5	71.2
	Cg3	80-100+	nd	8,56	3,56	0.3	65.5	2.0	0.2	0.8	0.4	0.3	23.6	3.8	10.4	12.2	0.5	36.6

**ESP**=exchangeable sodium percentage obtained by [Na] exchangeable/CEC; **CEC**= cation exchangeable capacity; **OC**= total organic carbon; **TN**= total nitrogen; **OC/S**= organic carbon/ total sulphur ratio

Generally, the organic C (OC) and total N (TN) content decreased along the soil profiles: higher values were detected in the hydromorphic soils than in the SASs, while distinct intercalations, characterized by different OC and TN values, were noticed in the S4 pedon, confirming the presence of buried organic matter-rich horizons.

The average content of Na, S, Ca and Mg in subaqueous soils was significantly higher ( $p<0.05$ ) than that detected in hydromorphic ones. In particular, the highest Na content was found in the N3 soil of the wetland area.

**Table 4.3.** Chemical properties of subaqueous soil profiles sampled in the wetland area.

Pedon	Horizon	Depth cm	pH		EC mS cm <sup>-1</sup>	OC	TN	Na	P	S	Ca g kg <sup>-1</sup>	Mg	Al	Fe	Mn	OC/S
			In.	Fin.												
N3	<i>Oeg</i>	0-14	7.9	6.9	21.5	53.8	6.2	31.7	1.4	8.6	94.5	13.4	4.3	44.7	1.6	6.3
	<i>Ase1</i>	14-20	8.0	7.0	16.2	33.8	3.6	19.8	0.8	5.5	101.2	11.8	5.7	34.7	1.6	6.2
	<i>Ase2</i>	20-38/40	8.3	7.1	11.5	17.1	1.6	7.6	0.5	3.2	81.0	10.1	6.5	15.6	1.2	5.3
	<i>Cg1</i>	38/40-45	8.6	7.9	6.8	3.4	0.2	3.7	0.3	1.5	44.2	9.5	7.2	11.2	0.4	2.2
	<i>Cg2</i>	45-100+	8.9	nd	nd	1.8	0.0	2.2	0.4	1.1	39.7	10.3	7.5	11.7	0.4	1.6
N4	<i>Oig</i>	0-8	nd	nd	nd	23.6	2.4	1.2	0.6	4.0	60.8	10.1	8.5	12.3	0.5	5.8
	<i>Ase</i>	8-18	8.5	7.5	9.9	3.2	0.2	0.8	0.4	1.8	42.3	8.2	6.4	9.8	0.4	1.8
	<i>Ag</i>	18-35	8.6	7.6	9.3	2.4	0.1	0.8	0.4	1.6	44.9	9.0	7.2	11.1	0.4	1.5
	<i>Cg1</i>	35-49	9.2	8.1	12.4	2.7	0.1	1.1	0.4	1.5	46.3	9.3	7.6	12.0	0.5	1.8
	<i>Cg2</i>	49-80+	8.9	nd	nd	1.9	0.1	1.9	0.3	1.8	45.9	10.3	8.7	13.4	0.5	1.0
S3	<i>Oi</i>	4-0	7.7	6.5	5.7	25.0	3.1	4.0	0.4	3.8	48.1	9.7	14.6	12.7	0.5	6.7
	<i>O/Ag</i>	0-6	7.8	6.5	4.4	20.6	1.9	3.0	0.3	3.3	40.8	8.8	12.3	11.4	0.4	6.3
	<i>A</i>	6-13	8	6.7	3.1	21.2	1.9	3.0	0.3	3.7	41.3	9.2	14.2	12.4	0.4	5.7
	<i>ACse1</i>	13-20	8.2	6.2	2.4	13.7	1.5	1.3	0.2	1.6	20.7	4.9	7.9	6.9	0.2	8.8
	<i>ACse2</i>	20-36	8.4	7.4	2.5	3.8	0.6	1.5	0.3	0.7	48.5	8.9	12.4	11.7	0.5	5.8
	<i>Cg1</i>	36-60	8.3	8.4	2.2	1.1	0.3	1.0	0.3	0.1	48.7	8.8	10.5	11.4	0.4	11.0
	<i>Cg2</i>	60-83+	8.3	8	2.4	1.2	0.3	1.3	0.3	0.1	49.1	8.8	11.9	13.2	0.4	11.8
S4	<i>Ag1</i>	0-6	8.2	6.5	5.1	7.4	1.1	4.0	0.3	2.4	52.7	8.6	11.8	9.9	0.3	3.0
	<i>Ag2</i>	6-13	8.5	6.8	7.8	10.6	1.1	4.6	0.4	8.3	52.8	12.8	24.6	18.2	0.5	1.3
	<i>Ag3</i>	13-20	8.3	6.6	6.8	11.1	0.9	4.2	0.3	5.8	53.4	9.8	14.0	13.4	0.5	1.9
	<i>O/Cg</i>	20-35	8.4	6.9	13.9	26.6	2.5	4.7	0.5	9.1	49.4	14.1	29.4	19.4	0.5	2.9
	<i>Cse1</i>	35-50	8.7	7.0	7.1	16.2	1.4	4.7	0.4	8.5	56.2	13.0	26.7	19.1	0.6	1.9
	<i>Cse2</i>	50-57	8.9	7.8	7.4	11.5	1.6	4.6	0.4	4.9	66.2	14.1	26.5	18.3	0.7	2.4
	<i>Cse3</i>	57-64	9.0	7.4	6.8	8.0	1.0	4.6	0.4	2.9	70.8	14.2	25.1	16.5	0.8	2.8
	<i>Cse4</i>	64-70	8.8	7.8	2.9	6.4	0.6	3.5	0.3	1.3	57.2	7.9	9.6	10.3	0.4	5.1
	<i>Cg</i>	70-80	8.5	6.9	2.01	4.2	1.3	2.8	0.3	1.1	62.5	7.0	7.9	9.8	0.4	4.0
	<i>O/Cg1</i>	80-90	8.1	6.1	4.46	10.5	1.3	3.2	0.2	4.8	54.9	5.9	6.5	8.5	0.4	2.2
	<i>O/Cg2</i>	90-98+	7.8	7.3	11.16	22.8	1.1	4.1	0.3	8.2	58.7	6.3	6.4	10.0	0.4	2.8

OC = total organic carbon; TN= total nitrogen; OC/S= organic carbon/ total sulphur ratio

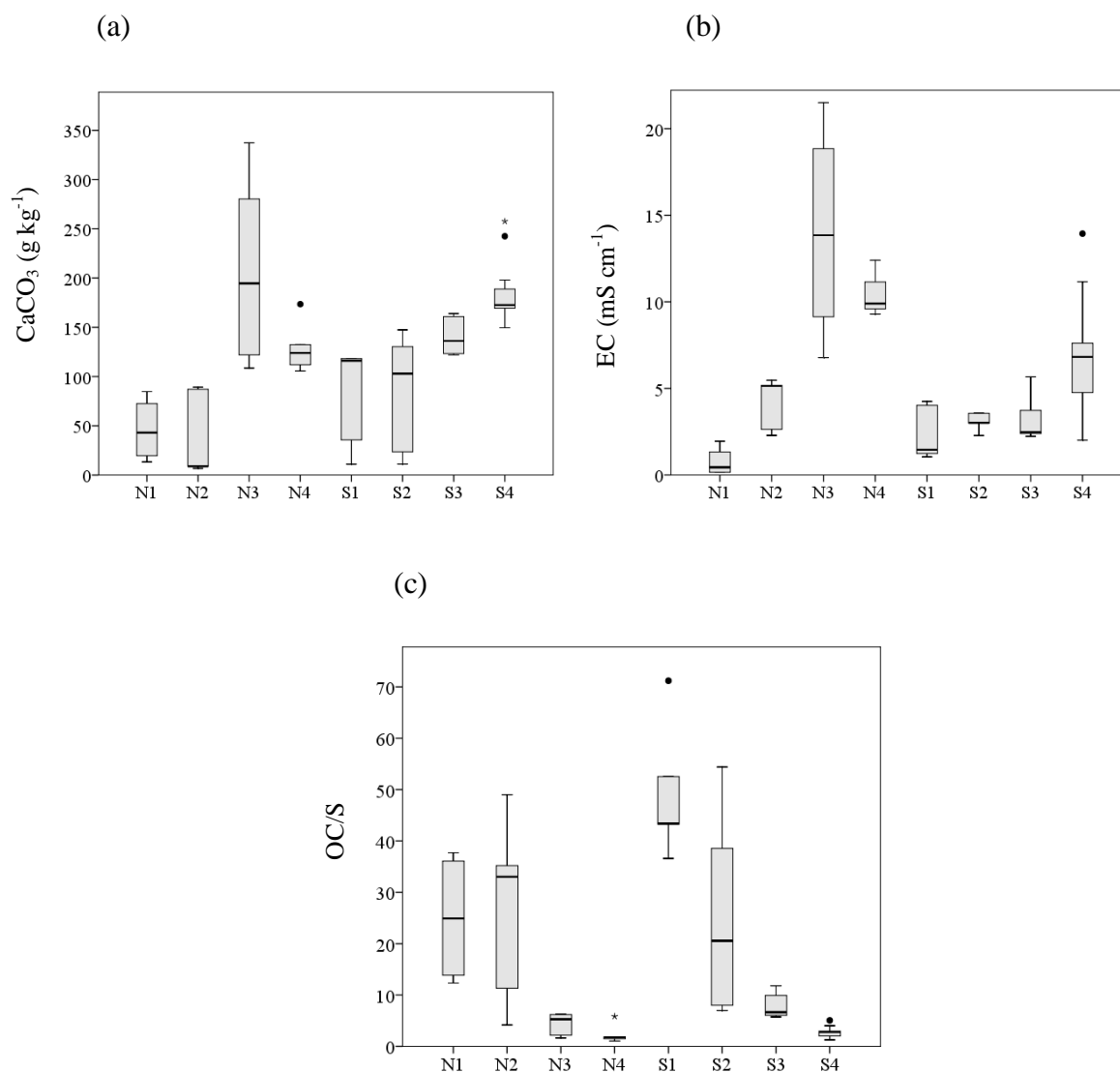
Carbonate contents (Figure 4.2a) were higher in wetland soils than in the interdunal ones. In the first case, carbonates content ranged from 105 to 337 g kg<sup>-1</sup>, while it decreased from top to sub-soil, ranging from 7 to 147 g kg<sup>-1</sup> in the hydromorphic pedons.

Similarly, the EC trend decreased from wetland to interdunal ecosystem (Figure 4.2b). In the S2 hydromorphic soil, the EC increased in the deep horizons, while in subaqueous ones an irregular EC value trend was noted in S3 and S4 (Table 4.2 and 4.3).

The processes linked to the evolving of anaerobic conditions in pedons were investigated using the organic carbon:sulphur ratio (OC/S) according to Ivanov et al. (1989), and OC/S boxplots of each pedons are shown Figure 4.2c.

The OC/S ranged from 11.8 to 1.3 in subaqueous soils (N3-4 and S3-4) while the ratio increased in interdunal hydromorphic soils depending on horizon depth and on its water saturation condition (Table 4.2). In these pedons, the OC/S ratio ranged from 4.2 to 71.2 and its values were lower than 10 only in deep gley horizons.

**Figure 4.2.** Minimum, maximum and quartile distribution of Carbonates  $\text{CaCO}_3$  (a), Electrical Conductivity EC (b) and OC/S (c) in the soil profiles.



High variability along the pedons for all chemical parameters were detected and in order to better understand the relationship between these variables, soil layers have been grouped into superficial organo-mineral aerated horizons and mineral deep anaerobic ones, assuming that strict anaerobic conditions in subaqueous soils generally occur below the first 10/20 cm (Reddy and DeLaume, 2008). All chemical variables have been correlated using two distinct correlation matrixes for superficial organo-mineral and deep mineral horizons, as shown in Table 4.4 (a) and (b) respectively.

In both matrixes  $\text{CaCO}_3$  and EC were positively correlated with the total concentration of Ca, Mg, Na, Fe, Mn and S, while OC and TN were correlated to these elements only in the deep mineral soil horizons group.

In both matrixes, total P showed significant positive correlations with Fe and Mn content while Mg, Ca and Na amounts were positively correlated between them.

In superficial organo-mineral horizons, S content showed a significant positive correlation with carbonate content ( $r=0.77$ ) while the former had a negative correlation with pH ( $r=-0.50$ ). In deep mineral horizons, S content was strongly positively correlated with OC ( $r=0.92$ ) and negatively with pH ( $r=0.69$ ).

**Table 4.4.** Matrix correlation between physicochemical variables in the superficial organo-mineral horizons (a) and in the deep mineral horizons (b) of all pedons. Only correlations with  $p \leq 0.05$  are shown.

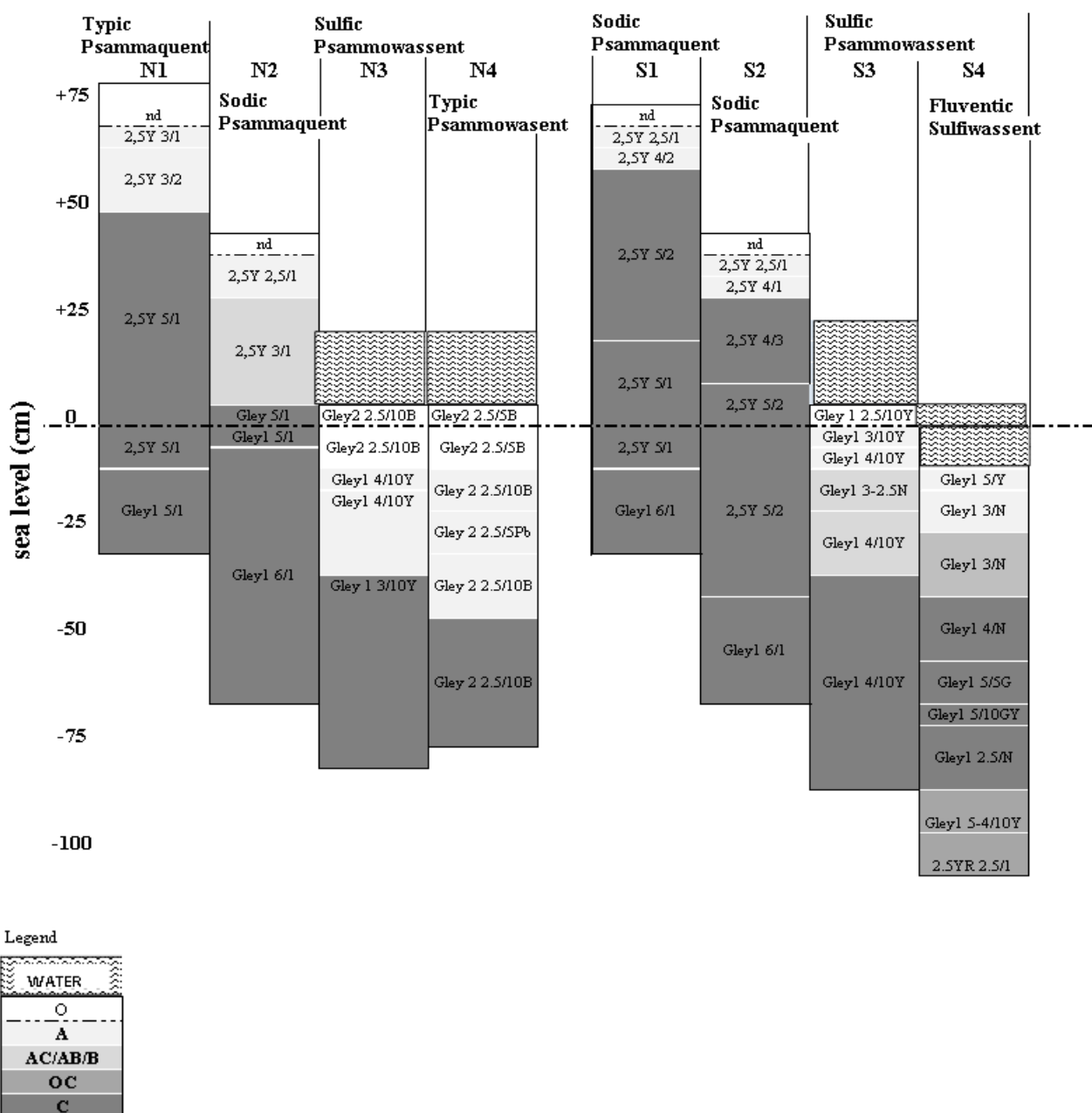
		$\text{CaCO}_3$	pH	EC	TN	OC	Al	Ca	Fe	K	Mg	Mn	Na	P	S
(a)	$\text{CaCO}_3$	1.00	1.00												
	pH	0.77		1.00											
	EC														
	TN				1.00										
	OC				0.95	1.00									
	Al						1.00								
	Ca	0.98		0.83				1.00							
	Fe	0.72		0.89				0.75	1.00						
	K						0.89			1.00					
	Mg	0.89	-0.49	0.72				0.94	0.62	0.50	1.00				
	Mn	0.85		0.88				0.86	0.95			1.00			
	Na	0.79		0.93				0.82	0.97		0.69	0.94	1.00		
	P	0.44		0.82	0.56		-0.47	0.51	0.91			0.80	0.88	1.00	
	S	0.77	-0.50	0.72				0.81	0.69	0.51	0.90	0.69	0.73	0.49	1.00
		$\text{CaCO}_3$	pH	EC	TN	OC	Al	Ca	Fe	K	Mg	Mn	Na	P	S
(b)	$\text{CaCO}_3$	1.00													
	pH	-0.53	1.00												
	EC		-0.48	1.00											
	TN	0.61	-0.73	0.53	1.00										
	OC	0.45	-0.64	0.71	0.84	1.00									
	Al	0.46			0.60	0.47	1.00								
	Ca	0.86	-0.71	0.59	0.63	0.54		1.00							
	Fe				0.52	0.47	0.87		1.00						
	K	0.63			0.68	0.54	0.97	0.42	0.78	1.00					
	Mg	0.70	-0.51	0.65	0.62	0.53	0.70	0.78	0.60	0.74	1.00				
	Mn	0.49						0.50	0.55		0.42	1.00			
	Na	0.74	-0.71	0.66	0.77	0.76		0.87		0.50	0.73	0.62	1.00		
	P								0.57			0.48		1.00	
	S	0.46	-0.69	0.72	0.80	0.92	0.55	0.55	0.46	0.63	0.61		0.71		1.00

#### 4.3.2. Soil classification and discriminant function analysis

Both hydromorphic and subaqueous soils have been ascribed to Entisols order and ranked into *Aquents* and *Wassents* suborder according to the Keys of Soil Taxonomy 12<sup>th</sup> edition (Soil Survey Staff, 2014).

The distribution of soil profiles according to their classification and morphological section is shown in Figure 4.3.

**Figure 4.3.** Soil classification and pedo-sequence of soil profiles.



The classification into the suborder has been driven firstly by the hydrological condition of the pedons. In fact, all hydromorphic soils are characterized by aquic conditions at a depth between 40 and 50 cm (*Aquent*), while SASs are distinguished by a positive water potential at the soil surface for more than 21 h of each day in all years (*Wassent*).

The sandy or sandy loam texture class and the presence of less than 35% by volume of rock fragments allowed both hydromorphic and SASs to be classified at great group level as *Psammaquents* and *Psammowassents* respectively, with the exception of the S4 pedon (*Sulfiwassent*).

Additional specific properties of each pedon have been identified at subgroup level.

Among the hydromorphic soils, the N1 pedon has been classified as *Typic Psammaquent*, while the other pedons in the interdunal area (N2, S1 and S2) were classified as *Sodic Psammaquent* because of the exchangeable sodium percentage (ESP) higher than 15% in some horizons (Table 2).

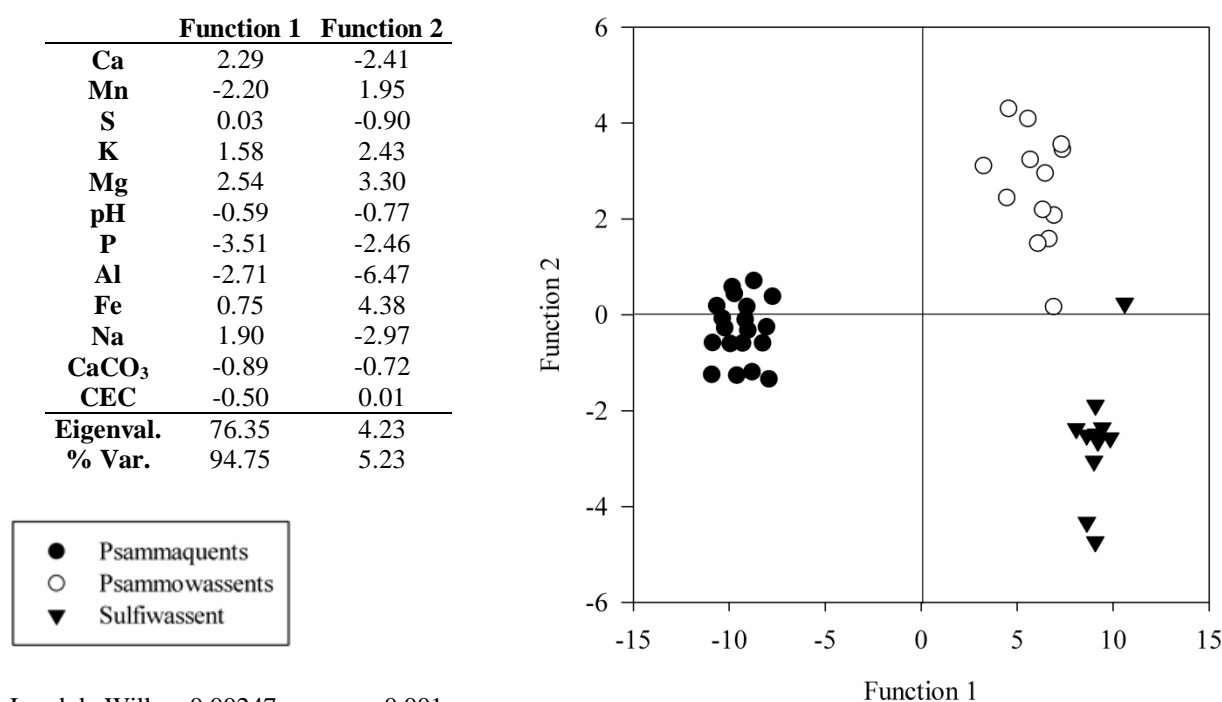
The classification of both N3 and S3 subaqueous soils as *Sulfic Psammowassent* was due the presence of an horizon with a combined thickness of 15 cm within 100 cm of the mineral soil surface than contain sulfidic materials.

The N4 pedon has been classified as *Typic Psammowassent*, despite the presence of sulfidic materials because the thickness of the sulfidic horizon did not meet the parameters of the Keys of Soil Taxonomy (Soil Survey Staff, 2014) for the sub-group classification.

The lowest subaqueous soil (S4) has been classified as *Fluventic Sulfiwassent* because of the presence of sulfidic materials in horizons of at least 15 cm thick within 50 cm of the mineral soil surface, and because of an irregular organic carbon distribution (Holocene age) between the depths of 25 and 125 cm.

A discriminant function analysis (DFA) has been performed using USDA great groups as pre-defined groups separation (i.e., *Psammaquent*, *Psammowassent*, *Sulfiwassent*) and the summary of the evaluations (standardized coefficients and score plot) is shown in Figure 4.4.

**Figure 4.4.** Canonical score plot and standardized coefficients (SCDC) of the discriminant function analysis (DFA) based on the great group classification (Soil Survey Staff, 2014). Only significant variables included in the model are shown.



Lambda Wilks> 0.00247 appros; <0.001

Figure 4.4 shows how Function 1 explained almost 95% of the total variance and it divided the hydromorphic soils (*Aquents*) from subaqueous ones (*Wassents*): Function 1, according to the positive and negative SCDCs, highlighted an increase of Mg, Ca and Na content in SASs and an enhancement of total P amount in hydromorphic ones.

Function 2, even if it represented only the 4% of the total variance, divided *Psammowassents* (N3-4 and S3) from *Sulfiwassent* (S4) allowing for the discrimination of the great groups within the *Wassent* suborder: the first group was characterized by an increase of total Fe, Mg and K content, while a higher content of Al, Na, P and Ca in *Sulfiwassent* than that of the *Psammowassents* was found.

#### 4.4. DISCUSSION

The soils genesis of S. Vitale park have been characterized by different processes linked to alluvial deposits sedimentation and wetland formation (Bondesan et al., 1995), and nowadays they are affected by different natural and anthropic phenomena, e.g. subsidence, saline intrusion, freshwater management (Buscaroli and Zannoni, 2010; Cidu et al., 2013).

Hydromorphic sandy soil (N1-*Typic Psammaquent*) in the highest micro-morphological part of the San Vitale park is not affected by the saline shallow water table, while in the lowest interdunal areas the saline intrusion affects hydromorphic soils. In the latter, the high sodium percentage is mainly adsorbed into organic colloids (N2, S1-2, *Sodic Psammaquents*), as suggested by the high values of OC, CEC and ESP values in the N2, S1 and S3 pedons.

The subaqueous soils of the wetland ecosystem are located in some brackish waterholes or in places exposed to the sea. For this reason, *Sulfic or Typic Psammowassents* have developed in closed areas which have no direct contact with sea water, while *Fluventic Sulfiwassent* has been found in the exposed areas, where marine depositions were evident.

All soils studied have developed on sandy/sandy-loam materials and are affected by salinity, which varied along the soil profile of both hydromorphic and subaqueous pedons due to the different effect of both the saline groundwater oscillations and surfacing phenomena (Zannoni, 2008), to salts accumulation and evaporation processes. The variation in EC trend among the hydromorphic pedons could be caused by a different intensity of superficial accumulation of salts due to marine aerosol depositions transported by wind, to precipitations and to evapotranspiration phenomena (Cidu et al., 2013; Rose and Waite, 2003; Salama et al., 1999). On the contrary, the irregular EC trend in some subaqueous profiles (S3 and S4) along the soil profiles is due to the combined effect of groundwater and surface water on the soil profile, because the S. Vitale park is deeply influenced by the leakage between different aquifers through confining beds (Buscaroli and Zannoni, 2010; Cidu et al., 2013; Zannoni, 2008).

The transition from subaqueous to hydromorphic soils can be well recognized by both carbonate and OC/S ratio trends. The decrease of carbonate content from SASs to hydromorphic soils suggests that the carbonate dissolution is mostly related to terrestrial ecosystems. This process, in fact, has already been detected in San



Vitale park, and it has been mainly related to soil acidification processes induced by microbial respiration in the aerated superficial soil horizons of hydromorphic soils (Buscaroli et al., 2009; Marinari et al., 2012).

Furthermore, the OC/S ratio decreases with soil wetness, highlighting how anaerobic reductive conditions occur due to progressive flooding. The OC/S ratio decrease is due to the availability of dissolved sulfate species, combined with the presence of organic matter and reactive  $\text{Fe}^{2+}$  (Berner, 1984; Hedges and Keil, 1995; Ivanov et al., 1989). This result is in agreement with the field observation of gley Munsell colors in wetland soils and in hydromorphic soil horizons affected by groundwater.

Moreover the low OC/S ratio seems to be related to the sulfidization process, and the high positive correlation between organic C and total S content, in the deep mineral horizons matrix, supports this hypothesis. In fact, in fresh, brackish and salt marsh soils, sulphur is reduced and forms carbon-bonded compounds (Kao et al., 2004; Krairapanond et al., 1992). In these conditions, the compounds formed by reduced S can react with free  $\text{Fe}^{2+}$ , inducing sulfidization processes (Demas and Rabenhorst, 1999; Fanning and Fanning, 1989) and thus developing sulfidic horizons.

With decreasing of the hydromorphic degree, reduced S compounds are oxidized back, forming other compounds (e.g.  $\text{H}_2\text{SO}_4$ ,  $\text{SO}_2$ , DMSO and DMS) which induces pH drift and soils acidification (Bradley and Stolt, 2003; Dent and Pons, 1995). In this study this process is stressed by the negative correlation between S and pH values in deep horizons. Nevertheless, the lowering of pH was not so intense as to cause the strong soil acidic conditions reported by other studies (Toivonen and Österholm, 2011; Vahedian et al., 2014) and this can be due to the relative high content of carbonates in the area, which act as a powerful soil buffer (Aller and Rude, 1988; Descostes et al., 2002; Fossing and Jorgensen, 1989; Nicholson et al., 1988).

The DFA identifies the chemical variables which better characterize and distinguish the different pedons according to their hydrological and morphological conditions. At suborder soil classification level, the DFA shows that hydromorphic soils located in highest morphological area of the park (*Aquents*) store a higher P amount than the subaqueous soils (*Wassents*). According to Schlesinger and Bernhardt (2013), P load of terrestrial biota is generally higher than that in marine system; however, inorganic P is generally stabilized into crystalline  $\text{Fe}^{3+}$  and  $\text{Al}^{3+}$  minerals in aerobic conditions (Reddy and DeLaume, 2008) while it is susceptible to translocations and leaching in reductive one (Needelman et al., 2007). In our study, this can also

be confirmed by the positive correlation between Fe and P in both superficial organo-mineral and deep mineral horizons.

The DFA also divides *Wassent* soils from *Aquent* ones because of the high content of soluble salt found in *Wassent* profiles (e.g. Ca, Mg and Na). The distribution of these elements is clearly linked to the intrusion of sea water in subaqueous soil profiles (Cidu et al., 2013) and the positive correlation among their concentration confirms the similar marine origin. In addition to the obvious difference in soil texture, the function 2 of DFA allows for the underlining of the chemical difference between *Sulfiwassent* profile (S4) and *Psammowassent* ones (N3-4 and S3) due to an increase in the amount of Fe, Mg and K in the latter. This can be ascribed to difference of sedimentation processes in the *Pialassa* and wetland area, to the transportation of nutrients through the surrounding canals and to nutrients accumulation in close areas. These hypotheses should be confirmed through further study on the dynamic of nutrients in waters of S. Vitale park.

#### 4.5. CONCLUSION

The S. Vitale park represents a very important natural area for investigating soil sequence from SASs to hydromorphic soil. The soil texture, the Munsell colour, the OC/S ratio and the carbonate distributions along the profiles can drive the characterization of the a *soil continuum* from SAS to hydromorphic soil sequences, as well as the hydromorphic transition from one system to another. The processes of sulfidization and carbonate depletion can be identify as the key pedogenetic features of soil transition, highlighting the important role of the soil water saturation and of the alternation of aerobic/anaerobic conditions.

The salinity trend along the soils profiles, highlights both the saline intrusion from the coast and the salts accumulation on the soil surface. However, only a further investigation on water isotopes could really explain the mixing of saline and fresh aquifers in these soils.

Subaqueous soils are prevalently characterize by the accumulation of salts form marine origin while hydromorphic soils by organic carbon accumulation on the topsoil and P store. These variables well define the morphological and diagnostic properties of soils, because they clearly highlight the differences among soils at both suborder (*Wassent* and *Aquent*) and great group (*Sulfiwassent* and *Psammowassent*) classification level according to the Keys to Soil Taxonomy.

## 4.6. REFERENCES

- Aller, R. C., and P. D. Rude. 1988. Complete oxidation of solid phase sulfides by manganese and bacteria in anoxic marine sediments. *Geochimica et Cosmochimica Acta* 52:751–765.
- Amorosi, A., M. C. Centineo, M. L. Colalongo, and F. Fiorini. 2005. Millennial-scale depositional cycles from the Holocene of the Po Plain, Italy. *Marine Geology* 222-223:7–18.
- Berner, R. A. 1984. Sedimentary pyrite formation: An update. *Geochimica et Cosmochimica Acta* 48:605–615.
- Bradley, M. P., and M. H. Stolt. 2003. Subaqueous Soil-Landscape Relationships in a Rhode Island Estuary. *Soil Science Society of America Journal* 67:1487.
- Buscaroli, A., E. Dinelli, and D. Zannoni. 2011. Geohydrological and environmental evolution of the area included among the lower course of the Lamone river and the Adriatic coast. *EQA- Environmental Quality* 5:11–22.
- Buscaroli, A., M. Gherardi, G. Vianello, L. Vittori Antisari, and D. Zannoni. 2009. Soil survey and classification in a complex territorial system: Ravenna (Italy). *EQA – Environmental quality* 2:15–28.
- Buscaroli, A., and D. Zannoni. 2010. Influence of ground water on soil salinity in the San Vitale Pinewood (Ravenna - Italy). *Agrochimica* 5:303–320.
- Castiglioni, G. B., A. Biancotti, M. Bondesan, G. C. Cortemiglia, C. Elmi, V. Favero, G. Gasperi, G. Marchetti, G. Orombelli, G. B. Pellegrini, and C. Tellini. 1999. Geomorphological map of the Po Plain, Italy, at a scale of 1:250 000. *Earth Surface Processes and Landforms* 24:1115–1120.
- Cidu, R., L. Vittori Antisari, R. Biddau, A. Buscaroli, S. Carbone, S. Da Pelo, E. Dinelli, G. Vianello, and D. Zannoni. 2013. Dynamics of rare earth elements in water–soil systems: The case study of the Pineta San Vitale (Ravenna, Italy). *Geoderma* 193-194:52–67.
- Demas, G., and M. C. Rabenhorst. 1999. Subaqueous Soils: Pedogenesis in a Submersed Environment. *Soil Science Society of American Journal* 63:1250–1257.
- Dent, D. L., and L. J. Pons. 1995. A world perspective on acid sulphate soils. *Geoderma* 67:263–276.
- Descostes, M. I., C. A. Beaucaire, F. L. Mercier, and S. É. Savoye. 2002. Effect of carbonate ions on pyrite (  $\text{FeS}_2$ ) dissolution:265–270.
- Fanning, D. S., and M. C. B. Fanning. 1989. *Soil: Morphology, genesis, and classification*. John Wiley & Sons, New York.

- Fanning, D. S., M. C. Rabenhorst, S. N. Burch, K. R. Islam, and S. A. Tangren. 2002. Sulfides and sulfates. Soil mineralogy with environmental applications. SSSA, Madison, WI.
- Ferronato, C., G. Vianello, and L. Vittori Antisari. 2014. The evolution of the Po Valley and Reno basin (North Italy) through the historical cartography: vicissitude of a land reclamation. Pages 741–752 Regional Symposium on Water, Wastewater and Environment: Traditions and Culture.
- Fossing, H., and B. Jorgensen. 1989. Measurement of bacterial sulfate reduction in sediments: Evaluation of a single-step chromium reduction method. *Biogeochemistry* 8.
- Gambolati, G. 1998. CENAS. (G. Gambolati, Ed.). Springer Netherlands, Dordrecht.
- Gee, G. W., and J. W. Bauder. 1986. Methods of Soil Analysis: Part 1—Physical and Mineralogical Methods. Pages 383–411 *Methods of Soil Analysis: Part 1—Physical and Mineralogical Methods*. Soil Science Society of America, American Society of Agronomy.
- Hedges, J. I., and R. G. Keil. 1995. Sedimentary organic matter preservation: an assessment and speculative synthesis. *Marine Chemistry* 49:81–115.
- Ivanov, M. V., A. Yu, M. S. Reeburgh, and G. W. Skyring. 1989. Interaction of sulphur and carbon cycles in marine sediments. Evolution of global biogeochemical sulphur cycle. John Wiley & Son Ltd.
- Kao, S. J., C.-S. Horng, A. P. Roberts, and K.-K. Liu. 2004. Carbon–sulfur–iron relationships in sedimentary rocks from southwestern Taiwan: influence of geochemical environment on greigite and pyrrhotite formation. *Chemical Geology* 203:153–168.
- Krairapanond, N., R. D. DeLaune, and W. H. Patrick. 1992. Distribution of organic and reduced sulfur forms in marsh soils of coastal Louisiana. *Organic Geochemistry* 18:489–500.
- Loeppert, R.H., Suarez, D.L., 1996. Carbonate and gypsum. In: Sparks, D.L. (Ed.), 532 *Method of Soil Analysis. Part 3, Chemical Methods*. SSSA and ASA, Madison, pp. 437–533 474. (n.d.). . USDA-ARS/UNL Faculty.
- Marinari, S., S. Carbone, L. Vittori Antisari, S. Grego, and G. Vianello. 2012. Microbial activity and functional diversity in Psamment soils in a forested coastal dune-swale system. *Geoderma* 173-174:249–257.
- McVey, S., P. J. Schoeneberger, J. Turenne, M. Payne, and D. A. Wysocki. 2012. SUBAQUEOUS SOILS (SAS) DESCRIPTION. Field Book for Describing and Sampling Soils. Third edition. National Soil Survey Center Natural Resources Conservation Service U.S. Department of Agriculture.
- Needelman, B. A., D. E. Ruppert, and R. E. Vaughan. 2007. The role of ditch soil formation and redox biogeochemistry in mitigating nutrient and pollutant losses from agriculture. *Journal of Soil and Water Conservation* 62:207–215.

- Nicholson, R. V., R. W. Gillham, and E. J. Reardon. 1988. Pyrite oxidation in carbonate-buffered solution: 1. Experimental kinetics. *Geochimica et Cosmochimica Acta* 52:1077–1085.
- Pinna, M. 1978. *L'atmosfera e il clima*. UTET, Torino.
- Reddy, R. K., and D. DeLaume. 2008. *Biochemistry of wetlands. Science and applications*. Taylor & Francis.
- Rose, A. L., and T. D. Waite. 2003. Kinetics of iron complexation by dissolved natural organic matter in coastal waters. *Marine Chemistry* 84:85–103.
- Salama, R. B., C. J. Otto, and R. W. Fitzpatrick. 1999. Contributions of groundwater conditions to soil and water salinization. *Hydrogeology Journal* 7:46–64.
- Schoeneberger, P., D. A. Wysocki, and E. C. J. Benham. 2012. *Field book for describing and sampling soils*, Version 3.0. Natural Resources Conservation Service, National Soil Survey Center, Lincoln, NE.
- Soil Survey Staff. 2010. *Keys to Soil Taxonomy*. 11th edition. United States Department of Agriculture, Natural Resources Conservation Service.
- Soil Survey Staff. 2014. *Keys to Soil Taxonomy*. 12th edition. United States Department of Agriculture, Natural Resources Conservation Service.
- Summer, M. E., and W. P. Miller. 1996. Cation exchange capacity and exchange coefficients. In: Sparks, D.L. (Ed.), *Methods of Soil Analysis, Part 3. Chemical Methods*. Soil Science Society of America and American Society of Agronomy, Madison, pp. 1201–1229.
- Teatini, P., M. Ferronato, G. Gambolati, W. Bertoni, and M. Gonella. 2005. A century of land subsidence in Ravenna, Italy. *Environmental Geology* 47:831–846.
- Toivonen, J., and P. Österholm. 2011. Characterization of acid sulfate soils and assessing their impact on a humic boreal lake. *Journal of Geochemical Exploration* 110:107–117.
- Vahedian, A., S. A. Aghdaei, and S. Mahini. 2014. Acid Sulphate Soil Interaction with Groundwater: A Remediation Case Study in East Trinity. *APCBEE Procedia* 9:274–279.
- Veggiani, A. 1974. *Le ultime vicende geologiche del ravennate. Influenza di insediamenti industriali sul circostante ambiente naturale – Studio sulla Pineta di San Vitale di Ravenna*.
- Vepraskas, M. J., C. B. Craft, and J. L. Richardson. 2000. *Wetland Soils: Genesis, Hydrology, Landscapes, and Classification*.

Vittori Antisari, L., G. Falsone, S. Carbone, S. Marinari, and G. Vianello. 2015. Douglas-fir reforestation in North Apennine (Italy): Performance on soil carbon sequestration, nutrients stock and microbial activity. *Applied Soil Ecology* 86:82–90.

Zannoni, D. 2008. Uso sostenibile dei suoli forestali di ambiente costiero in relazione ai fattori di pressione esistenti. University of Bologna.

# CHAPTER 5

## SALINE SYSTEMS

	<i>pp.</i>
5. Saline systems: the Grado lagoon.....	90
5.1. The study area.....	91
5.2. Materials and methods.....	92
5.2.1. Sampling ad experimental design.....	92
5.2.2. Morphological and ecological description of soil profiles.....	93
5.2.3. Water analysis and physicochemical characterization of soil profiles.....	94
5.2.4. Data analysis.....	94
5.3. Results .....	95
5.3.1. Climatic and ecological characterization.....	95
5.3.2. Morphological and physicochemical characterization of soils .....	96
5.3.3. Soil classification and ecological relationship.....	101
5.4. Discussion .....	105
5.5. Conclusion.....	107
5.6. References.....	109





## 5. SALINE SYSTEMS: THE GRADO LAGOON

The Italian lagoons, and in particular those of the Northern Adriatic Sea, are characterized by salt marshes, sandbanks and sub-tidal mudflats called “*velme*”, which represent important ecosystems for land management and wildlife protection (Ferrarin et al., 2010). Salt marshes, which undergo partial regular flooding at high tide, harbor several halophyte plant species and embody the habitat of several aquatic and migratory birds (de Groot et al., 2012; Koch et al., 2009). Their importance has been highlighted by the European community through the Directive 92/43/CEE “Habitat” and the development of Nature 2000 Network, in which the lagoon is considered as special protection areas (SPA) and special areas of conservation (SAC).

The relationship between SASs pedogenetic features and their topographic position on the landscape have been investigated by some authors (Bradley and Stolt, 2003; Osher and Flannagan, 2007; Vaughan et al., 2008) but to our knowledge, few informations on soils of low energy tidal ecosystems such as Italian lagoons are available.

Extending knowledge on sub-tidal habitats, offers a unique opportunity to understand the subaqueous pedogenesis and their relationship with the surrounding landscape in a perspective of climate change and environmental protection (Erich et al., 2010; Ferreira et al., 2007).

In this study, soils properties and ecosystem features were investigated in different salt marshes of Grado and Marano lagoon (Northern Italy), with the aim of (i) mapping hydromorphic/hydric and subaqueous tidal soils and (ii) understanding how the distance from the open sea, the vegetation and the morphology of these landforms influence soils characteristics.

This work has been realized thanks to the collaboration and logistic support of the Environmental Protection Agency of Friuli Venezia Giulia region (ARPA-FVG, Italy) and produced the following articles:

- Vittori Antisari, L., De Nobili, M., Ferronato, C., Natale, M., Pellegrini, E., Vianello, G., 2015. Subaqueous to hydromorphic soils transitions and vegetation distribution in the central Grado lagoon (Northern Adriatic Sea, Italy). – *Estuarine, Coastal and Shelf Science*, *submitted*.

## 5.1. THE STUDY AREA

The Grado and Marano lagoon (SPA/SAC Nature 2000: IT3320037) extends for 160 km<sup>2</sup> and spans between the Tagliamento and the Isonzo rivers estuaries in the Northern part of the Adriatic sea.

The lagoon is separated from the open sea by a barrier of islets and sandbanks which can be dated since the 4<sup>th</sup> century AD, and now occupy an area of 760 ha. According to Fontolan et al. (2012) different types of salt marshes can be recognized in the Grado lagoon on the basis of their geographical distribution and morphogenesis:

- fringing salt marshes bordering the inner margin of the lagoon and fluvial deltas near the mainland;
- tidal channel-fringing salt marshes, formed by sedimentation processes induced by abrupt morphological changes between channels and adjacent tidal flats;
- back-barrier salt marshes developed in the lee of barrier islands;
- salt marshes in recent para-lagoonal basins;
- isolated marshes.

The average height of these landforms above the mean sea level is quite low (<0.5 m a.s.l, on average) due to a slow but continuous soil subsidence and erosion process (Brambati, 1970; Fontolan et al., 2012). Among the different salt marshes, some areas has become permanently emerged lands, while some others are affected by hydric conditions caused by the tide oscillation.

Next to tidal channels and in sub-tidal zones, soils are permanently submerged and represent the border between the landforms and the sea bottom (Ferrarin et al., 2010).

In the lagoon, tidal fluctuations vary between  $\pm 65$  and  $\pm 105$  cm from the mean sea level, depending on the climate and seasonal conditions. The average salinity of surface sea water ranges from 20 to 35 mg L<sup>-1</sup> near the mainland and near the open sea respectively (ARPA, 2007), and the seasonal oscillation of the water temperature ranged between 5 and 7°C in winter and between 28 and 30°C in summer (Covelli et al., 2009; D' Aietti and Altobelli, 2007; Ferrarin et al., 2010).

The mean annual temperature in the lagoon is 13.1 °C, while the mean annual precipitation is 1106 mm yr<sup>-1</sup>. According to the Köppen-Geiger system the area is classified as “temperate/mesothermal climate of the mid-latitudes” (Peel and Blöschl, 2011), characterized by the moderating effect of the sea (Michelutti et al., 2003).

## 5.1. MATERIALS AND METHODS

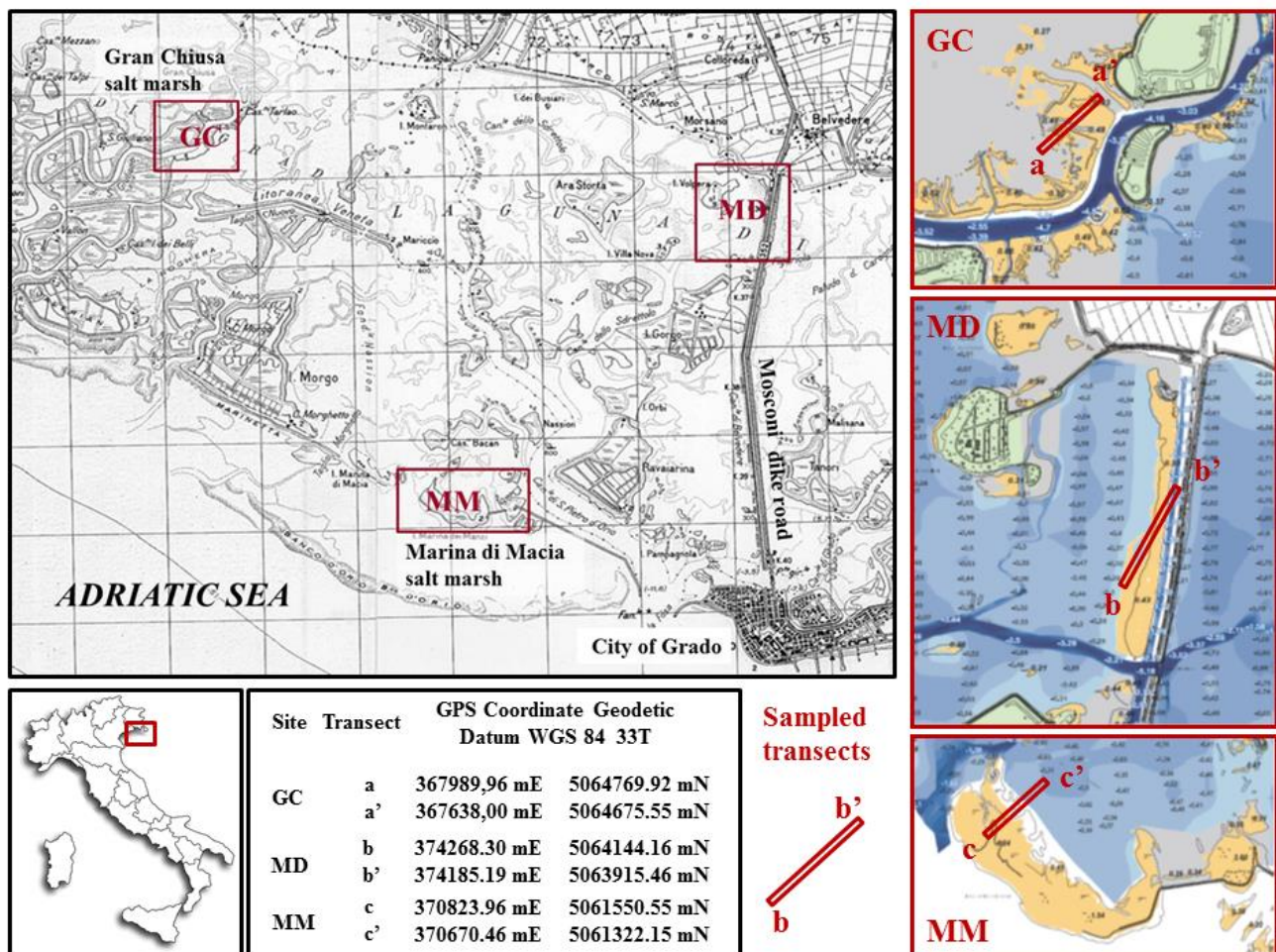
### 5.1.1. Sampling and experimental design

This study focused on three salt marsh, located in the between Bruso and Grado city, as shown in Figure 5.1.

The sampling points were chosen according to their representative location in the lagoon, prevalent vegetation pattern, and submerged condition.

The sampling survey was carried out in summer 2013, during low tide and soil profiles were collected and stored as described in section 4.2.1.

**Figure 5.1.** Map of Grado and Marano lagoon and geographical localization of the studied salt marshes.



The first study site (MM) was located on a back barrier salt marsh, in the Marina di Macia isle, and it was part of the old longshore bar that separated the Grado lagoon from the Adriatic sea. The studied pedons were sampled from the inner and most-elevated part of the salt marsh (MM-Lim1-2), to the tidal flat (MM-Sa1-2) and to the edge of the isle (MM-Zos).

The second study site (GC) was located in the Gran Chiusa isle, on a channel fringing marsh that has evolved from an ancient enclosed fish farm and it had been abandoned and re-naturalized long ago. The studied pedons were sampled from a prevalently emerged part of the isle (GC-Sar1), and a partially submerged part of the salt marsh (GC-Sar2).

The third study site (MD) was located in an artificial salt marsh, which was formed after the excavation of the adjacent Belvedere channel (1902-1920) and the consequent accumulation of dredged sediments. The isle lies parallel to the Mosconi dike road. The studied pedons were sampled in a permanently submerged areas in the inner part of the salt marsh, characterized by a different topographical height and land cover (MD-Sp1 and MD-Sp2).

Both hydric and subaqueous soil profiles and specific localization are shown in Appendix 5.

### **5.1.2. Morphological and ecological description of soil profiles**

The climatic data of the area were collected from the representative meteorological station of Portogruaro (VE, 5 m a.s.l.; about 20 km from the study site). The water balance was calculated for hydromorphic soils of the area according to the method described by Thornthwaite and Mather (1957) and revised by Black (2007). All data were processed with the Newhall Simulation Model (Newhall, 1972; Van Wambeke, 2000) to define the *temperatue and moisture regime* of the studied area.

*Vegetation communities* type was recorded observing presence and coverage of prevalent species. Phytosociological classes were recongnized according to Poldini et al. (1999), whereas nomenclature of plant species follows the latest Italian check list of vascular plants (Conti et al., 2005).

Each *genetic horizon* of both hydric and subaqueous soil profiles was described in field according to Schoeneberger et al. (2012) and to McVey et al. (2012) as presented in section 4.2.2.

### 5.2.3. Water analysis and physicochemical characterization of soil profiles

Analysis of *sea water* were carried out in field for pH, dissolved oxygen (DO), salinity (SAL) and temperature (T) and they were performed in both the upper and lower part of water column with portable immersion electrodes (Hach-Lange Instruments). All water samples were collected in glass bottles and analysis were replicated in laboratory.

*Soil analysis* were carried as described in section 4.2.3 for reduced sulphides observation, soil EC and pH, particle size distribution, total carbonates ( $\text{CaCO}_3$ ), organic carbon (OC), nitrogen (TN), Fe and S. All methods were accurately described in section 2.1.3 and 4.2.3. Salinity values ( $\text{g L}^{-1}$ ) were calculated from EC values using a correlation factor (0.64, Zannoni, 2008).

The *cation exchangeable capacity* (CEC) was determined according to Ciesielskui and Sterckeman (1997) using 0.05N  $[\text{Co}(\text{NH}_3)_6\text{Cl}_3]$ . Briefly 2.5g of soil were shaken for 2h with 50 mL of Co-examine solution. Samples were filtered with Watmann 42 filter paper and CEC ( $\text{cmol kg}^{-1}$ ) was estimated measuring the difference between initial and final  $\text{Co}^{2+}$  ions concentration in solution by ICP-OES (Aran et al., 2008).

### 5.2.4. Data analysis

All statistical analysis were performed with Statistica 10 software (Statsoft, Tulsa, OK, USA).

*Descriptive statistics* included the calculation of Mean, Minimum (min), Maximum (mas) and Standard Deviation (SD) values and were performed to summarize the variability of data.

*Linear regression* was performed to highlight the single correlation between variables.

*Discriminant function analysis* (DFA) was performed with forward stepwise method on different physicochemical properties (e.g. sand, silt and clay content, CEC, pH, EC, OC, TN, total contents of Fe and S) to highlight the differences between pedons according to their position in the lagoon (e.g. their morphological position, their water saturation level with respect to the high tide) and according to their prevalent vegetation cover. Wilk's lambda test and standardized canonical discriminate coefficients (SCDC) were used to rank the significance and the discriminate power of each function as described in section 2.2.6.

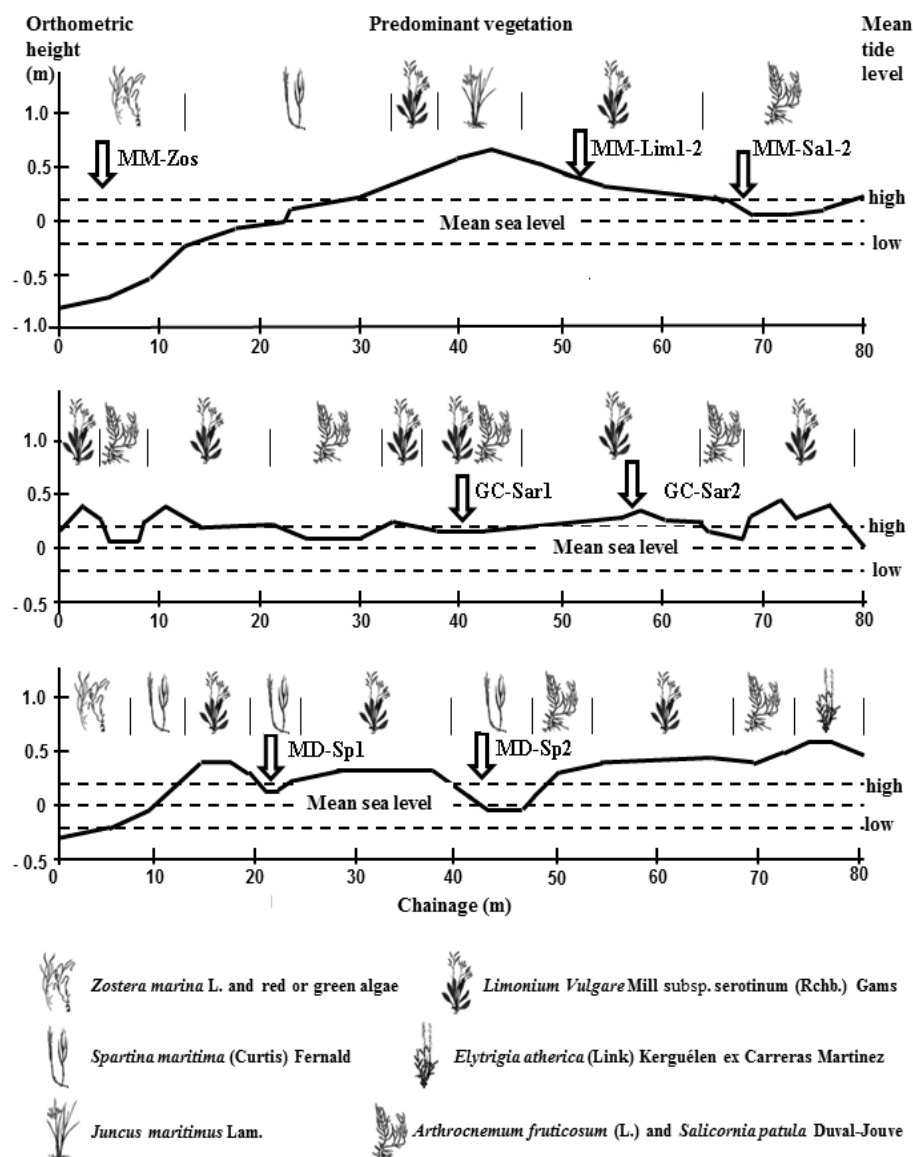
## 5.3. RESULTS

### 5.3.1. Climatic and ecological characterization

According to the climatic data from Portogruaro station, the temperate regime was defined as *Mesic* (annual average temperature of the soil between 8 and 15 °C, with a difference of average temperatures from summer to winter is above 5° C) and the moisture regime was defined as *Udic* as it presented more than 90 days of non-cumulative rainfall during the whole year (Soil Survey Staff, 2014).

The morphology of each salt marsh, its typical vegetation and the sampling points are shown in Figure 5.2.

**Figure 5.2.** Representation of vegetation species, based on soil morphology and sea level and of each salt marsh.



In Marina di Macia (MM), three different plant communities were recognized. The phytosociological class *Arthrocnemetea fruticosi* covered the inner part of the salt marsh; in particular, in MM-Lim1-2 sampling sites *Limonium vulgare* subsp. *serotinum* was the dominant species, whereas *Sarcocornia fruticosa* prevailed on MM-Sa1 and MM-Sa1-2 sampling points. At the edge of the salt marsh, on the MM-Zos pedon, eelgrass *Zostera noltii* was the predominant species, and it was associated with both red (e.g. *Gracilaria* genus) and green algae (e.g. *Ulva* genus).

In the Gran Chiusa salt marsh (GC), two different *facies* of the *Sarcocornietea fruticosi* class were found. In the GC-Sar1 studied site, *Limonium vulgare* subsp. *serotinum* was clearly the most abundant species while in the GC-Sar2, the compresence of *Limonium vulgare* subsp. *serotinum* and *Sarcocornia fruticosa* were noted.

At the Mosconi dike salt marsh (MD), only the *Spartinetea maritimae* phytosociological class was present: the MD-Sp1 site was mostly covered by *Spartina maritima*, while the MD-Sp2 studied site was located in a confined brackish waterhole, which was covered by an orange-red carpet and few examples of *S. maritima*.

### **5.2.2. Morphological and physicochemical characterization of soils**

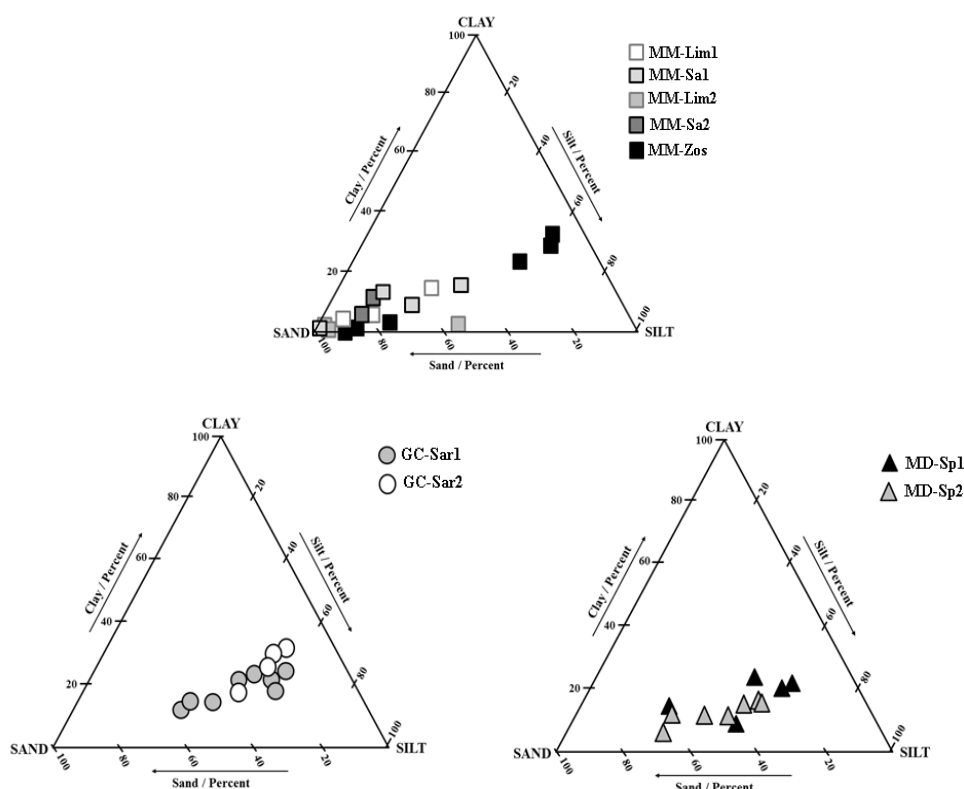
The morphological characterization of all genetic horizons of hydric and submerged soil profiles are shown in Appendix 6 while the percent distribution of sand, silt and clay determined in all sampled horizons is reported in Figure 5.3.

The soils were little developed, and their organo-mineral soil thickness varied from 10 cm in subaqueous soils (MD-Sp1-2 and MM-Zos) to 15/20 cm in MM hydric soils (MM-Lim1-2 and MM-Sa1-2) to 50 cm in GC hydric soils (GC-Sar1-2). Generally, the level of tide oscillations was associated to gley matrix colours and appearance of redoximorphic features (Appendix 5).

Sand predominated in the horizons of the MM saltmarsh soils, even if some loamy enrichments were observed in each pedon at different depths. In the hydric soil profiles (MM-Lim1-2 and MM-Sa1-2), several mottles and redoximorphic features were noted in all organo-mineral soil horizons, where depletion and accumulation of Fe occurred. Many coarse roots were present in MM-Lim1-2 pedons until deep mineral C horizons while fine roots were found only in organo-mineral horizons of MM-Sa1-2 pedons.

At the edge of the MM salt marsh, the subaqueous profile was characterized by several silty-clay-loam intercalations, which were associated to the presence of abundant shells and organic fragments (O/C horizons). Above these buried O/C horizons, sulfidic materials were detected by both odour description and soil wet incubation test.

**Figure 5.3.** Texture triangle of all soil horizons.



The Gran Chiusa and Mosconi Dike soils showed a completely different texture, where loamy and silty-loam texture predominated all along the soil profiles and sulfidic materials were detected in some C horizons.

GC pedons were strongly characterized by the presence of several roots and biological concentrations in all organo-mineral horizons, which disappeared in the deeper C ones. Many mottles and redoximorphic features were present until 80 cm depth, and under this level, gleyed colours and sulfidic Cse horizons were found.

In MD pedons, gley Munsell colours predominates all along the soil profiles and both shell coarse and organic fragments were mostly present in the superficial O and A horizons, although low decomposed fragments were observed all along the soil profile. Sulfidic materials were detected starting from 45 cm in MD-Sp1 and from 11 cm in MD-Sp2.



The physicochemical characteristics of tidal hydric and subaqueous soils profiles of MM, GC and MD salt marshes are shown in Tables 5.1, 5.2, and 5.3, respectively.

**Table 5.1.** Mean physicochemical properties determined in Marina di Macia salt marsh (MM) soil profiles.

Profile	Horizon	Depth cm	pH		CaCO <sub>3</sub>	OC	TN g kg <sup>-1</sup>	S	Fe	CEC mol <sup>+</sup> kg <sup>-1</sup>	C/N	OC/S	Fe/S
			initial	final									
MM-Lim1	<i>Oe</i>	3-0	nd	6.7	35	99.8	7.6	nd	nd	nd	13.0	nd	nd
	<i>A1</i>	0-5	nd	7.7	374	12.3	1.4	5.2	26.2	38.0	8.6	2.4	5.0
	<i>A2</i>	5-10	nd	7.8	108	48.1	3.8	1.2	10.0	10.7	12.5	39.1	8.1
	<i>Ab</i>	10-17	nd	8.0	366	15.5	1.9	2.8	26.0	15.0	8.2	5.5	11.0
	<i>C</i>	17-30	nd	8.3	759	2.7	0.8	0.4	2.2	5.8	3.4	6.6	5.4
	<i>Cg1</i>	30-80	nd	8.3	800	1.6	0.2	0.4	1.7	7.1	8.4	4.1	4.3
	<i>Cg2</i>	80-100	nd	8.1	443	2.5	0.7	2.4	7.3	4.7	3.5	1.1	2.6
MM-Lim2	<i>Oe</i>	1.5-0	nd	7.2	nd	98.8	7.6	nd	nd	nd	13.0	nd	nd
	<i>A1</i>	0-3	nd	7.6	227	46.6	5.2	2.9	13.0	24.6	8.9	16.1	4.5
	<i>A2</i>	3-6	nd	7.5	664	5.2	1.1	0.6	3.9	8.5	4.6	8.8	6.7
	<i>Ab</i>	6-20	nd	8.0	357	13.5	1.9	1.3	9.6	14.4	7.1	10.6	7.6
	<i>C</i>	20-35	nd	8.3	759	2.4	0.8	0.4	2.3	5.7	2.9	6.5	6.3
	<i>Cg1</i>	35-70	nd	8.3	800	1.3	0.2	0.4	1.7	6.2	6.2	3.6	4.7
	<i>Cg2</i>	70-100	nd	8.1	422	2.7	0.7	0.4	1.8	4.9	4.1	6.6	4.4
MM-Sa1	<i>A1</i>	0-0.5	nd	7.7	195	73.2	6.1	5.1	17.1	18.5	10.3	14.3	3.3
	<i>A2</i>	0.5-1.5	nd	7.6	299	30.3	3.4	4.3	14.6	10.0	8.9	7.1	3.4
	<i>C</i>	1.5-15	nd	8.4	348	0.7	0.6	0.3	3.2	3.4	1.3	2.3	10.3
	<i>AC</i>	15-20	nd	7.5	141	26.5	2.6	2.3	20.4	17.4	10.3	11.5	8.9
	<i>ACse</i>	20-35	nd	7.7	151	22.8	2.6	3.2	17.5	14.2	8.9	7.1	5.4
	<i>Cg</i>	35-65+	nd	7.9	699	1.9	0.5	0.7	3.0	6.3	4.1	2.9	4.5
MM-Sa2	<i>A1</i>	0-0.5	nd	7.0	294	74.1	6.3	4.7	8.0	19.2	11.7	15.9	1.7
	<i>A2</i>	0.5-1.5	nd	7.5	324	47.3	4.2	3.5	10.3	7.5	11.1	13.3	2.9
	<i>C</i>	1.5-20	nd	8.4	802	1.3	0.2	0.3	1.8	5.8	5.4	4.8	6.8
	<i>ACse</i>	20-32	nd	7.3	170	34.4	2.7	3.7	12.9	17.7	12.6	9.2	3.4
	<i>Cg1</i>	32-35	nd	8.2	750	1.7	0.4	0.4	2.8	6.7	3.9	4.0	6.8
	<i>Cg2</i>	35-70+	nd	8.2	750	1.4	0.2	0.5	2.9	6.6	6.4	2.5	5.2
MM-Zos	<i>Oig</i>	0.2-0	nd	nd	613	97.8	8.1	nd	nd	nd	12.0	nd	nd
	<i>Ase</i>	0-12	8.3	7.0	618	33.0	5.1	2.1	4.9	7.0	6.5	15.9	2.4
	<i>ACse</i>	12-22	8.2	7.1	170	40.0	4.3	3.1	5.7	8.2	9.3	12.9	1.8
	<i>O/Cg1</i>	22-37	8.6	7.5	80	53.2	7.3	3.9	22.9	17.1	7.3	13.8	5.9
	<i>O/Cg2</i>	37-52	8.5	7.6	90	66.1	8.5	3.9	28.3	20.0	7.8	17.1	7.3
	<i>Cg1</i>	52-63	8.4	7.5	609	71.0	9.1	3.5	20.7	17.6	7.8	20.2	5.9
	<i>Cg2</i>	63-67+	8.1	7.4	52	22.0	7.2	0.8	4.7	8.2	3.1	25.9	5.5

CEC= cation exchangeable capacity

In all pedons pH ranged between 6.7 and 8.6 and in SASs the pH values determined after 16 weeks decreased up to 1.3 pH.

The distribution of carbonates was irregular along the soil profiles but it generally ranged between 35 and 800 g kg<sup>-1</sup> in MM salt marsh, 23 and 120 g kg<sup>-1</sup> in GC salt marsh and between 38 and 320 g kg<sup>-1</sup> in MD salt marsh. Generally carbonates decreased in presence of sulfidic materials and of aerated horizons, but not significant correlation were noted.

**Table 5.2.** Mean physicochemical properties determined in Gran Chiusa salt marsh (GC) soil profiles.

Profile	Horizon	Depth cm	pH (H <sub>2</sub> O)		CaCO <sub>3</sub>	OC	TN g kg <sup>-1</sup>	S	Fe	CEC mol <sup>+</sup> kg <sup>-1</sup>	C/N	OC/S	Fe/S
			initial	final									
GC-Sar1	<i>Oe</i>	1-0	nd	7.2	52	61.1	5.1	nd	nd	nd	12.0	nd	nd
	<i>A1</i>	0-5	nd	7.0	23	43.5	3.9	2.6	42.0	22.1	11.2	17.0	16.4
	<i>A2</i>	5-10	nd	7.6	72	14.0	1.4	1.0	33.1	14.6	10.2	14.3	33.6
	<i>AB</i>	10-25	nd	7.8	124	7.1	1.3	0.8	34.8	17.0	5.3	9.3	46.0
	<i>AC</i>	25-50	nd	7.9	106	7.4	1.0	1.0	35.3	16.9	7.6	7.5	35.7
	<i>Cg1</i>	50-60	nd	7.8	103	9.1	1.2	2.3	34.6	21.8	7.4	3.9	15.0
	<i>Cg2</i>	60-80	nd	7.7	75	11.8	1.3	5.7	35.9	20.8	9.2	2.1	6.3
	<i>Cse3</i>	80-110	nd	7.8	72	12.3	1.3	9.4	42.1	24.0	9.1	1.3	4.5
	<i>Cse4</i>	110-120+	nd	7.4	71	21.5	1.8	11.9	38.4	23.7	11.7	1.8	3.2
GC-Sar2	<i>A1</i>	0-0.5	nd	7.3	29	37.1	3.6	3.9	37.0	15.7	10.3	9.5	9.5
	<i>A2</i>	0.5-5	nd	7.2	38	28.5	3.0	1.6	40.5	25.4	9.6	17.6	24.9
	<i>AB</i>	5-10	nd	7.7	48	13.2	1.6	0.8	42.3	21.4	8.4	17.1	54.5
	<i>AC1</i>	10-18	nd	7.8	76	8.1	1.2	0.6	43.2	19.8	6.9	12.5	66.3
	<i>AC2</i>	20-55	nd	7.9	100	6.2	1.1	0.6	39.5	17.3	5.8	10.3	65.6
	<i>Cg1</i>	55-75	nd	7.8	100	8.7	1.0	1.6	31.5	20.9	8.6	5.3	19.2
	<i>Cse2</i>	75-85	nd	7.7	81	11.1	1.2	4.1	32.8	21.3	9.3	2.7	7.9
	<i>Cse3</i>	80-95+	nd	7.8	79	12.2	1.3	9.3	42.7	24.1	9.0	1.3	4.6

CEC= cation exchangeable capacity

**Table 5.3.** Mean physicochemical properties determined in Mosconi Dike Road salt marsh (MD) soil profiles.

Profile	Horizon	Depth cm	pH (H <sub>2</sub> O)		CaCO <sub>3</sub>	OC	TN g kg <sup>-1</sup>	S	Fe	CEC mol <sup>+</sup> kg <sup>-1</sup>	C/N	OC/S	Fe/S
			initial	final									
MD-Sp1	<i>0/Ag1</i>	0-8	7.0	6.3	38	56.1	5.4	6.6	27.7	25.7	13.7	8.5	4.2
	<i>Ag2</i>	8-13	7.6	7.2	194	15.9	1.9	4.6	17.6	19.0	8.3	3.4	3.8
	<i>Cg1</i>	13-30.5	7.6	7.3	248	13.1	1.5	8.7	17.7	18.6	8.6	1.5	2.0
	<i>Cg2</i>	30.5-41	7.6	7.3	270	13.5	1.5	6.9	16.5	17.6	9.0	2.0	2.4
	<i>Cg3</i>	41-46	7.9	7.5	323	9.1	1.0	7.6	14.7	14.0	8.8	1.2	1.9
	<i>Cse4</i>	46-66.5	7.7	7.5	199	13.7	1.6	10.1	18.8	19.4	8.8	1.3	1.8
	<i>Cse5</i>	66.5-80	7.7	7.5	181	18.4	1.8	12.9	22.0	22.8	10.1	1.4	1.7
	<i>Cse6</i>	80-87+	7.7	7.6	200	21.3	2.2	12.4	21.0	23.9	9.6	1.7	1.7
MD-Sp2	<i>Oig</i>	0.5-0	nd	nd	nd	92.7	7.9	nd	nd	nd	11.7	nd	nd
	<i>Ag1</i>	0-1.5	7.9	7.1	111	29.3	3.1	10.4	37.8	8.6	9.5	2.8	3.6
	<i>Ag2</i>	1.5-4.5	7.9	6.9	56	55.7	5.0	12.5	42.6	17.0	11.2	4.4	3.4
	<i>Ag3</i>	4.5-8	7.7	6.5	68	52.8	4.7	17.2	47.6	17.0	11.2	3.1	2.8
	<i>A/Cg</i>	8-11	8.0	7.3	196	6.0	0.9	5.4	20.0	12.7	6.7	1.1	3.7
	<i>Cse1</i>	11-15.5	8.8	7.3	150	14.6	2.0	10.8	36.1	19.0	7.4	1.3	3.3
	<i>Cse2</i>	15.5-27.5	7.9	7.3	173	13.5	1.9	11.7	36.7	19.0	7.0	1.1	3.1
	<i>Cse3</i>	27.5-60+	7.9	7.3	198	15.5	1.7	12.3	39.4	19.0	9.1	1.3	3.2

CEC= cation exchangeable capacity

The OC/S ratio varied along the soil profiles and it was generally higher in hydric soils horizons than in SASs (MD-Sar1-2). Moreover, the OC/S ratio decreased from with soil depth, showing values  $>5$  in all C horizons. Exceptionally, MM-Zos soil horizons and those rich in OC presented high values of the OC/S.

The total S content ranged from 17.7 to 1.1 g kg<sup>-1</sup> in the superficial layers (e.g. A, Ag and Ase horizons) and from 12.2 to 0.2 g kg<sup>-1</sup> in deeper ones (e.g. C, Cg and Cse horizons).

The plotting Fe and S contents of soil profiles (Figure 5.4) highlighted a different linear correlation between these two elements ( $r^2 = 0.72, 0.45, 0.67, 0.31, 0.50$  for MM-Lim1-2, MM-Sa1-2, MM-Zos, GC-Sar1-2, MD-Sp1-2 respectively). Iron accumulation was detected in GC-Sar1-2 while large amount of both Fe and S were found in MD-Sp1-2 soil horizons.

**Figure 5.4.** Scatterplot between total sulphur (S) and iron (Fe), expressed as g kg<sup>-1</sup>, in all soil profiles.

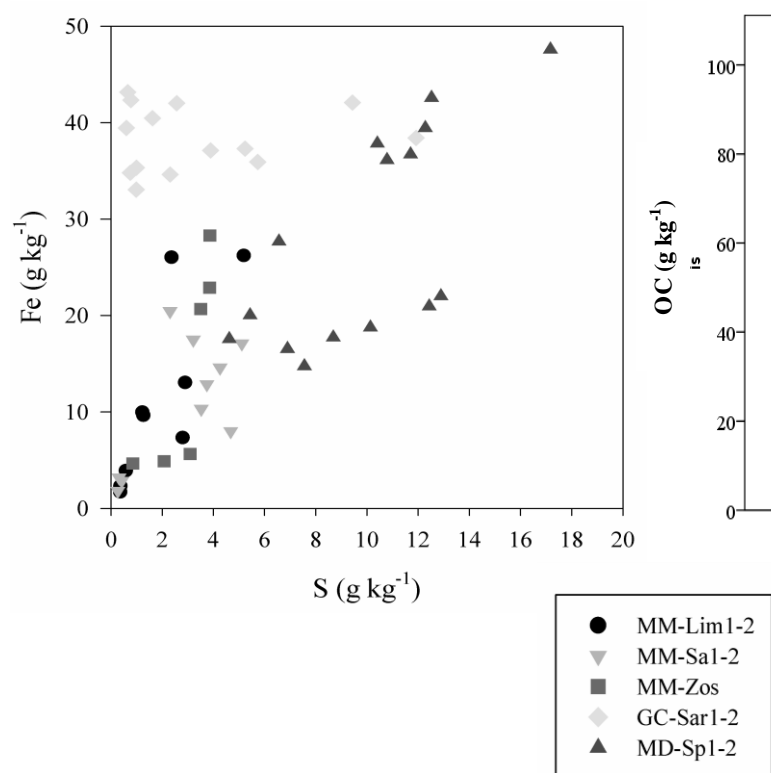
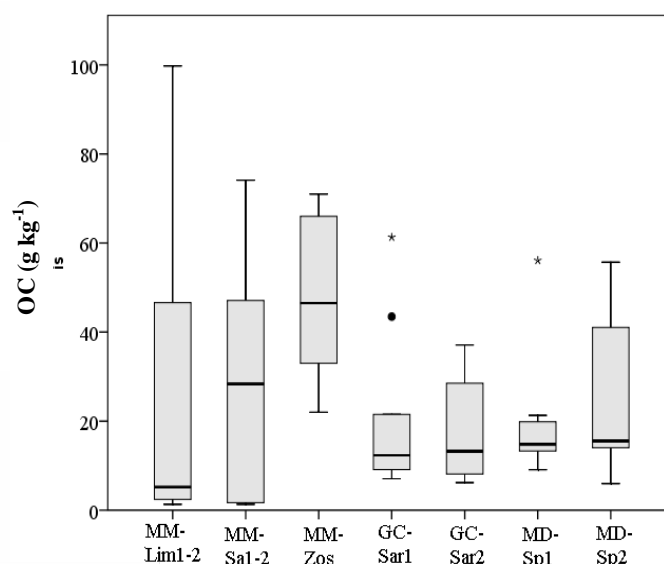


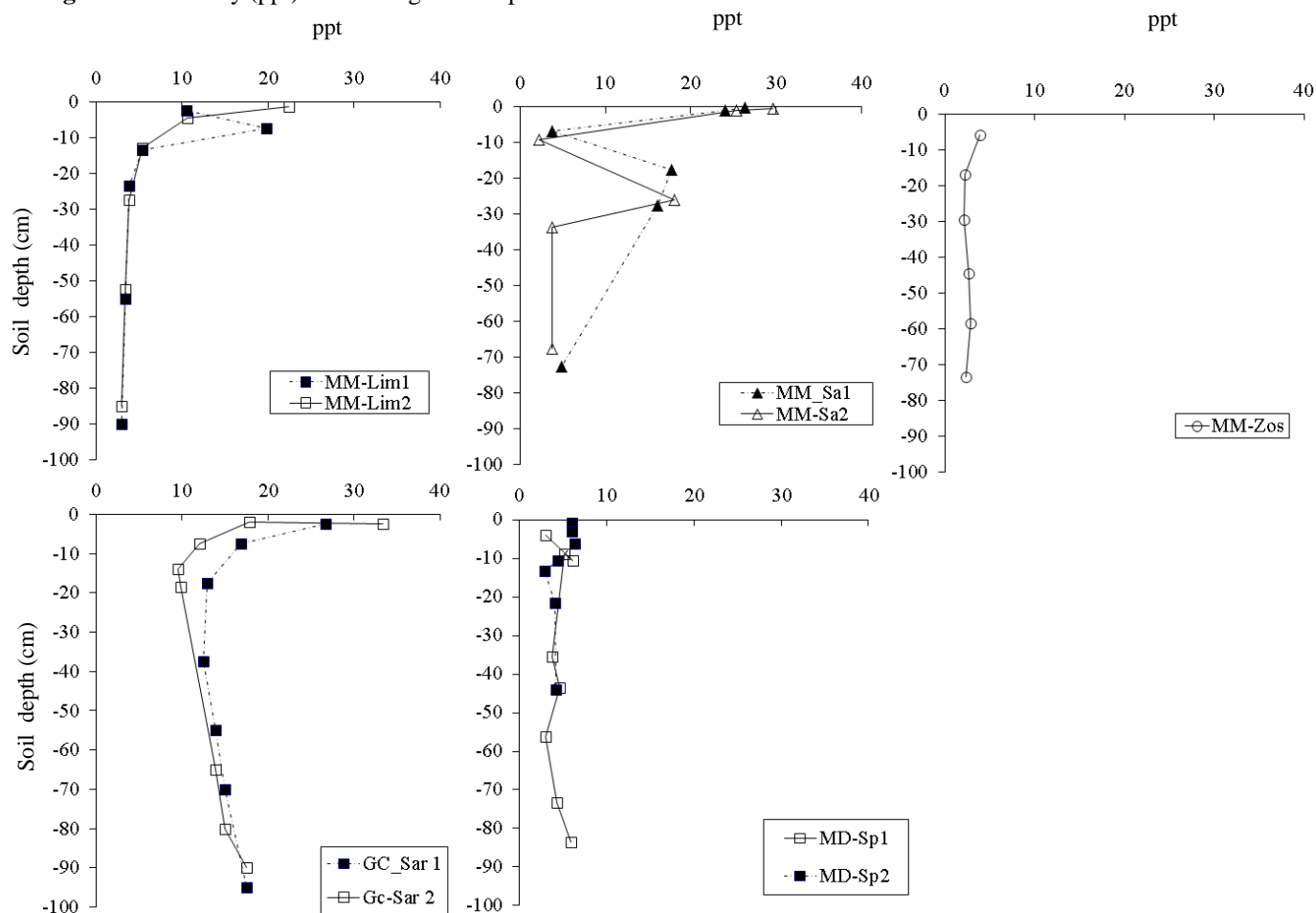
**Figure 5.5.** Quartile distribution of organic carbon (OC, g kg<sup>-1</sup>) in all soil profiles.



Generally, total OC and N strongly decreased with depth along soil profile of tidal soils, although some intercalations of organic matter was noted in MM pedons. MM-Zos was the richest OC pedon and it showed several organic fragments and buried O/C horizons along the soil profile. In MD and GC pedons, OC content slightly increase in the deep horizons and in MD one, OC content was associated with partially decomposed organic fragments all along the soil profile (Figure 5.5).

High salinity values (SAL) were detected in superficial soil horizons of all hydric soils, and they strongly decreased in deep C horizons and in all subaqueous soil profiles (Figure 5.6). Only MM-Lim1-2 pedons showed a graduate decrease of salinity along the soil profile, while in all the other pedons an irregular trend was noted: in MM-Sa1-2 pedons a deep decrease of salinity was found in horizons with 90% of sand and in GC ones SAL slightly increased in deep horizons.

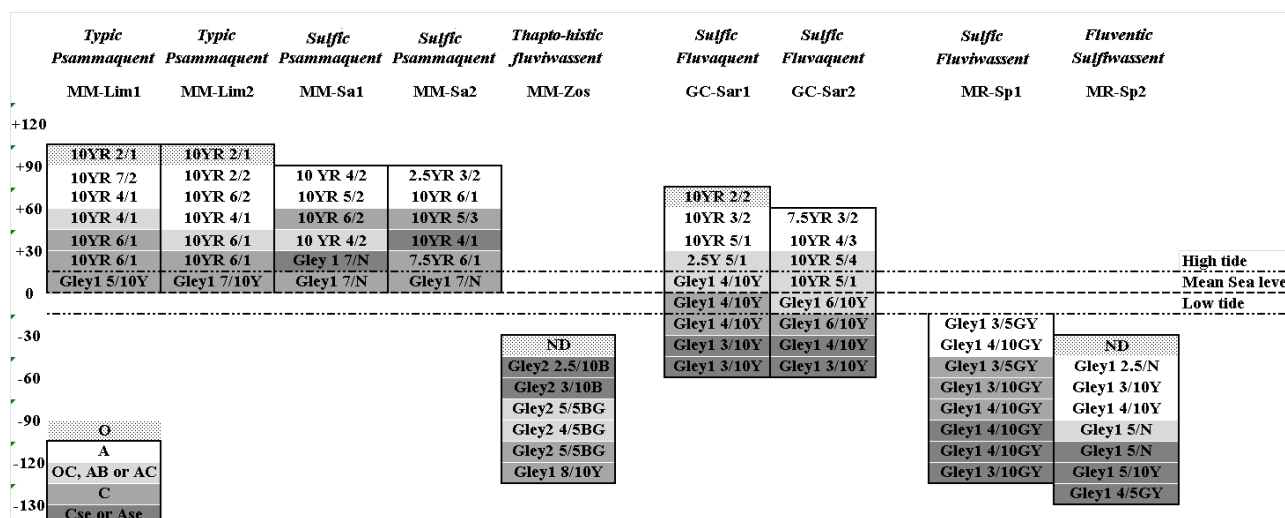
**Figure 5.6.** Salinity (ppt) trend along the soil profiles.



### 5.2.3. Soil classification and ecological relationship

The soil profiles were classified according to the Keys of Soil Taxonomy (Soil Survey Staff, 2014) and ranked into *Aquents* and *Wassents* suborders, according to their water saturation condition. The different soil profile classification and the morphological position with respect to the sea level is shown in Figure 5.7.

**Figure 5.7.** Representation of soil profiles and soil matrix colours, according to the soil morphology and the mean sea level.



In Marina di Macia salt marsh, MM-Lim1-2 soils displayed the same pedo-sequence (O/A/C) and were classified as *Typic Psammaquents*, because they both have sandy or loamy fine sand texture with less than 35% of rock fragments. Similarly MM-Sa1-2 were classified as *Sulfic Psammaquents* because they were also characterized by the presence of sulfidic materials within 50 cm of the mineral soil surface and therefore they. On the same salt marsh, MM-Zos profile was classified as *Thapto-histic Fluviwassent* because of a positive water potential for more than 21 hours per day, and because of the presence of a buried layer of organic materials, 20 cm or more thick, within 100 cm of the mineral soil surface (Table 5.1).

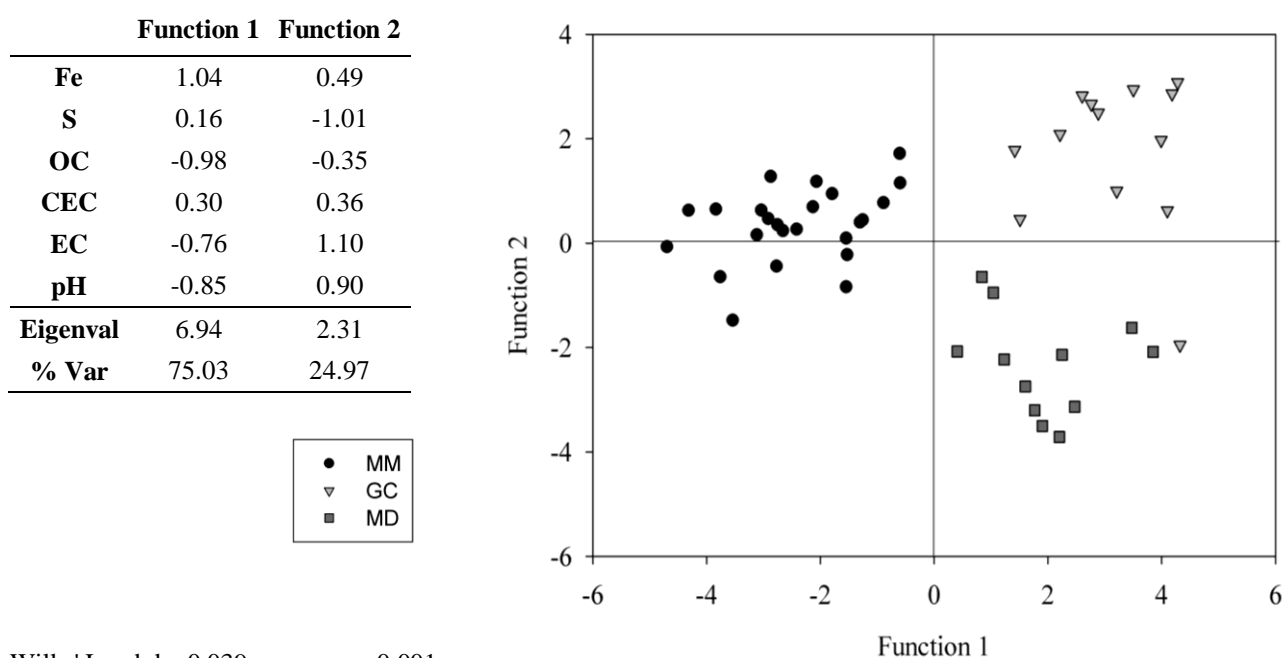
In Gran Chiusa salt marshes, both GC-Sar 1-2 pedons were classified as *Sulfic Fluvaquents* due to an irregular decrease of organic C content between a depth of 25 and 125 cm, and to the presence of sulfidic materials within 50 cm from the mineral soil surface (Table 5.2).

In Mosconi Dike road salt marsh both the studied pedons were ranked in in *Wassent* suborder. In the higher part of the salt marsh, MD-Sp1 was classified as *Sulfic Fluviwassent*, because it displayed an irregular decrease in organic C content between 25 and 100 cm below the mineral soil surface and because it contains sulfidic materials in horizons with a combined thickness of at least 15 cm, within 50 cm of the mineral soil surface, while in the lower part of the transect, MD-Sp2 was classified as *Fluventic Sulfwassent*, since it showed horizons with a combined thickness of a least 15 cm within 100 cm of mineral surface that contain sulfidic materials and an irregular decrease of organic C.

Two different Discriminant Function Analysis (DFA) were performed to identify the continuous variables related to the physicochemical properties of pedons which could discriminate the three salt marches geomorphological position in the lagoon, and their vegetation pattern.

The summary of the evaluation of the first DFA and its canonical score plot are shown in Figure 5.8.

**Figure 5.8.** Canonical score plot and standardized coefficients of the discriminant function analysis (DFA) based on the three salt marshes grouping. Only significant variables included in the model are shown.



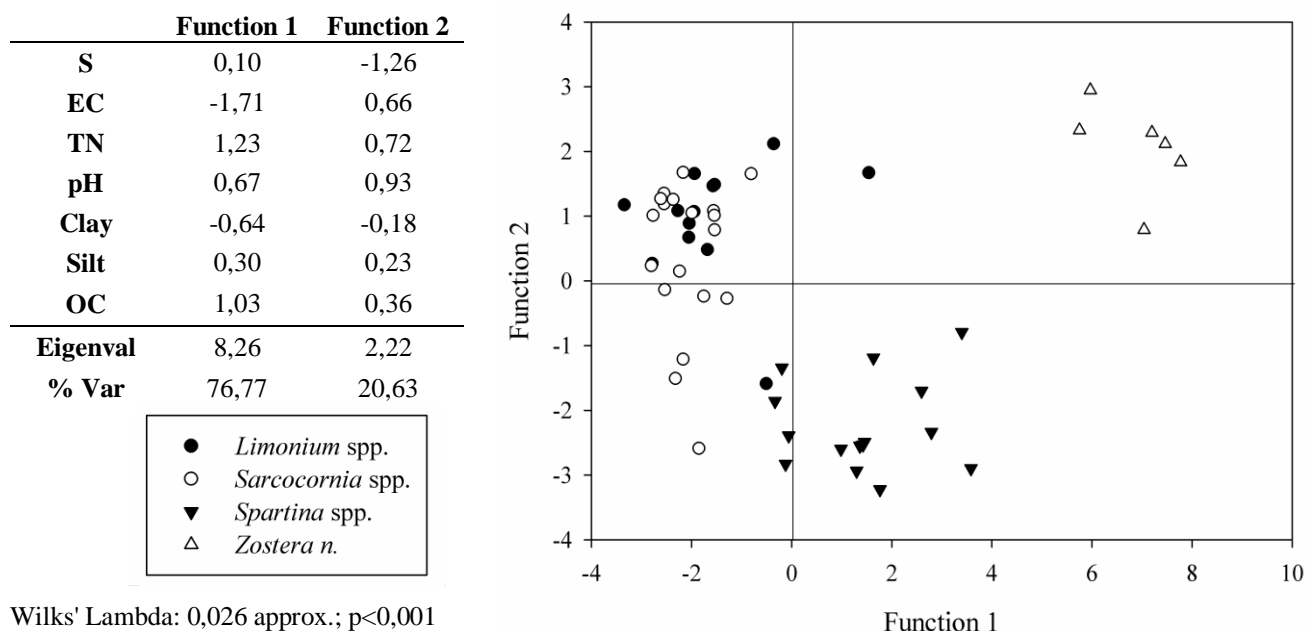
Wilks' Lambda: 0,039 approx.;  $p < 0.001$

Function 1 explained the 75% of the total variance between samples and it was driven by OC as negative standardized coefficient (SCDC) and by total Fe as positive factor: this allowed to discriminate MM salt marsh pedons, more rich in organic carbon, from those of CG and MD ones, which were characterized by a higher content of total Fe.

Function 2 explained the 25% of the total variance and it discriminated the subaqueous pedons of MD salt marsh from the hydric ones of GC study site. According to the discriminant power of the standardized coefficients, EC and total S content were identified as positive and negative discriminant variables, respectively, highlighting an increase of salinity from SAS to hydric soils and a decrease of S content.

A second discriminant analysis was performed on the same variables to highlight the influence of the vegetation cover on soil features. The summary of this evaluation is shown in Figure 5.9.

**Figure 5.9.** Canonical score plot and standardized coefficients of the discriminant function analysis (DFA) based on the different vegetation cover of soil profiles. Only significant variables included in the model are shown.



Function 1, mainly driven by EC in the negative sector and by OC and TN in the positive one, explained the 77% of the total variance and outlined all hydric soils from those submerged. According to this function, soils with a prevalent coverage of *Sarcocornia fruticosa* and *Limonium vulgare* subsp. *serotinum* (in MM and GC salt marshes) had high salinity level, mostly concentrated in the superficial organo-mineral horizons, while soil covered by *Spartina* spp. and by *Zostera n.* were characterized by higher OC and TN content. In this latter evaluation, the pedons discrimination in the positive sector of the scatter plot were mostly influenced by the high content of OC detected in MM-Zos and by the homogeneous distribution of OC in MD ones.

Moreover, according to Function 2, the pedon covered by *Zostera noltii* (MM-Zos) was discriminated from that covered with *Spartinetea maritimae* class in the MD salt marsh. The function was driven by pH in the positive sector and by S contents in the negative one, highlighting how MD subaqueous pedons covered by *Spartina* spp. were affected by high amount of reduced S compounds.

## 5.4. DISCUSSION

The Grado lagoon is characterized by salt marshes originated by different sedimentation processes from both Adriatic sea and Isonzo and Tagliamento rivers (Brambati, 1970), and by different human activities.

The effect of these processes, strongly influences the land morphology and the soil texture, highlighting how the riverine depositions in GC isle, and the artificial origin of MD one, have determined their loamy texture. On the contrary, the MM salt marsh lies parallel to the sea and it has been naturally formed by accumulation of calcareous sand deposits of marine origin.

In MM salt marsh, the low Fe content and the high EC values highlighted by the first DFA, confirm both the influence of the marine water intrusion within MM soils and the effect of the tide oscillation.

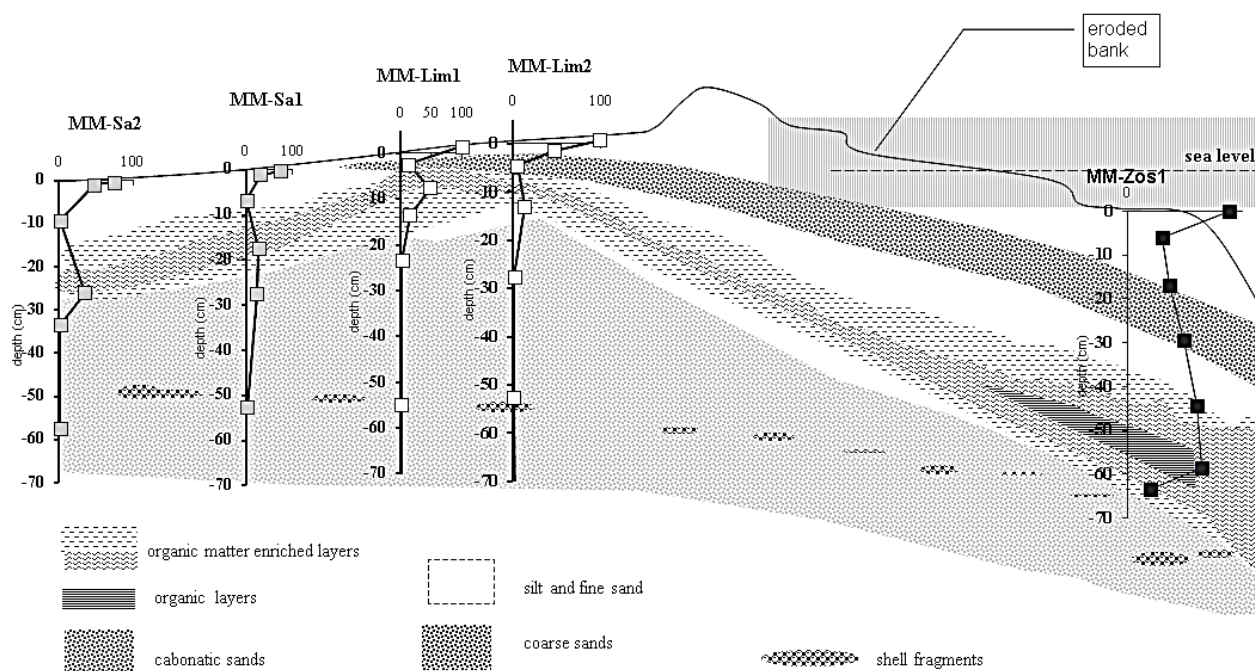
In the inner and most elevated soils (MM-Lim1-2 and MM-Sa1-2), the accumulation of salts in the superficial layer is related to aerosol depositions and evaporation phenomena (Cidu et al., 2013; Rose and Waite, 2003) while the high decrease of salinity along MM-Sa1-2 horizons and in MM-Zos pedons is due to the presence of a 90% sandy layer (Ashraf et al., 2010) and to the permanently saturated conditions of soil horizons. In these circumstances, in fact, the soluble ions which define the EC are leached through the marine flow (Bennett et al., 2009; Friedman, 2005).

The discontinuity of texture, the OC distribution in MM soil profiles and the presence of mottles, coats and organic fragments in their deep horizons suggest that an extraordinary sedimentation event has occurred in the past. The sequence of pedons from the inner MM salt marsh to the prospecting lagoon may not simply represent an hydrosquence, but reflect pedogenetic erosion/sorting/accumulation processes as in the Milne's second type of catena (hillslope with more than one type of parent rock). This hypothesis, is also strengthened by the presence of high organic matter content in MM-Zos, which can be due to the accumulation of eroded materials at the edge of the salt marsh (Bellucci et al., 2007).

The soil development under permanently submerged and anaerobic conditions, in fact, is usually characterized by low OC/S ratio, as confirmed by the trend of the OC/S ratio in most of the studied pedon (Ivanov et al., 1989). The only exception was the MM-Zos pedon which featured high OC/S ratios in gleyed horizons, probably due to the mixing of sandy deposits and eroded materials. A representation of the MM stratifications is presented in Figure 5.10.



**Figure 5.10.** Representation of OC distribution ( $\text{g kg}^{-1}$ ) and erosion processes in the MM salt marsh.



The silty-clay-loam texture and the high Fe content in GC and MD salt marshes suggest that their formation was more influenced by sedimentation of re-suspended silt riverine deposits enriched by Fe due to the weathering processes of rocks minerals (Krachler et al., 2005). The partial or permanent submerged soil conditions lead to a stronger TOC, Fe and S accumulation all along these profile compared to the surrounding hydromorphic soils. Under submerged conditions, all the studied pedons, in fact, act as an OC sink, due to the low degradation of the organic matter and the consequent increase of OC concentration in deep horizons. Moreover, under these conditions, the salinity decrease due to the salt leaching (Bennett et al., 2009).

The higher position on the tide level of GC pedons, the tide oscillation, and the presence of halophile species which allow the diffusion of oxygen in the topsoil, induce the formation of redoximorphic features along the soil profile and the development of some transition AC or AB horizons. On the other hand, in the deep horizons, where soil saturation is permanent and the vegetation is lacking, the clay-silt texture enable the formation of anaerobic zones in which sulfidic materials develop.

In MD salt marsh permanent subaqueous soils, the clay-silty texture promotes the formation of anaerobic conditions, and the high content of Fe and S suggests that the neoformation sulfidic materials are therefore favoured. The presence of *Spartina maritima* felt roots allows the accumulation of poorly humified organic

matter and induce oxygen diffusion only in a thin surface layer of the pedons (Pedersen et al., 2013; Zuo et al., 2012) triggering a slow pedogenetic process (Ding et al., 2010; Vann and Megonigal, 2003).

The tide oscillation clearly affects the kind of vegetation pattern on the soil surface, and promotes the formation of redoximorphic features, which results in the alternation of wet/dry cycle of soil horizons and in the consequently reduction, translocation and/or oxidation of iron and manganese oxides (Schaetzl and Anderson, 2005).

The development of redoximorphic features is also due to the presence of plants roots, which strongly contribute to diffuse oxygen and prevent anoxic conditions (Génin et al., 1998; Vepraskas et al., 2000). The vegetation growth, in fact, plays a fundamental role on the soil development influencing its physicochemical characteristics, and it as well function of several physical, chemical and biochemical factors, e.g. land morphology, salinity tolerance and submergence of the pedon (Silvestri et al., 2005).

The colonization of halophyte species such as *Limonium vulgare* and *Sarcocornia fruticosa*, which can survive only in partial submergence conditions and tolerate high salinity levels, has a very strong effect on soil aeration through roots respiration, and on soil horizons development, thus developing organic (O) and transitions (AB) horizons. Nevertheless, their tolerance mechanism should be investigated by further studies.

In soils submerged by shallow water, *Zostera noltii* and *Spartina maritima* contribute to mitigate salinity and to diffuse oxygen in the top soil, but they also enhance the accumulation of organic residues, contributing to the function of C sink of these pedons (Pedersen et al., 2013; Zuo et al., 2012). Under submerged conditions, the binding of reduced S species to the low-decompose organic matter favours the accumulation of sulphuric compounds, and the development of the sulfidization processes (Kao et al., 2004; Krairapanond et al., 1992), which strongly characterize the subaqueous marine environments covered by *Spartina maritima*.

## 5.5. CONCLUSION

The genesis of soils in Grado and Marano lagoon depends on a complex interaction of morphological, physical, chemical and biological factors. The tide oscillation and the different origin of the salt marshes deeply affect the soil development and their physicochemical characters.

The southernmost salt marsh (MM) is highly influenced by marine sandy depositions occurred during time and despite its well-constructed vegetation cover, the evidence of erosion processes has been highlighted by the analysis of the physicochemical properties of soils.

Completely different soils type were found in the inner GC and MD saltmarshes, which were characterized by silty-clay texture and the partial or total submergence condition. The effect of the tide oscillation is stronger in these sites, and it could be recognized by the presence of redoximorphic features, salinity and O/S trend, and by the distribution of organic carbon.

A clear relationship exists between vegetation species and salt marshes hydromorphism. The biodiversity observed within the same salt marsh is due to a very complex feedback mechanism, in which halophyte species growth as function of soil physicochemical characteristics and *viceversa* soil develops as function of the capacity of plants to accumulate organic matter, transfer of oxygen to roots and soil and mitigate salinity.

Further multidisciplinary studies should be carried out to understand the physiological, biochemical and microbiological interactions between these soils and their ecosystem.

## 5.6. REFERENCES

- D' Aietti, A., and A. Altobelli. 2007. Fish farming in Grado Lagoon: impacts and dynamics of two fishfarm. Pages 224–238 *Guidelines and case studies for the management of Natura 2000 sites in transitional environments*. TRIESTE. EUT., Grado (GO).
- Aran, D., A. Maul, and J.-F. Masfaraud. 2008. A spectrophotometric measurement of soil cation exchange capacity based on cobaltihexamine chloride absorbance. *Comptes Rendus Geoscience* 340:865–871.
- ARPA. 2007. Sistema georeferenziato GIS e monitoraggio delle barriere artificiali sommerse. Agenzia Regionale per la Protezione dell' Ambiente del Friuli Venezia Giulia: Gestione sostenibile delle risorse alieutiche marine e lagunari.
- Ashraf, M., O. Ozturk, and M. S. A. Ahmad. 2010. *Plant Adaptation and Phytoremediation*. Pages 1–481. Springer Netherlands, Dordrecht.
- Bellucci, L. G., M. Frignani, J. K. Cochran, S. Albertazzi, L. Zaggia, G. Cecconi, and H. Hopkins. 2007. <sup>210</sup>Pb and <sup>137</sup>Cs as chronometers for salt marsh accretion in the Venice Lagoon - links to flooding frequency and climate change. *Journal of environmental radioactivity* 97:85–102.
- Bennett, S. J., E. G. Barrett-Lennard, and T. D. Colmer. 2009. Salinity and waterlogging as constraints to saltland pasture production: A review. *Agriculture, Ecosystems & Environment* 129:349–360.
- Black, P. E. 2007. Revisiting the Thornthwaite and Mather Water Balance<sup>1</sup>. *JAWRA Journal of the American Water Resources Association* 43:1604–1605.
- Bradley, M. P., and M. H. Stolt. 2003. Subaqueous Soil-Landscape Relationships in a Rhode Island Estuary. *Soil Science Society of America Journal* 67:1487.
- Brambati, A. 1970. Provenienza, trasporto e accumulo dei sedimenti recenti nelle lagune di Marano e di Grado e nei litorali tra i fiumi Isonzo e Tagliamento. *Memorie della Società Geologica Italiana* 9:281–329.
- Cidu, R., L. Vittori Antisari, R. Biddau, A. Buscaroli, S. Carbone, S. Da Pelo, E. Dinelli, G. Vianello, and D. Zannoni. 2013. Dynamics of rare earth elements in water–soil systems: The case study of the Pineta San Vitale (Ravenna, Italy). *Geoderma* 193-194:52–67.
- Ciesielskui, H., and T. Sterckeman. 1997. Determination of cation exchange capacity and exchangeable cations in soils by means of cobalt hexamine trichloride. *Agronomie* 17:1–7.
- Conti, F., G. Abbate, A. Alessandrini, and C. Blasi. 2005. *An annotated check-list of the italian vascular flora*. Palombi ed. Roma.

- Covelli, S., A. Acquavita, R. Piani, S. Predonzani, and C. De Vittor. 2009. Recent contamination of mercury in an estuarine environment (Marano lagoon, Northern Adriatic, Italy). *Estuarine, Coastal and Shelf Science* 82:273–284.
- Ding, W., Y. Zhang, and Z. Cai. 2010. Impact of permanent inundation on methane emissions from a *Spartina alterniflora* coastal salt marsh. *Atmospheric Environment* 44:3894–3900.
- Erich, E., P. J. Drohan, L. R. Ellis, M. E. Collins, M. Payne, and D. Surabian. 2010. Subaqueous soils: their genesis and importance in ecosystem management. *Soil Use and Management* 26:245–252.
- Ferrarin, C., G. Umgiesser, M. Bajo, D. Bellafiore, F. De Pascalis, M. Ghezzi, G. Mattassi, and I. Scroccaro. 2010. Hydraulic zonation of the lagoons of Marano and Grado, Italy. A modelling approach. *Estuarine, Coastal and Shelf Science* 87:561–572.
- Ferreira, T. O., P. Vidal-Torrado, X. L. Otero, and F. Macías. 2007. Are mangrove forest substrates sediments or soils? A case study in southeastern Brazil. *Catena* 70:79–91.
- Fontolan, G., S. Pilon, A. Bezzi, R. Villalta, M. Lipizer, A. Triches, and A. D'Aietti. 2012. Human impact and the historical transformation of saltmarshes in the Marano and Grado Lagoon, northern Adriatic Sea. *Estuarine, Coastal and Shelf Science* 113:41–56.
- Friedman, S. P. 2005. Soil properties influencing apparent electrical conductivity: a review. *Computers and Electronics in Agriculture* 46:45–70.
- Génin, J.-M. R., G. Bourrié, F. Trolard, M. Abdelmoula, A. Jaffrezic, P. Refait, V. Maitre, B. Humbert, and A. Herbillon. 1998. Thermodynamic Equilibria in Aqueous Suspensions of Synthetic and Natural Fe(II)–Fe(III) Green Rusts: Occurrences of the Mineral in Hydromorphic Soils. *Environmental Science & Technology* 32:1058–1068.
- De Groot, R., L. Brander, S. van der Ploeg, R. Costanza, F. Bernard, L. Braat, M. Christie, N. Crossman, A. Ghermandi, L. Hein, S. Hussain, P. Kumar, A. McVittie, R. Portela, L. C. Rodriguez, P. ten Brink, and P. van Beukering. 2012. Global estimates of the value of ecosystems and their services in monetary units. *Ecosystem Services* 1:50–61.
- Ivanov, M. V., A. Yu, M. S. Reeburgh, and G. W. Skyring. 1989. Interaction of sulphur and carbon cycles in marine sediments. *Evolution of global biogeochemical sulphur cycle*. John Wiley & Son Ltd.
- Kao, S. J., C.-S. Horng, A. P. Roberts, and K.-K. Liu. 2004. Carbon–sulfur–iron relationships in sedimentary rocks from southwestern Taiwan: influence of geochemical environment on greigite and pyrrhotite formation. *Chemical Geology* 203:153–168.
- Koch, E. W., E. B. Barbier, B. R. Silliman, D. J. Reed, G. M. Perillo, S. D. Hacker, E. F. Granek, J. H. Primavera, N. Muthiga, S. Polasky, B. S. Halpern, C. J. Kennedy, C. V. Kappel, and E. Wolanski. 2009. Non-linearity in ecosystem services: temporal and spatial variability in coastal protection. *Frontiers in Ecology and the Environment* 7:29–37.

- Krachler, R., F. Jirsa, and S. Ayromlou. 2005. Factors influencing the dissolved iron input by river water to the open ocean. *Biogeosciences* 2:311–315.
- Krairapanond, N., R. D. DeLaune, and W. H. Patrick. 1992. Distribution of organic and reduced sulfur forms in marsh soils of coastal Louisiana. *Organic Geochemistry* 18:489–500.
- McVey, S., P. J. Schoeneberger, J. Turenne, M. Payne, and D. A. Wysocki. 2012. SUBAQUEOUS SOILS (SAS) DESCRIPTION. Field Book for Describing and Sampling Soils. Third edition. National Soil Survey Center Natural Resources Conservation Service U.S. Department of Agriculture.
- Michelutti, G., S. Zanolla, and S. Barbieri. 2003. Suoli e paesaggi del Friuli Venezia Giulia. ERSA.
- Newhall, F. 1972. of Soil Moisture Regimes from the climatic record.
- Osher, L. J., and C. T. Flannagan. 2007. Soil/Landscape Relationships in a Mesotidal Maine Estuary. *Soil Science Society of America Journal* 71:1323.
- Pedersen, O., T. D. Colmer, and K. Sand-Jensen. 2013. Underwater photosynthesis of submerged plants - recent advances and methods. *Frontiers in plant science* 4:140.
- Peel, M. C., and G. Bloschl. 2011. Hydrological modelling in a changing world. *Progress in Physical Geography* 35:249–261.
- Poldini, L., M. Vidali, and M. L. Fabiani. 1999. La vegetazione del litorale sedimentario del Friuli-Venezia Giulia (NE Italia) con riferimenti alla regione alto-adriatica. *Studia Geobotanica* 17:3–68.
- Rose, A. L., and T. D. Waite. 2003. Kinetics of iron complexation by dissolved natural organic matter in coastal waters. *Marine Chemistry* 84:85–103.
- Schaetzl, R. J., and S. Anderson. 2005. *Soils: Genesis and Geomorphology*. Cambridge University Press.
- Schoeneberger, P., D. A. Wysocki, and E. C. J. Benham. 2012. Field book for describing and sampling soils, Version 3.0. Natural Resources Conservation Service, National Soil Survey Center, Lincoln, NE.
- Silvestri, S., A. Defina, and M. Marani. 2005. Tidal regime, salinity and salt marsh plant zonation. *Estuarine, Coastal and Shelf Science* 62:119–130.
- Soil Survey Staff. 2014. *Keys to Soil Taxonomy*. 12th edition. United States Department of Agriculture, Natural Resources Conservation Service.
- Thornthwaite, C. W., and J. R. Mather. 1957. Instructions and tables for computing potential evapotranspiration and the water balance, Part 2. Page 254. Laboratory of Climatology.

- Vann, C. D., and J. P. Megonigal. 2003. Elevated CO<sub>2</sub> and water depth regulation of methane emissions: Comparison of woody and non-woody wetland plant species. *Biogeochemistry* 63:117–134.
- Vaughan, R. E., B. A. Needelman, P. J. A. Kleinman, and M. C. Rabenhorst. 2008. Morphology and Characterization of Ditch Soils at an Atlantic Coastal Plain Farm. *Soil Science Society of America Journal* 72:660.
- Vepraskas, M. J., C. B. Craft, and J. L. Richardson. 2000. *Wetland Soils: Genesis, Hydrology, Landscapes, and Classification*.
- Van Wambeke, A. R. 2000. The Newhall Simulation Model for estimating soil moisture & temperature regimes. Department of Crop and Soil Sciences, Cornell University, Ithaca, NY USA.
- Zannoni, D. 2008. *Uso sostenibile dei suoli forestali di ambiente costiero in relazione ai fattori di pressione esistenti*. University of Bologna.
- Zuo, P., S. Zhao, C. Liu, C. Wang, and Y. Liang. 2012. Distribution of *Spartina* spp. along China's coast. *Ecological Engineering* 40:160–166.





# CHAPTER 6

## CONCLUSIONS

*pp.*

6.	Conclusions.....	113
6.1.	Freshwater systems.....	113
6.2.	Brackish systems.....	113
6.3.	Saline systems.....	114



## 6. CONCLUSIONS

This research has explored different aquatic systems and in each case, an important environmental issue has been investigated (e.g. environmental quality and subaqueous soils development) to understand the key role of water on the soil characterization and land transformation.

### 6.1. FRESHWATER SYSTEMS

In the freshwater system of the Reno river basin, the strong exchange dynamic between water and sediment, highlighted the serious problem of the hydraulic security and of the environmental risk. In this contest, the evaluation of heavy metals risk assessment underlined that:

- sediments of the Reno river basin are differently affected by heavy metals contamination;
- heavy metals partitioning and fractionation techniques are more useful than the traditional ones for assessing the environmental hazard of freshwater sediments;
- the environmental hazard of some heavy metals increases after dredging operations and sediment drying;
- eco-friendly materials, such as natural clays and zeolites, can be used for water remediation and for the protection of sediment contamination avoiding the environmental problems linked to sediment dredging.

As final remark the applications of these materials for environmental protection needs to be improved and tested at large-scale, in order to consider all the environmental factors which are present in a real system.

### 6.2. BRACKISH SYSTEMS

In the brackish system of S. Vitale park, the ancient sediment depositions have formed different subaqueous and hydromorphic environments, where soils are subjects to different saturation degrees and different salinity levels. The characterization of soil profiles along distinct transects showed that:

- the formation of an unique *soil continuum* from subaqueous to hydromorphic soil includes subaqueous substrates in which pedogenetic processes can be recognized;
- both the physical features (e.g. texture) and the saline gradient represent common features among soil profiles highlighting the effect of the saline water intrusion oscillation and evaporation, along the soil

profiles while O/C ratio and carbonate distributions drive the transition from subaqueous to hydromorphic environments;

- some specific field indicators (e.g. matrix colour and redoximorphic features) as well as chemical indicators (e.g. OC/S ratio) and biochemical processes (e.g. carbon depletion and sulfidization) can be used to characterize and predict the soil transition processes from subaqueous to hydromorphic soils.

### **6.3. SALINE SYSTEMS**

In the saline system of the Grado lagoon, the study of the relationship between soil hydromorphism and its vegetation cover demonstrated that:

- soil development and characterization is function of the exposure to the open sea, the morphology of the area and of the tide oscillation level;
- the vegetation species on soil profiles are salt and sulphur-tolerant species, and they play an important role in the development of both hydric and subaqueous soils, through oxygen diffusion into the soil and organic matter accumulation along the soil profile.
- the study of the soil-vegetation cover relationship is a very important starting point for the mapping of hydric and subaqueous soils of Italian coasts and it can be used to define proper land-units for the management of aquatic resources.

As final remark, the study of subaqueous soils development should be carried on by involving others scientific disciplines. In fact, only a multidisciplinary approach, which include physical, chemical, biochemical, biological and microbiological expertise, could achieved a complete understanding of the complex reactions occurring in submerged systems.

## **APPENDICES**



## APPENDIX 1. River and canal sampling stations.

**Label**

F01 UpS

Reno river –Upstream

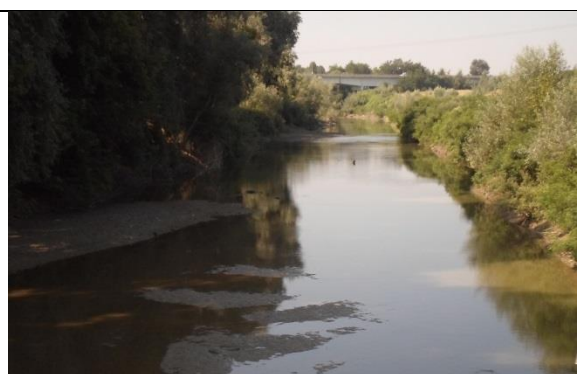
**Location**

Sasso Marconi (BO)

**Coordinates (UTM 32T)**

679865.00 m E

4917996.00 m N

**Label**

F02 DwS

Reno river – Downstream

**Location**

Bonconvento (BO)

**Geographical coordinates (UTM 32T)**

683806.00 m E

4942519.00 m N

**Label**

F03 UpS

Idice stream – Upstream

**Location**

Ozzano (BO)

**Geographical coordinates (UTM 32T)**

693376.00 m E

4916226.00 m N

**Label**

F04 DwS

Idice stream – Downstream

**Location**

Pieve di Budrio (BO)

**Geographical coordinates (UTM 32T)**

700104.00 m E

4935566.00 m N

**Label**

F05 UpS  
Samoggia stream – Upstream

**Location**

Monteveglia (BO)

**Geographical coordinates (UTM 32T)**

666724.00 m E  
4926760.00 m N

**Label**

F06 DwS  
Samoggia stream – Downstream

**Location**

Forcelli (BO)

**Geographical coordinates (UTM 32T)**

676938.00 m E  
4942926.00 m N

**Label**

F07 UpS  
Sillaro stream – Upstream

**Location**

S. Martino in Pedriolo (BO)

**Geographical coordinates (UTM 32T)**

710860.00 m E  
4907991.00 m N

**Label**

F08 DwS  
Sillaro stream – Downstream

**Location**

Sesto imolese (BO)

**Geographical coordinates (UTM 32T)**

727872.00 m E  
4924669.00 m N

---



**Label**

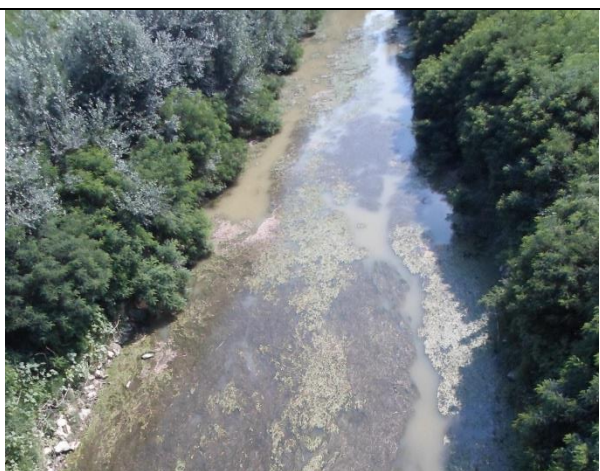
F09 UpS  
Santerno river – Upstream

**Location**

Codrignano (BO)

**Geographical coordinates (UTM 32T)**

704218.00 m E  
4914291.00 m N

**Label**

F10 DwS  
Santerno river – Downstream

**Location**

S. Agata in Santerno (BO)

**Geographical coordinates (UTM 32T)**

717693.00 m E  
4926952.00 m N

**Label**

C01 UpS  
Medicina canal- Upstream

**Location**

Medicina

**Geographical coordinates (UTM 32T)**

708281.00 m E  
4925607.00 m N

---

**Label**

C02 DwS  
Medicina canal- Wastewater plant

**Location**

Medicina

**Geographical coordinates (UTM 32T)**

710372.00 m E  
4929064.00 m N

**Label**

C03 DwS  
Medicina canal- Downstream

**Location**

Medicina

**Geographical coordinates (UTM 32T)**

711256.00 m E  
4930832.00 m N

**Label**

C04 UpS  
Zenetta canal- Upstream

**Location**

Quarto inferiore (BO)

**Geographical coordinates (UTM 32T)**

692640.00 m E  
4932057.00 m N

**Label**

C05 DwS  
Zenetta canal – Downstream

**Location**

Quarto inferiore (BO)

**Geographical coordinates (UTM 32T)**

692115.00 m E  
4933830.00 m N

---



**Label**

C07 UpS  
Dosolo – Upstream

**Location**

Calderara di Reno (BO)

**Geographical coordinates (UTM 32T)**

681227.00 m E  
4937578.00 m N

**Label**

C10 DwS  
Dosolo – Downstream

**Location**

Calderara di Reno (BO)

**Geographical coordinates (UTM 32T)**

681191.00 m E  
4937880.00 m N

**Label**

C09 -UpS  
Riolo – Upstream

**Location**

S. Venanzio (BO)

**Geographical coordinates (UTM 32T)**

693504.00 m E  
4957379.00 m N

**Label**

C11 - DwS  
Riolo – Downstream

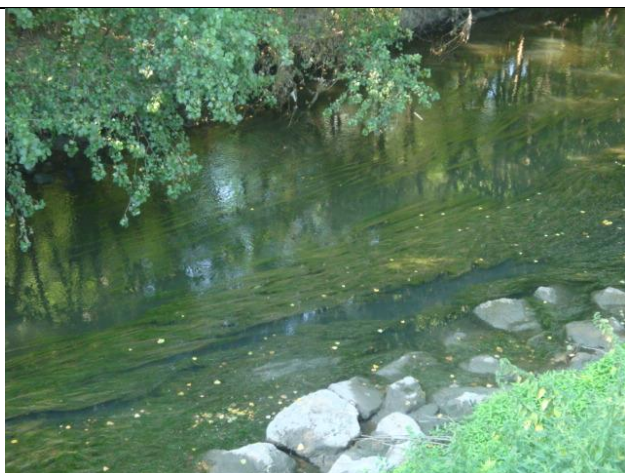
**Location**

S. Venanzio (BO)

**Geographical coordinates (UTM 32T)**

692106.00 m E  
4957656.00 m N

---

**Label**

C12 -UpS  
Navile – Upstream

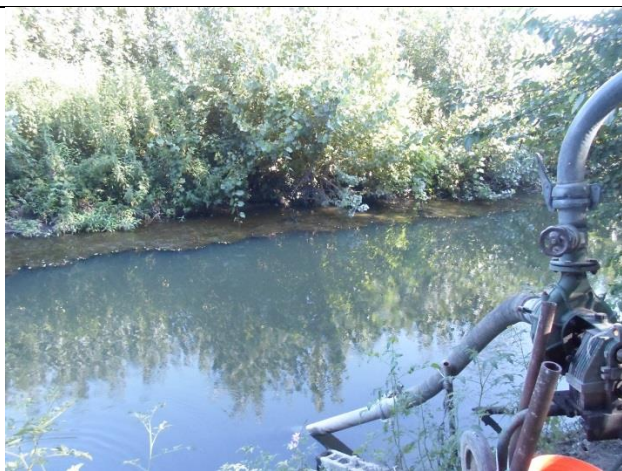
**Location**

Bologna (BO)

**Geographical coordinates (UTM 32T)**

687916.00 m E

4936497.00 m N

**Label**

C13 - DwS  
Navile – Downstream

**Location**

Bologna (BO)

**Geographical coordinates (UTM 32T)**

690042.00 m E

4940446.00 m N

---

**APPENDIX 2.** River and canal waters properties (RUpS, RDwS, CUpS and CDwS respectively). Mean, Standard deviation (SD), Maximum (Max), Minimum (Min) and p level (p) are reported.

		Mean	SD	Min	Max	p		Mean	SD	Minimum	Maximum	P	
pH	RUpS	8,21	0,27	7,25	9,01	0,00	Al (mg L <sup>-1</sup> )	RUpS	24,29	14,43	0,00	76,70	0,00
	RDwS	8,12	0,23	7,35	8,57			RDwS	26,89	26,20	0,00	147,00	
	CUpS	7,77	0,27	6,95	8,19			CUpS	70,19	120,02	1,12	562,00	
	CDwS	7,67	0,35	6,90	8,27			CDwS	30,58	28,86	0,71	136,00	
EC (mS cm <sup>-1</sup> )	RUpS	0,62	0,29	0,23	1,84	0,00	Fe (mg L <sup>-1</sup> )	RUpS	19,93	7,58	4,84	38,80	0,00
	RDwS	0,75	0,33	0,25	1,85			RDwS	24,89	9,89	7,16	52,30	
	CUpS	0,81	0,39	0,24	1,95			CUpS	154,09	233,39	17,30	1007,00	
	CDwS	0,86	0,37	0,25	1,74			CDwS	101,46	106,02	17,60	523,00	
HCO <sub>3</sub> <sup>-</sup> (mg L <sup>-1</sup> )	RUpS	140,92	69,43	30,74	289,90	0,00	Mn (mg L <sup>-1</sup> )	RUpS	3,94	5,42	0,52	19,30	0,00
	RDwS	160,42	82,27	61,49	488,95			RDwS	11,07	23,80	0,56	101,00	
	CUpS	253,13	80,05	101,50	395,80			CUpS	245,38	404,92	3,62	1884,00	
	CDwS	252,95	66,48	85,40	466,25			CDwS	69,65	53,84	4,12	253,00	
DOM (mg L <sup>-1</sup> )	RUpS	3,23	1,00	1,39	5,71	0,00							
	RDwS	4,38	1,80	1,26	12,55								
	CUpS	7,59	4,17	0,18	18,96								
	CDwS	8,01	2,66	3,74	14,24								
DON (mg L <sup>-1</sup> )	RUpS	0,93	0,67	0,27	3,84	0,00							
	RDwS	2,23	1,99	0,27	11,23								
	CUpS	4,34	3,59	0,61	14,49								
	CDwS	6,49	4,05	0,60	14,27								
K (mg L <sup>-1</sup> )	RUpS	0,55	1,68	0,00	8,18	0,00							
	RDwS	0,67	2,04	0,01	10,80								
	CUpS	15,69	16,26	3,61	92,00								
	CDwS	18,58	9,39	2,79	41,50								
P (mg L <sup>-1</sup> )	RUpS	57,76	25,99	0,01	107,00	0,00							
	RDwS	72,02	33,88	0,01	132,00								
	CUpS	0,42	0,38	0,10	1,51								
	CDwS	0,93	0,89	0,04	3,27								
Mg (mg L <sup>-1</sup> )	RUpS	32,38	18,44	5,41	87,60	0,00							
	RDwS	37,52	18,45	5,84	80,70								
	CUpS	26,26	11,03	9,93	55,60								
	CDwS	24,89	11,97	11,20	64,40								
S (mg L <sup>-1</sup> )	RUpS	44,11	55,53	0,71	285,00	0,05							
	RDwS	24,01	21,08	0,71	80,90								
	CUpS	29,94	14,40	8,63	59,40								
	CDwS	36,53	19,81	13,00	110,00								
Na (mg L <sup>-1</sup> )	RUpS	3,58	7,37	0,08	42,60	0,00							
	RDwS	4,25	9,71	0,01	59,40								
	CUpS	44,44	29,09	8,32	121,00								
	CDwS	73,38	56,51	0,02	256,00								
Ca (mg L <sup>-1</sup> )	RUpS	22,00	30,58	0,36	180,00	0,00							
	RDwS	31,99	27,00	0,36	130,00								
	CUpS	91,84	36,72	42,70	165,00								
	CDwS	95,12	33,39	42,70	169,00								

**APPENDIX 3.** River and canal sediments properties (RUpS, RDwS, CUpS, CDwS). Mean, Minimum (Min), maximum (Max) Standard deviation (SD) and ANOVA.









		Label	Mean	Min	Max	SD	ANOVA
<b>Ph</b>		RUpS	7,8	3,4	8,8	1,5	0,00
		RDwS	8,2	7,6	8,7	0,2	
		CUpS	7,6	7,0	8,2	0,3	
		CDwS	7,5	6,8	8,2	0,4	
<b>CE</b>	<b>μS cm-1</b>	RUpS	293,2	150,0	908,0	148,7	0,00
		RDwS	363,4	156,5	1850,0	291,7	
		CUpS	823,5	256,0	2345,0	574,0	
		CDwS	798,6	382,8	2142,0	308,5	
<b>CaCO<sub>3</sub></b>	<b>%</b>	RUpS	27,7	15,1	43,8	7,3	0,00
		RDwS	20,9	13,6	37,0	5,7	
		CUpS	13,2	7,0	29,6	4,7	
		CDwS	15,8	9,1	30,6	4,7	
<b>TN</b>		RUpS	1,3	0,1	25,5	3,9	0,02
		RDwS	1,1	0,1	19,7	3,1	
		CUpS	2,4	0,8	6,4	1,3	
		CDwS	2,6	0,4	5,0	0,9	
<b>TOC</b>		RUpS	5,4	0,2	25,5	5,4	0,00
		RDwS	5,5	0,1	19,7	4,7	
		CUpS	23,3	5,3	63,0	13,9	
		CDwS	23,4	3,6	49,7	9,6	
<b>K</b>		RUpS	5,9	0,7	15,2	3,7	0,00
		RDwS	5,6	1,0	17,8	3,9	
		CUpS	10,3	4,0	25,8	5,1	
		CDwS	9,2	1,5	23,2	4,7	
<b>P</b>		RUpS	0,3	0,1	0,9	0,2	0,00
		RDwS	0,4	0,1	1,2	0,3	
		CUpS	1,6	0,2	4,1	1,0	
		CDwS	2,1	0,1	8,7	1,7	
<b>S</b>	<b>g kg<sup>-1</sup></b>	RUpS	1,0	0,2	3,1	0,6	0,0
		RDwS	0,7	0,1	3,9	0,6	
		CUpS	1,7	0,4	5,5	1,0	
		CDwS	2,0	0,3	4,3	0,9	
<b>Ca</b>		RUpS	99,6	22,0	293,7	62,9	0,06
		RDwS	91,1	12,4	231,0	53,0	
		CUpS	72,2	28,4	134,2	27,6	
		CDwS	78,7	37,9	223,1	32,9	
<b>Mg</b>		RUpS	10,0	3,5	23,9	4,6	0,00
		RDwS	9,2	2,1	27,1	5,0	
		CUpS	12,8	5,7	27,7	5,9	
		CDwS	12,5	3,6	23,2	5,2	
<b>Fe</b>		RUpS	35,9	10,7	143,4	25,3	0,38
		RDwS	29,3	8,8	64,1	14,6	
		CUpS	35,3	13,9	68,4	16,2	
		CDwS	31,7	7,3	70,9	17,5	

		Label	Mean	Min	Max	SD	ANOVA
<b>Mn</b>		RUpS	1537,2	624,7	4524,0	943,8	0,01
		RDwS	1348,2	424,7	3036,3	662,6	
		CUpS	1253,0	547,7	4750,1	765,9	
		CDwS	997,3	332,4	2841,3	551,2	
<b>Cd</b>		RUpS	0,1	0,0	0,2	0,0	0,00
		RDwS	0,1	0,0	0,2	0,0	
		CUpS	0,9	0,1	4,8	1,2	
		CDwS	0,5	0,1	1,8	0,4	
<b>Co</b>		RUpS	11,8	3,7	29,8	6,0	0,00
		RDwS	11,2	3,2	26,2	5,6	
		CUpS	23,8	8,5	72,3	14,1	
		CDwS	16,8	4,6	45,4	8,6	
<b>Cr</b>		RUpS	89,4	22,5	222,4	49,0	0,00
		RDwS	100,5	25,7	239,8	55,2	
		CUpS	147,2	47,7	398,6	86,5	
		CDwS	139,9	58,0	378,0	79,9	
<b>Cu</b>	<b>mg kg<sup>-1</sup></b>	RUpS	28,4	5,2	69,0	17,7	0,00
		RDwS	25,7	7,4	59,9	15,3	
		CUpS	132,3	25,2	538,9	105,2	
		CDwS	175,2	52,2	498,9	105,6	
<b>Zn</b>		RUpS	70,9	18,3	189,1	35,5	0,00
		RDwS	71,3	23,1	192,9	39,8	
		CUpS	707,9	65,2	4927,4	997,6	
		CDwS	563,0	98,6	3768,5	715,3	
<b>Ni</b>		RUpS	47,0	16,7	102,4	21,1	0,00
		RDwS	44,7	16,2	104,9	20,9	
		CUpS	80,2	27,9	175,9	38,0	
		CDwS	71,0	24,1	236,5	41,2	
<b>Pb</b>		RUpS	11,2	3,0	19,4	4,1	0,00
		RDwS	15,2	4,7	68,7	12,4	
		CUpS	73,2	10,3	365,9	81,4	
		CDwS	68,4	14,5	208,4	46,8	











**APPENDIX 4.** Northern (a) and southern (b) soil profiles of S. Vitale park.

Northern site

<p>N1- Intedunal forest</p> 	<p>Soil profile</p> 	<p>Coordinates (UTM -32T)</p> <p>279845 m E</p> <p>4934006 m N</p>
<p>N2- interdunal forest/grassland</p> 	<p>Soil profile</p> 	<p>Coordinates (UTM -32T)</p> <p>280408 m E</p> <p>4933986 m N</p>
<p>N3- brackish waterhole</p> 	<p>Soil profile</p> 	<p>Coordinates (UTM -32T)</p> <p>280300 m E</p> <p>4933916 m N</p>
<p>N4- Wetland</p> 	<p>Soil profile</p> 	<p>Coordinates (UTM -32T)</p> <p>280183 m E</p> <p>4931633 m N</p>

(b) Sothern site

S1-Interdunal forest	Soil profile	Coordinates (UTM -32T) 279731 m E 4928557 m N
		
S2- Interdunal grassland	Soil profile	Coordinates (UTM -32T) 280253 m E 4928520 m N
		
S3- Wetland	Soil profile	Coordinates (UTM -32T) 280334 m E 4929135 m N
		
S4- Pialassa	Soil profile	Coordinates (UTM -32T) 280483 m E 4929167 m N
		



**APPENDIX 5.** Landscape and geographical localization of salt marshes soils in Grado Lagoon.

Marina di macia salt marsh

MM-Lim1-2	Soil profile		Coordinates (UTM -32T)
	Lim1	Lim2	370823 m E
			5061550 m N
MM-Sa1-2	Soil profile		Coordinates (UTM -32T)
	Sa1	Sa2	370769 m E
			506110 m N
MM-Zos	Soil profile		Coordinates (UTM -32T)
			370670 m E
			5061322 m N

Gran Chiusa salt marsh

GC-Sar1



Soil profile



Coordinates (UTM -32T)

367989 m E

5064769 m N

GC-Sar2



Soil profile



Coordinates (UTM -32T)

367638 m E

504675 m N

Moskoni Dike salt marsh

MD-Sp1



Soil profile



Coordinates (UTM -32T)

374268 m E

5064144 m N

MD-Sp2



Soil profile



Coordinates (UTM -32T)

374185 m E

5063915 m N

**APPENDICE 6.** (a) Main descriptive elements of investigated Hydromorphic soil (Aqueunts) profiles. Codes according to Schoeneberger et al. (2012).

Profile and prevalent species	Horizons			Matrix Color Munsell (Moist)	Mottles Q/C/Color	Texture	Structure T/G/S	Consistence S/P	RMFs (K/Q/S) Q/K/Color	Roots Q/S	Biological concentration Q/K	Peroxide color change	Odor (K/I)
	Master	Depth (cm)	Boundary Q/T										
MM-Lim1 <i>Limonium vulgare</i> subsp. <i>serotinum</i>	Oe	3-0	A/S	10YR 2/1		MK	PL/2/m	s/p		m/vf		N	N
	A1	0-5	C/W	10YR 7/2		LS	GR/1/f	so/ps		m/f	c/RSB	N	N
	A2	5-10	C/S	10YR 4/1		S	ABK/2/m	s/p		f/m	f/RSB	N	N
	Ab	10-17	C/W	10YR 4/1	f/d/7.5YR 5/6	SL	ABK/2/m	ss/ps		c/fm		N	N
	C	17-30	C/W	10YR 6/1	f/d/7.5YR 6/8	S	SG/0	ss/po		c/m		N	N
	Cg1	30-80	A/S	10YR 6/1		S	SG/0	so/po		f/m	f/SFB	N	N
	Cg2	80-100	U	Gley1 5/10Y		SL	SG/0	so/po			f/SFB	N	N
MM-Lim2 <i>Limonium vulgare</i> subsp. <i>serotinum</i>	Oe	1.5-0	A/S	10YR 2/1		MK						N	N
	A1	0-3	C/W	10YR 2/2		LS	PL/1/f	ss/p		m/fm	m/RSB	N	N
	A2	3-6	C/S	10YR 6/2	f/d/7.5YR 5/8	S	ABK/1/f	ss/ps		c/m	f/SFB&RSB	N	N
	Ab	6-20	C/W	10YR 4/1	f/d/7.5YR 5/8	SL	ABK/2/m	ss/ps		c/fm	f/SFB&RSB	N	N
	C	20-35	C/W	10YR 6/1		S	SG/0	ss/po	FEF/f/3	c/m		N	N
	Cg1	35-70	A/S	10YR 6/1		S	SG/0	so/po		f/m	c/SFB	N	N
	Cg2	70-100	U	Gley1 7/10Y		SL	SG/0	so/po		f/m		N	N
MM-Sa1 <i>Sarcocornia fruticosa</i>	A1	0-0.5	A/S	10YR 4/2		SL	GR/1/f	so/ps		m/f		N	N
	A2	0.5-1.5	C/W	10YR 5/2		SL	SG/0	so/ps		m/f	c/RSB	N	N
	C	1.5-15	C/W	10YR 6/2	f/d/7.5yr 2.5/2	S	SG/0	ss/ps		c/f	f/SFB&RSB	N	N
	AC	15-20	D/S	10YR 4/2	f/d/7.5yr 2.5/2	L	PL/2/f	s/p		f/f	c/RSB	N	S/SL
	ACse	20-35	D/I	Gley1 7/N		SL	PL/2/f	s/p	F2M/c/3	f/m		Y	S/MD
	Cg	35-65+	U	Gley1 7/N		S	SG/0	so/po	FED/f/2			N	S/SL
MM-Sa2 <i>Sarcocornia fruticosa</i>	A1	0-0.5	C/W	2.5YR 3/2		SL	PL/1/f	ss/p		m/fm		N	N
	A2	0.5-1.5	C/W	10YR 6/1		S	GR/2/f	ss/po		m/f		N	N
	C	1.5-20	D/S	10YR 5/3	f/f/7.5 YR 4/5	SL	SG/0	ss/po	OSFc/2	f/f	f/SFB	N	S/SL
	ACse	20-32	A/S	10YR 4/1		S	SBK/2/f	ss/p		c/f		Y	S/MD
	Cg1	32-35	C/W	10YR 6/1		S	SG/0	so/po	OSF/f/2			N	S/SL
	Cg2	35-70+	U	Gley1 7/N		S	SG/0	so/po	FED/f/2		f/SFB	N	N
GC-Sar1 <i>Sarcocornietea fruticosi</i> (Prev. <i>Limonium vulgare</i> subsp. <i>serotinum</i> )	Oe	1-0	A/S	10YR 2/2		MK	PL/1/f			m/f		N	N
	A1	0-5	C/W	10YR 3/2	f/f/10YR 4/3	L	GR/1/f	s/p		f/m		N	N
	A2	5-10	C/W	10YR 5/1	c/d/10YR 4/3	SL	ABK/1/f	s/p		f/m		N	N
	AB	10-25	C/W	2.5Y 5/1	c/d/10YR 4/3	L	SBK/1/f		OSF/f/2	m/f/m	f/RSB	N	N
	AC	25-50	D/I	Gley1 4/10Y	f/d/10YR 5/6	L	ABK/1/f	sv/pv	OSF/f/1	f/f		N	N
	Cg1	50-60	D/I	Gley1 4/10Y	f/f/5YR 5/4	SIL	SG/0	sv/pv	OSF/c/2			N	N
	Cg2	60-80	D/I	Gley1 4/10Y	f/f/5YR 5/4	SIL	SG/0	sv/pv	OAF/f/2			N	S/SL
	Cse3	80-110	D/I	Gley1 3/10Y		SIL	SG/0	sv/pv	OAF/f/1			Y	S/MD
GC-Sar2 <i>Sarcocornietea fruticosi</i> (prevalence <i>Sarcocornia fruticosa</i> )	Cse4	110-120+	U	Gley1 3/10Y		SIL	SG/0	sv/pv				Y	S/MD
	A1	0-0.5	C/W	7.5YR 3/2		L	GR/1/f	ss/ps		m/f		N	N
	A2	0.5-5	C/W	10YR 4/3		L	ABK/1/fm	ss/p		c/f		N	N
	AB	5-10	D/I	10YR 5/4	f/f/10YR 5/3	SIL	ABK/2/m	ss/p		f/f	f/RSB	N	N
	AC1	10-18	D/I	10YR 5/1	c/d/10YR 5/3	SICL	ABK/2/m	s/p	OSF/c/2	f/m		N	N
	AC2	20-55	D/I	Gley1 6/10Y	c/d/10YR 4/3	SICL	ABK/1/m	sv/p	OSF/c/1	f/m	c/RSB	N	N
	Cg1	55-75	D/I	Gley1 6/10Y	f/f/5YR 4/4	SIL	SG/0	sv/pv	OAF/f/1			N	S/SL
	Cse2	75-85	D/I	Gley1 4/10Y	f/f/5YR 5/4	SIL	SG/0	sv/pv				Y	S/MD
	Cse3	80-95+	U	Gley1 3/10Y		SIL	SG/0	sv/pv				Y	S/MD

**Horizon master:** g=gleying, se=sulphides. **Horizon boundary:** (D)Distinctness: A=abrupt, C=clear, G=gradual, D=diffuse - (T) Topography: S=smooth, W=wavy, I=irregular, U=unknown. **Field texture class:** S=sand, SL=Sandy Loam, L=Loam, LS=Loamy Sand, SCL= Silty Clay Loam; **Structure.** (T) Type: GR = granular, ABK= angular blocky, SBK = subangular blocky, PL = platy, SG = single grain / (G) Grade: 0 = structureless, 1 = weak, 2 = moderate - (S) Size: vf = very fine, f = fine, m = medium; **Consistence.** (S) Stickiness: so = non-sticky, ss = slightly sticky, s = moderately sticky, sv = very sticky / (P) Plasticity: po = non-plastic, ps = slightly plastic, p = moderately plastic, pv = very plastic; **Mottles/redoximorphic features (RMFs):** (K) Kind: FED=iron depletions, FEF=ferriargillans, F2M=reduced iron FeS, OAF=organoargillans, OSF=organic stains; (Q) Quantity: f=few, c=common, m=many; (S) size: 1=fine, 2=medium, 3=coarse, 4=very coarse, 5=extremely coarse - **Roots.** (Q) Quantity: 1=few, 2=common, 3=many / (S) Size: vf=very fine, f=fine, m=medium, co=coarse. **Peroxide color change:** Y=yes; N=no. **Odor.** (K) Kind: N = none, S = sulphurous - (I) Intensity: SL = slight, MD = moderate, ST = strong.



(b). Morphological properties determined in Subaqueous soils (SASs) profiles. Main descriptive elements according to McVey et al. (2012).

Profile and dominant SAV	Water column measurements information		Horizons		Matrix Color Munsell	Texture	Coarse Frags	Organic fragments	Fluidity class	Peroxide color change	pH		Odor	
			Master	Depth										
	Top	Bottom		(cm)			%	%			Init	16 wks	K/I	
MM-Zos	T ( °C)	27	25	Oig	0.2-0		MK	45	45					
(Water depth cm 60 at low tide)	pH	8.5	8.5	Ase	0-12	Gley2 2.5/10B	MK S	9	9	SF	Y	8.3	6.1	S/ST
Zostera noltii and green algae (Ulva gen.)	DO (mg/l)	13.5	9.6	ACse	12-22	Gley2 3/10B	S	7	7	SF	Y	8.2	7.1	S/MF
	SAL (ppt)	29.7	33.4	O/Cg1	22-37	Gley2 5/5BG	MK SICL	12	22	SF	N	8.6	7.5	N
				O/Cg2	37-52	Gley2 4/5BG	MK SICL	21	31	SF	N	8.5	7.6	N
				Cg1	52-63	Gley2 5/5BG	SIL	6	6	MF	N	8.4	7.5	N
				Cg2	63-67+	Gley1 8/10Y	LS	0	2	MF	N	8.1	7.4	N
MD-Sp1	T ( °C)	27	26	0/Ag1	0-8	Gley1 3/5GY	MK SL	24	24	MF	N	7	6.3	N
(Water depth cm 20 at low tide);	pH	8.8	8.7	Ag2	8-13	Gley1 4/10GY	L	18	18	MF	N	7.6	7.2	N
Spartina maritima	DO (mg/l)	10.3	9.2	Cg1	13-30.5	Gley1 3/5GY	L	11	11	MF	N	7.6	7.3	N
	SAL (ppt)	33	34.2	Cg2	30.5-41	Gley1 3/10GY	L	9	9	MF	N	7.6	7.3	N
				Cg3	41-46	Gley1 4/10GY	SL	12	12	NF	N	7.9	7.5	N
				Cse4	46-66.5	Gley1 4/10GY	SIL	14	14	MF	Y	7.7	7.5	S/ST
				Cse5	66.5-80	Gley1 4/10GY	SIL	6	6	MF	Y	7.7	7.5	S/ST
				Cse6	80-87+	Gley1 3/10GY	SIL	18	5	VF	Y	7.76	7.6	S/ST
MD-Sp2	T ( °C)	27	25	Oig	0.5-0		MK	20	20					
(Water depth cm 25 at low tide);	pH	8.4	8.5	Ag1	0-1.5	Gley1 2.5/N	MK L	12	12	SF	N	7.9	7.1	N
Spartina maritima and reddish carpets (sulfobacter spp)	DO (mg/l)	10.3	9.3	Ag2	1.5-4.5	Gley1 3/10Y	L	15	15	MF	N	7.9	6.9	N
	SAL (ppt)	33.1	33.9	Ag3	4.5-8	Gley1 4/10Y	L	17	17	SF	N	7.7	6.5	N
				ACg	8-11	Gley1 5/N	L	9	9	MF	N	8.0	7.3	N
				Cse1	11-15.5	Gley1 5/N	SIL	5	5	NF	Y	8	7.3	S/MD
				Cse2	15.5-27.5	Gley1 5/10Y	SIL	10	10	MF	Y	7.9	7.3	S/MD
				Cse3	27.5-60+	Gley1 4/5GY	SIL	0	4	VF	Y	7.9	7.3	S/SL

**Horizon master:** g=gleying, se=sulphides. **Texture:** MK=mucky, L= Loam, LS = Loamy Sand, S = sand, SL = Sandy Loam, SICL = Silty Clay Loam, SIL = Silt Loam; **Fluidity class:** NF = non fluid, SF = slightly fluid, MF = moderately fluid, VF = very fluid; **Peroxide color change:** Y=yes; N=no. **Odor.** (K) Kind: N = none, S = sulphurous – (I) Intensity: SL = slight, MD = moderate, ST = strong.

**Water column measurements information:** **Top** = within 5 cm of the water surface; **Bottom** = within 5 cm of the bottom; **T** = temperature; **DO** = Dissolved oxygen; **SAL** = salinity

## List of tables:

**Table 2.1:** Summary of heavy metals concentration in river (a) and canal (b) waters according to their upstream (UpS) and downstream (DwS) position. Data are presented as  $\mu\text{g L}^{-1}$ .

**Table 2.2.** Geoaccumulation Index and qualitative classification in river and canal sediments, in upstream and downstream stations (Muller, 1969).

**Table 2.3.** Availability percentage of metals, determined by DTPA extraction of rivers and canals sediments in wet and dry samples. Data presented as percentage values of DTPA extract on the total fraction.

**Table 3.1.** Removal percentage and uptake of microbial macro elements and heavy metals in the effluent after 2 and 12h of laminar flux on a clinoptilolite bed.

**Table 4.1.** Morphological features of the hydromorphic (a) and subaqueous soils (b). Codes according to Shoenenberg et al (2012) and McVey et al. (2012) respectively.

**Table 4.2.** Chemical properties of hydromorphic soil profiles sampled in the interdunal area.

**Table 4.3.** Chemical properties of subaqueous soil profiles sampled in the wetland area.

**Table 4.4.** Matrix correlation between physicochemical variables in the superficial organo-mineral horizons (a) and in the deep mineral horizons (b) of all pedons. Only correlations with  $p \leq 0.05$  are shown.

**Table 5.1.** Mean physicochemical properties determined in Marina di Macia salt marsh (MM) soil profiles.

**Table 5.2.** Mean physicochemical properties determined in Gran Chiusa salt marsh (GC) soil profiles.

**Table 5.3.** Mean physicochemical properties determined in Mosconi Dike Road salt marsh (MD) soil profiles.



## List of Figures:

**Figure 1.1.** The catchment-coast continuum. Origin, transport and accumulation of sediments and their impact on the downstream areas. (European Sediment Research Network, 2004).

**Figure 1.2.** Representation of sediment disposal from the river catchment to the estuarine and coastal zones (Owens and Batalla, 2003).

**Figure 1.3.** Schematic presentation of reduction zones in subaqueous sediments/soils (modified from Žiljus (2011)).

**Figure 1.4.** Redoximorphic features on a soil profile (Grado lagoon, Northern Italy).

**Figure 1.5.** Sulfidic horizon in subaqueous soil (a) and pyrite accumulation associated with Fe oxidation (b).

**Figure 2.1.** Reno river basin (Northern Italy) and localization of the monitoring network. Rivers (R) and Canals (C) are shown.

**Figure 2.2:** Standardized coefficients (SCDC) and scatter plot of the Discriminant Function Analysis (DFA) based on the macro physicochemical properties of water samples. Only significant variables included in the model are shown.

**Figure 2.3:** Texture triangle of river and canal sediments.

**Figure 2.4.** Factor loadings of Principal Component Analysis (PCA) and score plot obtained from the analysis.

**Figure 2.5.** Dendrogram obtained by cluster analysis of log (K<sub>d</sub>) values.

**Figure 2.6.** Histograms of metals distribution between Exchangeable, Carbonate, Oxide/ Hydroxide bonds, Sulphur/ Organic bonds and Residual phase according to a five-step sequential extraction. Data are presented as % values.

**Figure 3.1.** Chemical and mineralogical composition of Ecolin clinoptilolite sample obtained by X-ray diffraction pattern.

**Figure 3.2.** Laminar flux system for water remediation in a clinoptilolite bed.

**Figure 3.3.** Uptake of ammonium (3.2.a) and microbial faecal indicators (3.2.b) at different sorbent: adsorbate ratio.

**Figure 3.4.** Plexiglas column and open-system set-up (*Experiment 3*).

**Figure 3.5.** Cu and Zn removal percentage (D) and uptake (Q) from different amounts of vermiculite

**Figure 3.6.** Adsorption kinetic of Cu and Zn on vermiculite permeable barrier (VPB) and bio-barrier (VPB.Bio). Standard Deviation was always < ±5%.

**Figure 3.7.** SEM image of the biofilm grown in Dil.LB medium and supported on vermiculite.

**Figure 3.8.** Mass balance of Cu and Zn throughout sediment, barrier and water the open system assay. VPB is vermiculite barrier while VPB-Bio is vermiculite bio-barrier system. Standard Deviation was always  $< \pm 5\%$ .

**Figure 3.9.** FT-IR spectra of characteristic functional groups of pure vermiculite (VPB) and vermiculite loaded with biomass (VPB-Bio) before and after metals treatment.

**Figure 4.1.** Localization of the study area, and morphological distribution of soil profiles.

**Figure 4.2.** Minimum, maximum and quartile distribution of Carbonates  $\text{CaCO}_3$  (a), Electrical Conductivity EC (b) and OC/S (c) in the soil profiles

**Figure 4.3.** Soil classification and pedo-sequences of soil profiles.

**Figure 4.4.** Canonical score plot and standardized coefficients (SCDC) of the discriminant function analysis (DFA) based on the great group classification (Soil Survey Staff, 2014). Only significant variables included in the model are shown.

**Figure 5.1.** Map of Grado and Marano lagoon and geographical localization of the studied salt marshes.

**Figure 5.2.** Representation of the vegetation species, based on soil morphology and sea level on each salt marsh.

**Figure 5.3.** Texture triangle of all soil horizons.

**Figure 5.4.** Scatterplot between total sulphur (S) and iron (Fe), expressed as  $\text{g kg}^{-1}$ , in all soil profiles.

**Figure 5.5.** Quartile distribution of organic carbon (OC,  $\text{g kg}^{-1}$ ) in all soil profiles.

**Figure 5.6.** Salinity (ppt) trend along the soil profiles.

**Figure 5.7.** Representation of soil profiles and soil matrix colours, according to the soil morphology and the mean sea level.

**Figure 5.8.** Canonical score plot and standardized coefficients of the discriminant function analysis (DFA) based on the three salt marshes grouping. Only significant variables included in the model are shown.

**Figure 5.9.** Canonical score plot and standardized coefficients of the discriminant function analysis (DFA) based on the different vegetation cover of soil profiles. Only significant variables included in the model are shown.

**Figure 5.10.** Representation of OC distribution ( $\text{g kg}^{-1}$ ) and erosion processes in the MM salt marsh.



## List of papers:

- **Ferronato, C.**, Modesto, M., Stefanini, I., Vianello, G., Biavati, B., Antisari, L.V., 2013. Chemical and Microbiological Parameters in Fresh Water and Sediments to Evaluate the Pollution Risk in the Reno River Watershed (North Italy). *J. Water Resour. Prot.* 05, 458–468. doi:10.4236/jwarp.2013.54045
- **Ferronato, C.**, Vittori Antisari, L., Modesto, M., Vianello, G., 2013. Speciation of Heavy metals at water-sediment interface. *EQA – Environ. Qual.* 10, 51–64. doi:10.6092/issn.2281-4485/3932
- **Ferronato, C.**, Vianello, G., Vittori Antisari, L., 2015. Adsorption of pathogens microorganisms,  $\text{NH}_4^+$  and heavy metals of wastewater through a clinoptilolite using bed laminar flow. *Clay minerals. Clay Minerals*, *in press*.
- **Ferronato, C.**, Vianello, G., Vittori Antisari, L., 2015. Heavy metals risk assessment after oxidation of dredged sediments through speciation and availability studies in the Reno river basin, Northern Italy. *J. Soil and Sediments*. doi: 10.1007/s11368-015-1096-4. – *in press*.
- **Ferronato, C.**, Silva, B., Costa, F., Tavares, T., 2015. Vermiculite bio-barriers for Cu and Zn remediation: an eco-friendly approach for freshwater and sediments protection. *Int. J. of Environ. Sci. and Tech.* *submitted*.
- **Ferronato, C.**, Falsone, G., Natale, M., Zannoni, D., Buscaroli, A., Vianello, G., Vittori Antisari, L., 2015. Chemical and pedological features of subaqueous and hydromorphic soils sequence in an intradune-wetland system (San Vitale park, Northern Italy). *Geoderma*- *submitted*.
- Vittori Antisari, L., De Nobili, M., **Ferronato, C.**, Natale, M., Pellegrini, E., Vianello, G., 2015. Subaqueous to hydromorphic soils transitions in the central Grado lagoon (Northern Adriatic Sea, Italy). – *Estuarine, Coastal and Shelf Science*, *submitted*.

## List of publications in congress acts:

- **Ferronato C.**, Stefanini I., Modesto M., Biavati B., Vianello G., Vittori Antisari L., 2012. Microbial pollution of the water of Reno river basin (North Italy). Abstract in: III Convegno Nazionale Società Italiana di Microbiologia Agraria, Alimentare e Ambientale (SIMTREA), Bari, June, 26<sup>th</sup>-28<sup>th</sup>, 2012.
- Vittori Antisari L., **Ferronato C.**, Gruppioni A., Vianello G., 2013. Treatment of wastewater by zeolites associated with a fluid processing device for EPT and microbial removal. Abstract in: Workshop: Biogeochemical processes at air-water-soil interfaces. Imola, May, 14<sup>th</sup>-15<sup>th</sup> 2013.
- **Ferronato C.**, Simoni A., Vianello G., Vittori Antisari L., 2013. Nutrient availability (P, K, S) changing red-ox condition in freshwater sediments of Reno river Basin (North Italy). Abstract in: 8th international SedNet conference, Lisbon (PT), November 6<sup>th</sup>-9<sup>th</sup>, 2013.
- **Ferronato C.**, Silva, B., Costa F., Vittori Antisari L., Tavares T., 2014. Biorecovery of Heavy Metals Using Vermiculite for Sediment and Water Protection. Abstract in: 12th International Chemical and Biological Engineering Conference (CHEMPOR 2014). Porto (PT), September 10<sup>th</sup>-12<sup>th</sup>, 2014.
- **Ferronato, C.**, Vianello, G., Vittori Antisari, L., 2014. The evolution of the Po Valley and Reno basin (North Italy) through the historical cartography: vicissitude of a land reclamation. Conference proceedings in: Regional Symposium on Water, Wastewater and Environment: Traditions and Culture. ISBN:97 8-960-538-921-5.